

1-2001

APPLICATION OF GEOPHYSICAL, HYDROGEOLOGIC L AND GIS TECHNIQUES FOR INVESTIGATION OF GROUNDWATER RESOURCES IN THE AL DHAID AREA, UAE

MOHAMED MUSTAFA MOHAMED AL MULLA

Follow this and additional works at: https://scholarworks.uaeu.ac.ae/all_theses

Part of the [Environmental Sciences Commons](#)

Recommended Citation

MOHAMED AL MULLA, MOHAMED MUSTAFA, "APPLICATION OF GEOPHYSICAL, HYDROGEOLOGIC L AND GIS TECHNIQUES FOR INVESTIGATION OF GROUNDWATER RESOURCES IN THE AL DHAID AREA, UAE" (2001). *Theses*. 72.

https://scholarworks.uaeu.ac.ae/all_theses/72

This Thesis is brought to you for free and open access by the Electronic Theses and Dissertations at Scholarworks@UAEU. It has been accepted for inclusion in Theses by an authorized administrator of Scholarworks@UAEU. For more information, please contact fadl.musa@uaeu.ac.ae.

0154 - 20660

**APPLICATION OF GEOPHYSICAL,
HYDROGEOLOGICAL AND GIS TECHNIQUES FOR
INVESTIGATION OF GROUNDWATER RESOURCES IN
THE AL DHAID AREA, UAE**

By

**MOHAMED MUSTAFA MOHAMED AL MULLA
(B. Sc. Agricultural Sciences, 1994)**

**A Thesis Submitted to the Faculty of Science of the
United Arab Emirates University in Partial Fulfillment of the
Requirements for the Degree of Master of Science
in
ENVIRONMENTAL SCIENCE**

**Faculty of Science
United Arab Emirates University**

January 2001

The Thesis of Mohamed Mustafa Mohamed Ali for the Degree of Master of Science in Environmental is approved.

.....
Examining Committee Member, Dr. Asma Al-Farraj

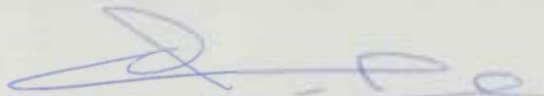


.....
Examining Committee Member, Prof. Abdel-Rahman Alsharhan



.....
Examining Committee Member, Prof. Ahmed Mahmoud El - Bershamgy

Ahmed El-Bershamgy



.....
Dean of Graduate Studies, Dr. Hadeef Rashed Al-Owais

**The Thesis of Mohamed Mustafa Mohamed Al Mulla for the degree of
Master of Science in Environmental Science is approved.**

.....
Chair of Committee, Prof. Dr. Abdulrahman S. Al Sharhan

.....
Examining Committee Member, Prof. Dr. Ahmed El Bershamgi

.....
Examining Committee Member, Dr. Asma Al-Farraj

**United Arab Emirates University
2001**

ACKNOWLEDGMENTS

I have to thank Almighty Allah above all for His Blessings and for providing me with the ability to complete this study successfully.

I would like to express my sincere appreciation to my supervisors, Prof. Dr. Mahdy M. Abdul Rahman, Geology Department, U.A.E. University and Dr Asma Al Farraj, Geography Department, U.A.E. University for their supervision and continuous guidance throughout this study. My thanks are due to Mr. Yasser Hammam, Geography Department, U. A. E. University for his continuous help in the GIS laboratory.

I would like also to extend my deep thanks and appreciation to Dr. Zeinelabidin S. Rizk, Geology Department, U.A.E. University (formerly) for his supervision, advice and help during the study and preparation of the thesis.

I wish to thank the Ministry of Agriculture and Fisheries for the support and valuable data provided to me for this study. My thanks are due to the Department of Soil and Water and the Central Agriculture Region of the Ministry of Agriculture and Fisheries for the support to me in the completion of this study.

My deep thanks and appreciation to my friends and my great family for their help, patience and encouragement during the time of the study.

Mohamed Mustafa Mohamed Al Mulla

ABSTRACT

In this thesis, geophysical, hydrological and GIS techniques were applied for evaluation of groundwater potentiality and land use planning for agricultural purposes in the Al Dhaid area, United Arab Emirates.

The gravity anomalies yielded three fault trends, ENE-WSW, NNW-SSE and E-W. The fault displacements range from 70 m to 320 m, with downthrown sides towards the northwest. The saturated thickness of sedimentary section above the ophiolite series varies between 700 m in the northwest and more than 3500 m at the northwest. The result of the resistivity and TDEM surveys produced a four-layers model based on thickness, resistivity, and total dissolved solids (TDS) contents. The four layers, from top to base, are: the superficial layer (thickness = 1.5 to 5 m, resistivity = 500 to 2000 ohm.m and TDS = 10 to 50 ppm), the upper aquifer (thickness = 5 to 15 m, resistivity = 205 to 605 ohm.m and TDS = 200 to 2000 ppm), the aquiclude (thickness = 28 m to 150 m, resistivity = 10 to 1000 ohm.m and TDS = 100 ppm to 300 ppm) and the lower aquifer (thickness = 80 to 450 m, resistivity = 20 to 100 ohm.m and TDS = 100 – 7500 ppm). Analysis of well logs indicated that porosity values ranges from 5% in some limestones to 47% in fractured dolomities. Temperature, conductivity and hydrochemistry logs showed the directions of groundwater flow and saline-water intrusion.

The hydrogeologic units identified in the Al Dhaid area include an upper free to semi-confined aquifer, an aquiclude and a lower confined aquifer. The regional groundwater flow direction is from the main recharge area in Northern Oman Mountain in the east toward the natural discharge area; the Arabian Gulf in the west. Between 1984 and 1999, a 20 km diameter cone-of-depression centered around the observation well GP-15 resulted from excessive groundwater pumping for all purposes. The average hydraulic gradient varies from 0.025 in the east to 0.005 in the west. The TDS content in groundwater of the Al Dhaid area changes from <750 mg/l in the northeast to 3000 mg/l in the central area and >7500 mg/l in the southwest. The sequence of cation dominance is $\text{Na}^+ > \text{Mg}^{2+} > \text{Ca}^{2+}$ and the sequence of anion dominance is $\text{Cl}^- > \text{SO}_4^{2-} > \text{HCO}_3^-$. The TDS content and total hardness show that the groundwater in some localities at the study area is not suitable for drinking and domestic purposes. Because of the agricultural activity at and around the Al Dhaid area, the concentration of NO_3^- in some samples is above the WHO recommended limit for drinking water (10 mg/l NO_3^- -N).

The results of GIS modeling indicate that the eastern strip of the study area has a high groundwater potentiality because of the intersection of more than one structural trend and low salinity (TDS =1500 gm/l). The areas of the Al Dhaid city and its surrounding and the south central area are most favorable for agriculture because groundwater in both areas has moderate salinity (TDS =3000 mg/l), low SAR (<10), shallow depth to groundwater (<45 m) and soil types suitable for agriculture.

TABLE OF CONTENTS

	Page
CHAPTER I - INTRODUCTION	1
1.1 General statement	1
1.2 Location of the study area.....	2
1.3 Objectives	2
1.4 Methods of study	4
1.4.1 Field measurements	4
1.4.2 Laboratory analyses.....	4
1.4.3 Office work.....	5
CHAPTER II – GEOMORPHOLOGY AND GEOLOGY	6
2.1 Geomorphology	6
2.1.1 Northern Oman Mountains.....	8
2.1.2 Piedmont and gravel plains.....	9
2.1.3 Inland plains and sand dunes.....	10
2.2 Geology.....	12
2.2.1 Surface geology	12
2.2.1.1 Semail ophiolite sequence	12
2.2.1.2 Allochthonous unit	14
2.2.1.3 Juweiza Formation.....	14
2.2.1.4 Neoautochthonous Sediments	15
2.2.1.4.1 Qahlah Formation	15
2.2.1.4.2 Maastrichtian-Lower Tertiary sediments	16
2.2.2 Subsurface geology.....	17
CHAPTER III – GEOPHYSICAL INVESTIGATIONS.....	20
3.1 Gravity investigation.	20
3.1.1 Gravity survey.....	20
3.1.2 Gravity interpretation.....	21
3.1.2.1 Qualitative analysis of Bouguer anomalies.....	21
3.1.2.2 Quantitative analysis of gravity anomalies.	24

	Page
3.1.2.2.1 Fault displacements	24
3.1.2.2.2 Thickness of sedimentary section.....	24
3.2 Geoelectrical investigations.....	27
3.2.1 Geoelectrical survey	27
3.2.1.1 Geoelectrical resistivity survey	27
3.2.1.2 Electromagnetic survey	28
3.2.1.2.1 Introduction.....	28
3.2.1.2.2 TDEM survey.....	31
3.2.1.2.2.1 TDEM instrument.....	31
3.2.1.2.2.2 Measurement layout.....	32
3.2.1.2.2.3 Stations positioning	32
3.2.1.2.3 TDEM data processing and interpretation	32
3.2.1.2.3.1 TDEM data processing	32
3.2.1.2.3.2 TDEM data interpretation.....	32
3.2.1.3 Geoelectrical interpretation of resistivity profiles	34
3.2.1.3.1 First layer	34
3.2.1.3.2 Second layer.....	34
3.2.1.3.3 Third layer.....	37
3.2.1.3.4 Fourth layer.....	37
3.2.1.4 Total dissolved salts.....	40
3.2.1.4.1 First layer	40
3.2.1.4.2 Second layer.....	40
3.2.1.4.3 Third layer.....	43
3.2.1.4.4 Fourth layer.....	43
3.2.1.5 Thickness distribution maps	46
3.2.1.5.1 First layer	46
3.2.1.5.2 Second layer.....	46
3.2.1.5.3 Third layer.....	46
3.2.1.5.4 Fourth layer.....	46
3.3 Borehole logging	51
3.3.1 Introduction.....	51
3.3.2 Geophysical logs.....	52
3.3.3 Interpretation of well logs	57
3.3.3.1 Interpretation of well logs in borehole 1	57
3.3.3.1.1 Formation litology	57
3.3.3.1.2 Fluid characteristics.....	59
3.3.3.2 Interpretation of well logs in borehole 2	60
3.3.3.2.1 Formation lithology	60
3.3.3.2.2 Fluid characteristics.....	62
3.4 Water salinity	63

CHAPTER IV – HYDROGEOLOGY & HYDROCHEMISTRY... 65

4.1 Climatic conditions	66
4.2 Hydrogeology	70
4.2.1 Hydrogeologic units	70
4.2.1.1 The upper aquifer.....	70
4.2.1.2 The aquiclude	71
4.2.1.3 The lower aquifer	74
4.2.2 Hydraulic heads	75
4.2.3 Water balance	83
4.3 Hydrogeoch	83
4.3.1 Physical properties.....	88
4.3.2 Major cations	93
4.3.3 Major anions	98
4.3.4 Ionic ratios	100
4.3.5 Water quality	106
4.3.6 Water types	113

CHAPTER V - GIS MODELING 117

5.1 Introduction	117
5.2 Model construction	117
5.3 Discussion of results.....	126
5.3.1 Zoned maps.....	126
5.3.2 Cross-correlation models.....	132
5.3 Discussion of results.....	126
5.3.2 Cross-correlation models.....	132

CHAPTER VI – CONCLUSIONS 146

6.1 Introduction	146
6.2 Conclusions based on geophysical investigations	146
6.3 Conclusions based on hydrogeological studies.....	149
6.4 Conclusions based on hydrogeochemical studies.....	150
6.5 Conclusions based on GIS modeling	151

REFERENCES..... 153

LIST OF FIGURES

Figure		Page
1.1	Location map of the study area.....	3
2.1	Geomorphologic map of the Al Dhaid area.....	7
2.2	Geologic map of east central UAE, including the study area.....	13
2.3	A NW-SE geologic cross section across the study area....	18
3.1	Geological interpretation of detailed gravity effects.....	26
3.2	Bouguer gravity anomalies and interpretation of major fault trends affecting the study area.....	25
3.3	Calculated sedimentary-ophiolite interface in the Al Dhaid area.....	29
3.4	Schematic representation of the propagation of the electromagnetic waves.....	30
3.5	Resistivity distribution in the first geoelectric layer.....	35
3.6	Resistivity distribution in the second geoelectric layer....	36
3.7	Resistivity distribution in the third geoelectric layer.....	38
3.8	Resistivity distribution in the fourth geoelectric layer.....	39
3.9	Distribution of total dissolved salts in the first geoelectric layer.....	41
3.10	Distribution of total dissolved salts in the second geoelectric layer.....	42

Figure		Page
3.11	Distribution of total dissolved salts in the second geoelectric layer.....	44
3.12	Distribution of total dissolved salts in the second geoelectric layer.....	45
3.13	Thickness distribution of the first geoelectric layer.....	47
3.14	Thickness distribution of the second geoelectric layer....	48
3.15	Thickness distribution of the third geoelectric layer.....	49
3.16	Thickness distribution of the third geoelectric layer.....	50
3.17a	Well log and lithologic interpretation in well No.1.....	53
3.17b	Fluid characteristic well log in well No. 1.....	54
3.18a	Well log and lithologic interpretation in well No.2.....	55
3.18b	Fluid characteristic well log in well No. 2.....	56
3.19	Water salinity versus depth in borehole No. 1.....	64
4.1	Location of the Ministry of Agriculture and Fisheries observation wells in the Al Dhaid area	67
4.2	Isopach map of the upper aquifer in the Al Dhaid area, in meters.....	72
4.3	Isopach map of the Paleocene aquiclude in the Al Dhaid area, in meters.....	73
4.4	Hydraulic head contour map of the upper aquifer in the Al Dhaid area, in meters above sea level in 1999.....	76
4.5	Hydraulic head contour map of the upper aquifer in the Al Dhaid area, in meters above sea level in 1984.....	77

Figure	Page
4.6 Hydraulic head contour map of the lower aquifer in the Al Dhaid area, in meters above sea level in 1999.....	78
4.7 The change in groundwater levels at nine observation wells in the Al Dhaid area during 1985-1998.....	81
4.8 Contour map showing the cone-of depression associated with groundwater extraction between 1984 and 1999 in the Al Dhaid area.....	82
4.9 Annual runoff volume of five major wadis in the Al Dhaid area during the period 1975-1998.....	84
4.10 The rainfall-groundwater level relationship of the Siji area for the period 1985-1998.....	85
4.11 The rainfall-groundwater level relationship of the Al Dhaid area for the period 1985-1998.....	86
4.12 A summary of water balance in the Al Dhaid area for the period 1977-1995	87
4.13 Location map of water wells sampled for chemical analysis from the Al Dhaid area during the period 1996-1999	89
4.14 Iso-temperature (°C) contour map of groundwater in the Al Dhaid area during 1995-1996.....	90
4.15 Iso-pH contour map of groundwater in the Al Dhaid area during 1995-1996.....	92
4.16 Iso-EC contour of groundwater in the Al Dhaid area during 1995-1996.....	94
4.17 Iso-concentration contour map of the calcium ion in groundwater of the Al Dhaid area in 1996.....	95
4.18 Iso-concentration contour map of the magnesium ion in groundwater of the Al Dhaid area in 1996.....	96

Figure	Page
4.19 Iso-concentration contour map of the sodium ion in groundwater of the Al Dhaid area in 1996.....	97
4.20 Iso-concentration contour map of the bicarbonate ion in groundwater of the Al Dhaid area in 1996.....	99
4.21 Iso-concentration contour map of the sulphate ion in groundwater of the Al Dhaid area in 1996.....	101
4.22 Iso-concentration contour map of the chloride ion in groundwater of the Al Dhaid area in 1996.....	102
4.23 Contour map showing the distribution of $\text{Ca}^{2+}/\text{Mg}^{2+}$ ratio in groundwater of the Al Dhaid area in 1996.....	104
4.24 Contour map showing the distribution of $\text{C}^{-}/(\text{CO}_3^{2-} + \text{HCO}_3^{-})$ ratio in groundwater of the Al Dhaid area in 1996.....	105
4.25 Contour map showing the distribution of $\text{SO}_4^{2-}/\text{Cl}^{-}$ ratio in groundwater of the Al Dhaid area in 1996.....	107
4.26 Contour map showing the distribution of $\text{Na}^{+}/\text{Cl}^{-}$ ratio in groundwater of the Al Dhaid area in 1996.....	108
4.27 Iso-concentration contour map of the nitrate ion in groundwater of the Al Dhaid area in 1996.....	110
4.28 Iso-concentration contour map of the total iron in groundwater of the Al Dhaid area in 1996.....	111
4.29 Iso-total hardness contour map of groundwater in the Al Dhaid area in 1996.....	112
4.30 Iso-SAR contour map of groundwater in the Al Dhaid area in 1996.....	114
4.31 A trilinear plot of all groundwater samples collected from the Al Dhaid area in 1996.....	115

Figure	Page
5.1 A flow chart of the GIS analytical model of the Al Dhaid area.....	118
5.2 Zoned distribution of total dissolved solids <1500 mg/l in groundwater of the al Dhaid area in 1996.....	121
5.3 Zoned distribution of total dissolved solids <3000 mg/l in groundwater of the al Dhaid area in 1996.....	122
5.4 Zoned distribution of total hardness (TH <80 mg/l) in groundwater of the al Dhaid area in 1996.....	123
5.5 Zoned distribution of sodium adsorption ration (SAR <10) in groundwater of the al Dhaid area in 1996.....	125
5.6 Zoned distribution of depth to groundwater (<45 m) in groundwater of the al Dhaid area in 1996.....	128
5.7 Soil classification of the Al Dhaid area.....	129
5.8 Re-grouping of JICA's soil classification of the Al Dhaid area into tow major classes.....	130
5.9 The main drainage lines within the Al Dhaid area, traced from the soil classification map.....	131
5.10 The major fault trends affecting the Al Dhaid area, as interpreted from the gravidata.....	133
5.11 Influence of major structural trends on the drainage network of the Al Dhaid area.....	134
5.12 Zones of groundwater with TDS <3000 mg/l and total hardness <80 mg/l in the Al Dhaid area in 1996.....	135
5.13 Zones of groundwater with TDS <1500 mg/l and sodium adsorption ratio (SAR) <10 in the Al Dhaid area in 1996.....	136

Figure		Page
5.14	Zones of groundwater at depth <45 m and TDS <1500 mg/l in the Al Dhaid area in 1996.....	138
5.15	Zones of groundwater with TDS <1500 mg/l, SAR <10 and soil types suitable for agriculture in the Al Dhaid area in 1996.....	138
5.16	Zones of shallow groundwater (depth <45 m), moderate salinity (TDS <3000 mg/l) and low sodium adsorption ratio (SAR <10) in the Al Dhaid area in 1996.....	140
5.17	Zones of shallow groundwater (depth <45 m), moderate salinity (TDS <3000 mg/l), low sodium adsorption ratio (SAR <10) and soil types suitable for agriculture in the Al Dhaid area in 1996.....	141
5.18	Combination of groundwater salinity, drainage lines and major structural zones affecting the Al Dhaid area.....	143
5.19	Suggested protection zones along the sides of major stream channels in the Al Dhaid area.....	144
5.20	Recommended protection zones of groundwater observation wells in the Al Dhaid area.....	145

LIST OF TABLES

Table		Page
2.1	Topographical subdivisions and geological units in the Al Dhaid area.....	11
2.2	Subsurface lithology in two boreholes (B1 and B2) at the Al Dhaid area.....	19
4.1	A summary of hydraulic properties of the upper and lower aquifers in the Al Dhaid area.....	74
4.2	Water-table elevations, in meters above sea level, at nine observation wells in the Al Dhaid area during 1985-1998.....	80
4.3	Comparison of the water quality parameters in the Al Dhaid area with the WHO and GCC standards for drinking water.....	116

CHAPTER 1

INTRODUCTION

CHAPTER 1

INTRODUCTION

1.1 General Statement

The close proximity of the Al Dhaid area to Northern Oman Mountains in UAE and availability of reasonable groundwater resources have made it a favorable site for intensive agricultural activities since early 1970s. The wide application of mechanical submersible pumps in numerous water wells has led to acute aquifer depletion due to excessive groundwater discharge compared with the limited recharge. This unbalanced situation has resulted in a sharp decline of groundwater levels, increasing groundwater salinity, dryness of shallow wells and deterioration of groundwater quality.

The Ministry of Agriculture and Fisheries (MAF) has early realized these problems and conducted intensive field survey using geophysical, hydrogeological and hydrogeochemical techniques for assessment of groundwater problems in the Al Dhaid area. In this regard, the MAF cooperated with international agencies, such as IWACO Consultants for Water and Environment (1986) and Japan International Cooperation Agency (JICA) in 1996.

Since these studies were concluded in 1995, the researcher found it necessary to continue field investigations and make use of recent

applications of Geographic Information System (GIS) techniques for evaluation of groundwater resources in the Al Dhaid area. For this purpose, integration of previous data as well as present field and laboratory results were used to develop a comprehensive GIS model for water resources evaluation, planning and protection.

1.2 Location of the Study Area

The study area is a part of the central agricultural region in UAE. It covers 850 km² and is bounded by Longitudes 55° 50' and 56° 00' E, and Latitudes 25° 00' and 25° 23' N. It extends from the Northern Oman Mountains in the east to the Fayah Mountains in the west. The northern agricultural region limits the study area in the north and the Al-Madam plain represents its southern boundary (Fig.1).

1.3 Objectives

The present study employed available field-measured geophysical data, hydrogeologic investigation, groundwater chemistry and soil classification, along with the ESRI GIS package, for evaluation groundwater potentiality of Al Dhaid area.

The study also included identification of major surface and subsurface geologic structures, assessment of groundwater quality, distinction of different hydrogeologic units and evaluation of land use for agriculture.

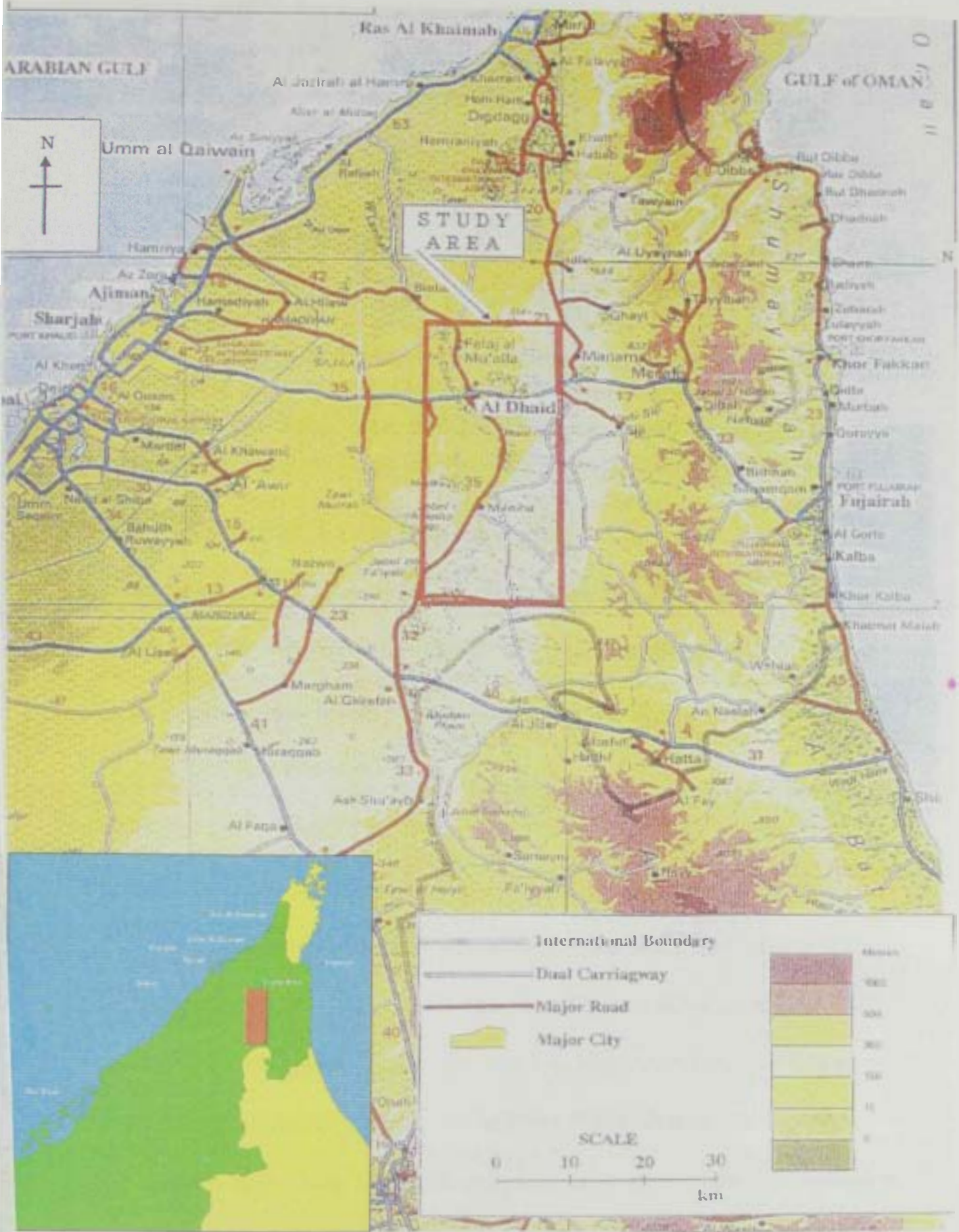


Figure 1.1. Location map of the study area.

1.4 Methods of Study

1.4.1 *Field-measurements*

The field-measured data include depth to groundwater in the observation wells of the Ministry of Agriculture and Fisheries within the study area for the period of 1995-1999.

The physical parameters of groundwater samples including temperature ($^{\circ}\text{C}$), electrical conductivity (EC) in $\mu\text{S}/\text{cm}$ and hydrogen ion concentration (pH) were also measured in the field. In addition to pumping test experiments, infiltration measurements, geoelectrical and well logging field surveys which was participated with the Ministry of Agriculture and Fisheries.

1.4.2 *Laboratory Analyses*

Groundwater samples from about 100 private wells were analyzed for major cations (Ca^{2+} , Mg^{2+} , Na^{+} and K^{+}) and anions (CO_3^{2-} , HCO_3^{-} , SO_4^{2-} and Cl^{-}) in the central laboratories of the Ministry of Agriculture and Fisheries. The results were plotted on Piper (1944) diagram and presented as contour maps using SURFER computer program version 5.01 surface mapping system (Golden Software Inc., 1994).

1.4.3 Office Work

Office work includes analysis and presentation of field-measured data, laboratory analyses and results of previous geophysical investigations on relevant charts and graphs. These data include geophysical information, groundwater levels and analyses of groundwater chemistry.

The GIS modeling was carried out in the Department of Geography, UAE University, using ArcView GIS 3.2 package (ESRI products) with ArcView Spatial Analyst, under Windows NT 4.0 platform.

CHAPTER 2

**GEOMORPHOLOGY AND
GEOLOGY**

CHAPTER 2

GEOMORPHOLOGY AND GEOLOGY

2.1 Geomorphology

The study area is located within wadi flats and desert that stretches from the foothills of the Northern Oman Mountains in the east to the Arabian Gulf in the west (Fig.2.1). The monotonous terrain consists of vast flood plains with minor dunes of an uneven configuration. A number of wadi channels traverse the study area from the east towards the west. The largest of these are Wadi Al Dhaid, Wadi Siji, Wadi Kadrah, Wadi Hamdah and Wadi Thiqebah. The presence of silt in flat, low lying ground between the wadi terrace and fluvial fans indicates that the study area is prone to periodic flooding from the Northern Oman Mountains. Although the floodwater is temporarily retained in such silt flats, low lying land and sand dunes, most of the water may be lost by evapotranspiration (Ministry of Communications, 1996).

This topography is very common in the western foothills of the Northern Oman Mountains and similar types of alluvial fans align and connect with each other to form what is called a bahada plain. Large fluvial fans such as the Madam plain and Jiri plain also lie on a similar alignment of the Al Dhaid bahada plain (JICA, 1996; Al Farraj, 1996).



- Af = Alluvial Fan
- Fp = Flood Plain
- Rd = River Bed
- Sd = Sand Dune
- Tr = Trace
- Pd = Pediment plain

Figure 2.1. Geomorphologic map of the study area (JICA, 1996)

2.1.1 Northern Oman Mountains

The Northern Oman Mountains extend to the east of the study area and is characterised by a rugged terrain with steep slopes and a number of scarps. Most of the area lies between elevations of 200 m and 1200 m. The drainage lines downgradient of the mountain area generally display a dendritic pattern (Al- Frraj, in prap.), controlled in places by protruding rock mass, joints and faults. Along Wadi Sifuni, Wadi Shawkah and Wadi Thiqebah, a relatively dense dendritic drainage pattern is seen (JICA 1996). However, the northern watersheds, such as Wadi Siji and Wadi Ghayl, display a linear drainage pattern close to the structural zones (Al- Farraj, 1996;Al- Farraj, in prap.).

The wadi valleys are generally filled by Mid Pleistocene gravel and sand, which are locally cemented forming conglomerate. More extensive flood plain deposits mixed with recent loose gravels and sands overlies these sediments. The continued down cutting develops many stepped river terraces and forms deep grooves along the wadi courses at the foothills of the mountains (Al- Farraj, 1996;Al- Farraj, in prap.).

Most seepage and water sources of shallow wells come from groundwater concentrated at the junctions between rock mass and the aforesaid gravel layer. Evidence of groundwater storage is clearly apparent in the ophiolite mass itself and occasional seepage breaks out during the rainy season where the fractures and weathered zones are highly integrated.

2.1.2 Piedmont and Gravel Plains

Most of the study area is covered by terrace, alluvial fans and floodplain deposits (JAICA,1996;Al-Farraaj,2000). The alluvial fans extend from the foothills of the mountain to sand dunes, which spread out from the Jebel Fayah – Jebel Mileiha line to the coast of the Arabian Gulf. In the study area, numerous small wadi channels gather into the main channels of Wadi Al Dhaid, Wadi Kadrah and Wadi Hamdah. Between these channels, broad flood plains are found in the middle of the gravel plain. In the downstream area, all such channels merge into Wadi Lamhah and the flood plain becomes restricted to its course.

The runoff from the Northern Oman Mountain leaves a faint indication on the gravel plain. However, the deposits originate from a series of older fans. Coarser particles or a thin silt layer generally covers the surface of the plain. The size of the sediment is clearly graded along the wadi courses. At Wadi Kadrah, which is located on the border between the Northern Oman Mountains and the gravel plain, large gravels ranging from pebble to boulder are scattered. Downstream near the Wadi Lamhah, coarse sands to fine gravel are mainly distributed even in the centre of the wadi course. Most gravel is composed of weathered serpentinite derived from the Ophiolite Series. However, in some places around the limestone ridges, calcareous and siliceous gravel is occasionally dominant. A dry wadi pattern or a series of ridges of

Maastrichtian limestone breaks the gentle slope of the plain (e.g. Jebel Mileiha and Jebel Fayah). Sand dunes bordering the western edge of the gravel plain form a natural barrier against surface runoff (Al- Farraj,2000).

2.1.3 Inland Plains and Sand Dunes

These areas form a rectangular bounded by the gravel plain and the hills that straddle Jebel Mileiha and Jebel Fayah. To the west, the coastal sabkha and the Gulf coast bound the area. The dune sand is composed mostly of either carbonate or quartz derived from shell fragments and quartz-bearing rocks. The carbonate sand is found mostly near the coastline while the quartz sand is inland. The quartz sand of this area is easily distinguished by its reddish colour caused by iron oxide staining the grains (Al- Frraj, in prap.).

Most of the dunes are generally aligned in the ENE-WSW direction, approximately perpendicular to the prevailing wind direction. These are recent dunes and are mobile; often forming a series of sand dunes strung out in a NW-SE direction (Glennie et al., 1994). Otherwise, the older series of dunes are in general recognised by being larger and higher than the recent dunes. The largest dune is found in the north of the study area and is 209 m in elevation. This older dune type is occasionally fixed by vegetation and is composed of more ancient dune materials constructed over several cycles of on-shore sedimentation.

Field observation of the depth of saturated sand after rain storms indicated that a high infiltration rate might be possible, which can contribute to groundwater recharge from local drainage in the dune area (JAICA, 1996). The basic geomorphologic features recognized in the study area are summarized in Table 2.1

Table 2.1 Topographical subdivisions and geological units in the study area (JICA, 1996).

Topographical Division	Land Formation Type	Geological Unit
Northern Oman Mountains	Erosional slopes	(Os) Semail ophiolite sequence (Hy) Hayabi complex (Hw) Hawasina assemblages
Piedmont and gravel plains	(Tr) Trace or dissected limestones and carbonates (Pd) Pediment plain	Maastrichtian-Tertiary sediments (Jw) Juweiza Formation (Qh/Uar) Qahlah Formation (Esh) Eocene shale
Inland plains and sand dunes	(Af) Old dissected alluvial fan (Af) New active alluvial fan (Fp) Flood plain (Rd) River bed of active wadi (Sd) Sand dunes and troughs	(Gre/Ufa) Cemented gravel and terrace deposits of the Upper Far Formation (AI) Superficial deposits of Recent alluvial gravels and sands

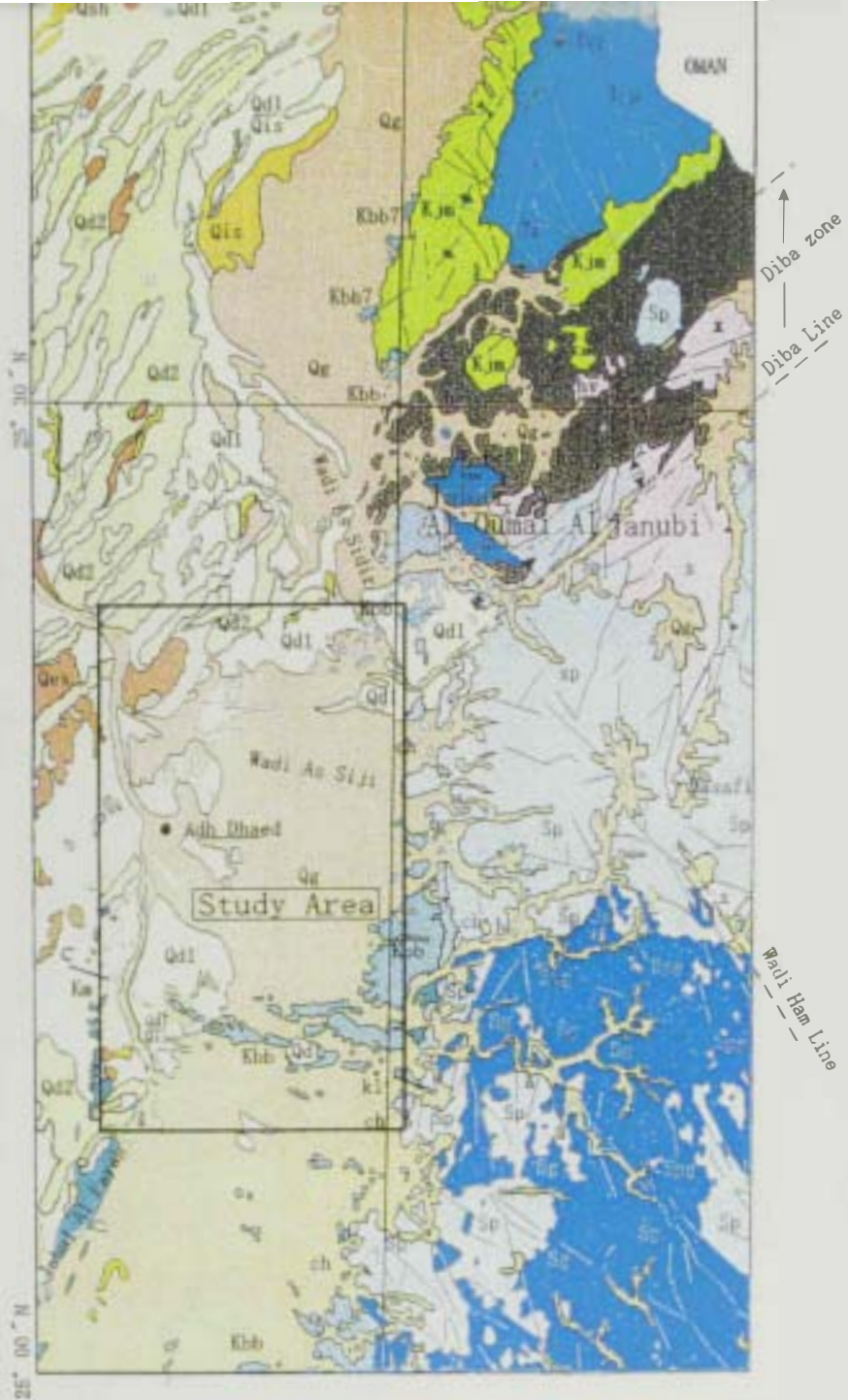
2.2 Geology

2.2.1 Surface Geology

The major geological units in the study area comprise the Semail Ophiolite sequence, allochthonous unit (the Batinah complex) and neoautochthonous Maastrichtian sediments (Fig. 2.2). The following is a summary of lithological characteristic and geologic structure of these units, based on JICA's (1996) study mainly and (Alleman and Peters, 1972; Alsharhan and Kendall, 1986; Alsharhan and Nairn, 1988).

2.2.1.1 Semail Ophiolite Sequence (Op)

This is the largest and most extensive unit within the study area and its major outcrops are confined to the Northern Oman Mountains. As a result of syn- and post emplacement faulting and folding, the ophiolite nappe has been broken into a number of more or less intact structural blocks. The whole sequence represents a complete section up to 20 km thick through mid-Cretaceous oceanic lithosphere. Many of the faults in the upper part of the ophiolite can be demonstrated to be oceanic structures even though they may have been reactivated during and after emplacement. The base of the nappe is marked by a zone of mylonitized and highly sheared peridotite, known as the "banded unit", the structures of which clearly overprint an earlier mantle tectonite fabric and which appear to have formed during amphibolite facies metamorphism.



Autochthonous and Par-Autochthonous units			
Qz	Fluviatile deposits	Boulders gravel, mud and silt in drainage Channels and minor undifferentiated terrace deposits Terrace deposits and piedmont gravel beds, scree and outwash fans. Boulder to gravel size debris in a fine grained matrix, in places well cemented, local sand and silt interbeds	Holocene
Qcs	Coastal sabkha	Calcareous silt, waddy sand with considerable salt content, salt crusts, flooded by storm and spring tides	Pleistocene and Holocene
Qim	Inland sabkha	Silt and muddy sand, flooded by wadi or rising ground water	
Qm	Desert plain deposits	Lag gravels, locally sand or silt, from low-lying flat or gently undulating surface with isolated dunes. May include areas of thin eolian sand cover, sabkha	
Qd1	Eolian sand	Low dunes	
Qd2	Eolian sand	High dunes	
Kbb	Boulder beds	Pebbles, cobbles and boulders, principally of brown chert, gabbroic and ultrabasic rocks in a siliceous limestone matrix	?
Kl	Limestone	White to buff, fine grained, porous, nodular weathering, contains fragments of chert, basic and ultrabasic rocks	Upper Cretaceous
Kul	Maastrichtian Limestone	Brown, purplish, grey and white fossiliferous limestone, locally with nodular varieties, limestone conglomerata and reef deposits Occasional chert bands and nodules. Minor interbeds of marl, mudstone and shale. Local thick basal conglomerata in Jabal Al Fayah area	
Kjm	Musandam Group	Grey, massive to well bedded limestones, locally oolitic, fossiliferous, dolomitic with chert nodules	
	Elphinstone Group	Limestone, dolomitic limestone, dolomite, shale, marl, siltstone, sandstone, local chert and conglomerata (Fr)	Lower Jurassic to Lower Cretaceous
	Ru'us Al Jibal Group	Dolomite, dolomitic and argillaceous limestone and occasional shale (Fr)	Mid-Permian to Triassic
	Rasqa Formation	Limestone, dolomite, sandstone, marl and local shales outcropping in Jabal Al Qamar Al Janubi (Ra)	Ordovician
Or	Rann quartzite Formation	Quartzitic sandstone and shale	Upper Cretaceous to Pre-Permian
Allochthonous units			
Gabbro	Gabbros	Coarse grained leucocratic and melanocratic varieties, commonly layered and with minor serpentinite zones; breccias, microgabbroic and pegmatitic types occur locally	
Ultrabasic	Gabbros and ultrabasics	Complex zones of gabbro with intermixed ultrabasic rocks	
Sp	Ultrabasics	Peridotite, serpentinitized peridotite and serpentinite, locally banded. Magnetite and thin chrysotile veins widespread Serpentinite generally highly fractured. Silicified alteration products (ch) hatched	
Metamorphic series			
Metamorphics	Metamorphics	Quartzite, quartz schist, quartz mica schist, chloritic schist, bands of brown, buff and white crystalline marble. Local calc silicate rocks include amphibolite and epidote schist	
Chert/limestone facies	Chert/limestone facies	Maroon and greenish grey chert commonly well bedded, grey brown and white limestone, occasional green/grey and maroon shale, local volcanics (h) Larger areas of chert (hc)	
Volcanics	Volcanics	Mainly dark green intermediate and basic lavas, vesicular, locally porphyritic and in places with pillow structures, agglomerate and ? tuff beds	
Geological boundary			Fault or fracture (mark on downthrow side)
Geological boundary, approximate			Fault or fracture, inferred or approximate
Dip and strike of strata			Thrust fault (barbs point to overthrust rocks)
Anticline			Wadi
Syncline			Tom

Figure 2.2. Geologic map of the east central of UAE including the Study area (JICA, 1996)

Radiometric dating of metamorphic rocks yields mid to late-Cretaceous age. The K-Ar and Rb-Sr mineral ages ranging from 70 to 95 million years. During the later stage of nappe emplacement and post-emplacement, the lower ultramafic part of the ophiolite has been extensively serpentinized. Apart from these effects, the Semail Ophiolite nappe represents a more or less complete and largely unaltered section of mid-Cretaceous oceanic upper mantle and crust.

2.2.1.2 Allochthonous Unit (The Batinah Complex)

This facies comprises several allochthonous units, which overlie the Semail nappe along the western edges of the mountains. It consists of a lower melange, composed of blocks of the Semail Ophiolite (Os), exotic limestones, Hayabi volcanics (Hy), Hawasina sediments (Hw), metamorphic rocks and serpentinite, which locally has a depositional contact with the top of the ophiolite.

2.2.1.3 Juweiza Formation (Jw)

The Oman Mountains were subjected to a major deformation in the Cretaceous (Turonian - Campanian period), with the emplacement of far-travelled thrust nappes from northeast to southwest onto the Arabian Peninsula margin. The nappe emplacement onto the Arabian foreland was preceded by a deepening of Arabian shelf margin in the mid to late

Cretaceous Period. This emplacement was associated with the deposition of deep-water sediments disconformably above the Cenomanian shelf and slope limestone following subsidence of the continental margin. Deep-water sedimentary melanges, found in the upper part of the Hawasina and Hayabi complexes, were probably developed at an earlier time in a more distant setting. Syn-emplacement flysch deposits of Campanian age (Juweiza Formation) were deposited in fore deep in front of the advancing nappes. Post-emplacement folding, uplift and erosion of the nappes were complete by the Maastrichtian Period when a transgressive series of clastic sediments and shallow water limestone were deposited across the mountainous area. Late Cretaceous nappes emplacement in the Oman Mountains has several features in common with the each other.

2.2.1.4 Neoautochthonous Sediments and Tertiary Structures

The Maastrichtian, Palaeocene and Eocene sediments, mainly limestone with a total thickness of up to 600 m, unconformably overlie the late Cretaceous allochthonous units of the Oman Mountain Range along its eastern and western flanks. There are two facies:

2.2.1.4.1 Qahlah Formation

The coarse grained clastic are largely restricted to the eastern side of the mountains, whereas, by contrast, on the western side, the limestone

rests directly on older rocks. In places, subaerial exposure and lateritic weathering of the ophiolite occurred before Maastrichtian sedimentation took place.

2.2.1.4.2 Maastrichtian Lower Tertiary Sediments

These sediments were deformed during the mid-Tertiary Eocene Period. The tectonism was particularly severe in the north, along the western side of the Musandam Peninsula. The Mesozoic limestone of the Ru'us Al Jibal Massif was displaced several kilometres westward along the Hagab thrust. Along the line of the thrust, the limestone is locally overturned and thrustover the Eocene shale. In general, the Tertiary fold axes trend parallel to the mountains from N-S in the north to NW-SE and E-W further south. It has been suggested that the Tertiary folding is the result of reactivation of basement faults and local uplift, perhaps partly due to salt doming. A regional origin is, however, suggested by the widespread development and consistency of trends and directions of the fold axes.

The post-Miocene history of the area is one of repeated uplift of the mountains and subsidence of the flanks with thick sediment deposition. Over 4000 m of the Neogene sediments in an offshore borehole on the Oman continental margin where extensive slumping of the thick semi-consolidated sediments have been identified on seismic profiles. Cycles

of repeated uplift are recorded by a series of gravel-capped terraces on the flanks of the mountains. Elevated terraces above sea level are found in some places, but are as yet undated. In the major mountain wadis cemented gravel are pushed up to 50 m above the present valley floors.

2.2.2 Subsurface Geology

Figure 2.3 is a NW-SE geologic cross section across the study area illustrating the subsurface stratigraphic units. The figure also clearly indicate the influence of major faults on the thickness of each of these units.

Table 2.2 summaries the subsurface lithologies encountered in the study area, based on the data obtained from two boreholes (B1 and B2) and from geophysical investigations.

Table 2.2 Subsurface Lithology in two boreholes B1 and B2 at the Al Dhaid area (JICA 1996)

Formation	Lithology (Borehole 1)	Lithology(Borehole 2)
Alluvium	Sand and gravel (0-17m), dominated by limestone with an average porosity of 35%. Some thin clays are noted	Sand and gravel (0-29m), limestone and dolomite with an average porosity of 32% to 50%
Limestone	Limestone (17-85 m) with interbedded dolomite. The average porosity of 40%. The porosity is identified as primary in origin.	Limestone (29-101m) with intercalated limestone. Formation porosity averages 42%. Primary porosity is dominant. Thin dolomites are identified by their low density porosity and formation resistivity
Dolomite	Dolomite (85-133 m) with an average porosity of 36%. Some secondary porosity is identified, especially between 122 m and 133 m where joints and fractures are noted in cores. Dolomitic Limestone (133-200 m) in places with a variable porosity of 20%. Some thin clays are present and secondary porosity is between 169 and 190 m.	Dolomite (101-219 m) with interbedded limestones. Formation porosity averages 40%. Primary porosity is dominant. The thin limestone is identified by high formation resistivity. The formation porosity decreases to less than 20% in some of the limestones.
Marl and Marly Limestone	Not observed	Marland Marly Limestone (219-300 m) with interbedded limestone and dolomite. Formation porosity averages 32%. Limestones are identified by high formation porosity resistivity. The formation porosity decreases to less than 20% in some of the limestones.

CHAPTER 3

GEOPHYSICAL INVESTIGATION

CHAPTER 3

GEOPHYSICAL INVESTIGATIONS

Geophysical investigations were conducted in the study area aiming at delineating different hydrogeologic units, evaluating groundwater quality, studying petrophysical characteristics of the water bearing layers and defining subsurface geologic structures controlling aquifer boundaries and the courses of buried wadi channels.

Three types of geophysical methods were applied in the study area. The first method has made use of the gravitational field. The second required input of artificially generated energy into the ground, such as electrical and electromagnetic fields. The third technique was the geophysical well logging.

The geophysical measurements at the Al Dhaid and surrounding areas were conducted during two different episodes, the first was in 1986 (IWACO) including gravity, DC-electrical and well-logging surveys. The second was in early June of 1996 (JICA) including natural gamma ray, TDEM survey and well logging in two wells.

3.1 Gravity investigation

3.1.1 Gravity Survey

IWACO (1986) has conducted geophysical survey in the study area including gravity with main purpose of determining sites of new water

wells. However, 386 gravity stations were used and the gravity field was measured by the La Coaste Gravimeter. The gravity values were corrected for the base zero in the vicinity of Al Dhaid.

3.1.2 Gravity Interpretation

A gravity survey determines variation in the earth's gravitational field caused by differences in the density of subsurface rocks. The gravity method deals with the variation of the gravitational acceleration and is used most extensively in the search for oil traps, in addition to engineering and archaeological applications.

Two different approaches are used for interpretations of the Bouguer anomaly data. One is direct, where the original data are analysed to produce an interpretation. The other is indirect, where models were constructed to compute synthetic gravity anomalies, which were then compared with the observed Bouguer anomalies.

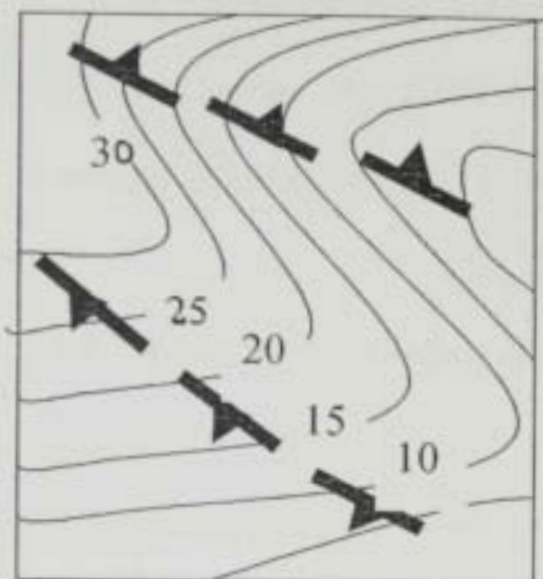
3.1.2.1 Qualitative Analysis of Bouguer Anomalies

The IWACO (1986) Bouguer gravity map of the Al Dhaid plain has been subjected to qualitative analysis aiming at delineation of the subsurface structural trends which control the course of groundwater flow. However, the best method of subsurface mapping of faults is the Linsser's (1967) technique, which stated that the faults could be

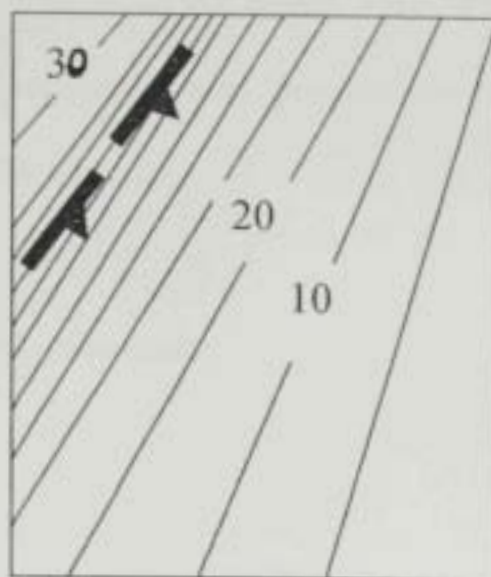
delineated by gravity detailing. In this context, four principles are considered:

1. Gravity gradient: Areas occupied by dense parallel Bouguer anomaly contours in a continuously decreasing manner represent a fault axis in the same direction of gravity contours (Fig. 3.1.a). The downthrown side is at the direction of Bouguer anomaly decrease. Faults of this type are shallow and close to the ground surface.
2. Gravity contour undulations: The Bouguer gravity contours of deep-seated faults are of sinusoidal shapes. Fault axes bounding either positive or negative undulations (Fig. 3.1.b). Downthrown sides of the faults are in the direction of Bouguer anomaly reduction.
3. Change of gravity gradient: A abrupt change of the gravity gradient indicates a fault axis perpendicular to the direction of gravity contours (Fig. 3.1.c). This type represents faults of intermediate depth.
4. Change of gravity amplitude in the same closure: The presence of closures having different sizes inside closed Bouguer gravity contours represent fault axis perpendicular to the elongation of the close anomaly (Fig. 3.1.d).

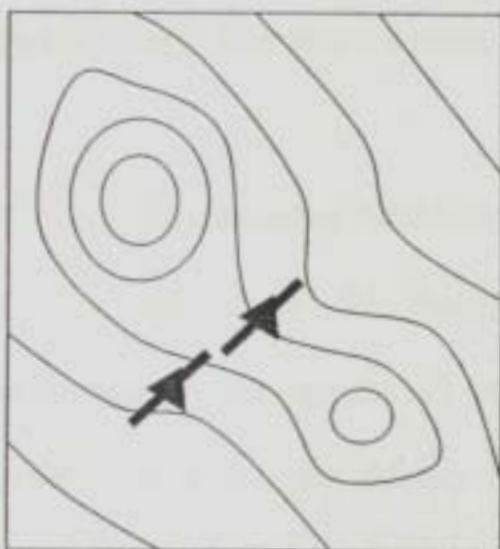
Applying the four principles of gravity detailing mentioned above; the subsurface structural picture of the Al Dhaid area can easily be delineated



a



b



c



d

Fig.3.1. Structural interpretation of detailed gravity effects

a. Gravity gradient;

b. Contour undulations;

c. Change in gravity gradient;

d. Change of gravity amplitude within the closure.

(Fig.3.2). The major structural trends in this area are mostly ENE-WSW to E-W. Besides, the NNW-SSE direction is also present but less dominant compared with the ENE-WSW direction.

3.1.2.2 Quantitative Analysis of Gravity Anomalies

3.1.2.2.1 Fault Displacements

The fault displacements in the study area range from 320 m to 70 m. The NNE-SSW faults have large throw values, while the NNW-SSE faults possess low throw values.

3.1.2.2.2 Thickness of Sedimentary Section

The analysis of the Bouguer anomaly profile (A-B) (Fig. 3.2), according to the system of equations suggested by Grant and West (1965), in which the density contrast between the sediments and the underlying ophiolites $\rho = 0.5 \text{ gm/cm}^3$, has been applied. The calculated shape of the sedimentary - ophiolite contact is depicted in Figure 3.3. On this figure, the depth of the contact reflects a general increase in the thickness of the sedimentary section towards the northwest. Thickness of sediments varies between 700 m at the southeastern end of the profile and

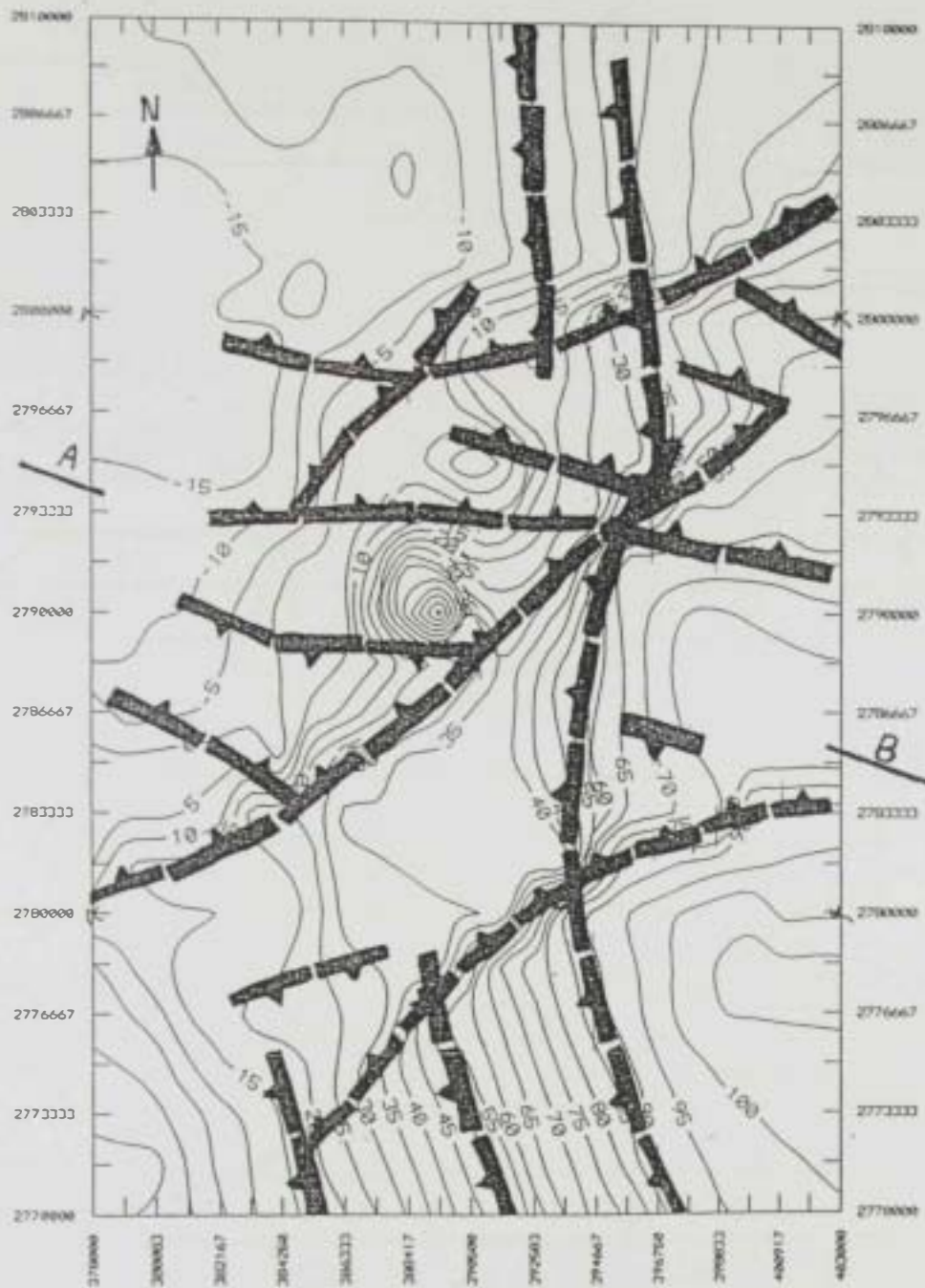


Figure 3.2 Bouguer gravity anomalies deduced from IWACO (1986) data and interpretation of major fault trends affecting the study area.

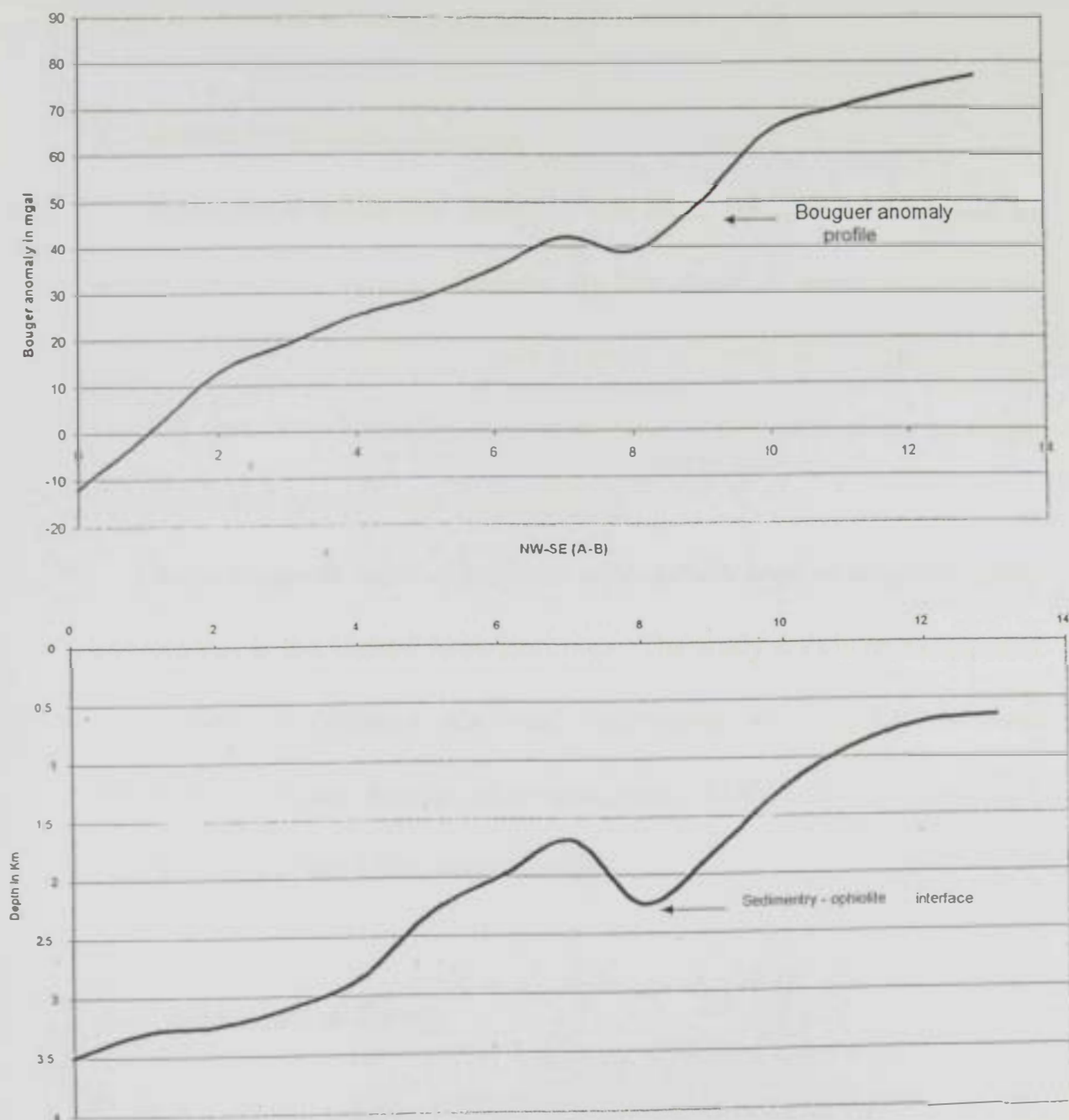


Fig.3.3. Calculated Sedimentary – Ophiolite interface in Al-Dhaid area
 a. Bouguer anomaly profile, and
 b. Calculated depths of the interface.

more than 3500 m at its northwestern end. Also, a number of faults have their throw towards the northwest.

3.2 Geoelectrical Investigations

Geoelectrical resistivity survey is the most common tool applied in groundwater exploration. Besides its low cost, it provides complete information needed for subsurface evaluations, such as layer succession, vertical and lateral changes in lithological facies, subsurface geologic structures and groundwater potentialities.

Electromagnetic method has been successfully applied in groundwater exploration in the United Arab Emirates. The study area is an example of application of different electrical techniques such as DC-electrical resistivity and time domain electromagnetic (TDEM) in two successive episodes (1986 and 1996, respectively).

3.2.1 Geoelectrical Survey

3.2.1.1 Geoelectrical Resistivity Survey

The direct current geoelectrical survey in the study area has been conducted by IWACO (1986), where 143 vertical electrical soundings were carried out. The schlumberger arrangement has been employed in

this survey. In making a resistivity survey with vertical electrical soundings an electric current is introduced into the ground via two outer electrodes in the arrangement and the produced potential difference is measured between two inner electrodes. The current intensity (I), the potential difference (ΔV) and the geometrical factor (K) are used to evaluate the apparent resistivity curve. True resistivities of the different geoelectrical layers are calculated using special templates (Keller and Frisknecht, 1979)

3.2.1.2 Electromagnetic Survey

3.2.1.2.1 Introduction

The electromagnetic methods have the broadest range of applications. Measurements of the rate of decay of the waning eddy currents provide a means of locating anomalously conducting bodies and estimating their conductivity. A form of depth sounding can be made utilizing time domain electromagnetic (TDEM). Only short offsets of transmitter and receiver are necessary and the array therefore crosses minimum geological boundaries such as faults and lithological contacts. By contrast, vertical electrical soundings (VES) are much more affected by near surface conductivity inhomogeneities since long arrays are required.

The transient electromagnetic, or time domain electromagnetic (TDEM) survey conducted over an area includes a steady current to be passed through a loop of wire on the surface of the earth, which is inductively linked to the earth layers. After a discrete period of time (a few tens of milliseconds), during which any effects due to switching the current on would have died away (known as turn on transients), the applied current is interrupted abruptly (Reynolds, 1998). If a conductor is present within the vicinity, the sharp change in the primary field will induce eddy currents within the conductor. The eddy currents migrate from the transmitter loop into the earth and the pattern resembles a downward and outward propagation of the eddy current filament at successive intervals of time (t_2, t_3, \dots, t_n) over a homogeneous ground (Fig.3.4), rather like smoke rings. The rate of change of the magnetic field depends upon the underground resistivity distribution. In low conductive layers, the receiver output voltage, which is proportional to the rate of change of the secondary magnetic field with time, is initially large but decays rapidly. In good conductors, however, the response is initially lower but the voltage decays slowly. The receiver coil can measure the time derivative of the transient magnetic field.

In theory, the depth of investigation is a function of time after the shut off of the primary current rather than loop radius, however, in practice the late stage signal must be sufficiently strong with respect to the electro-

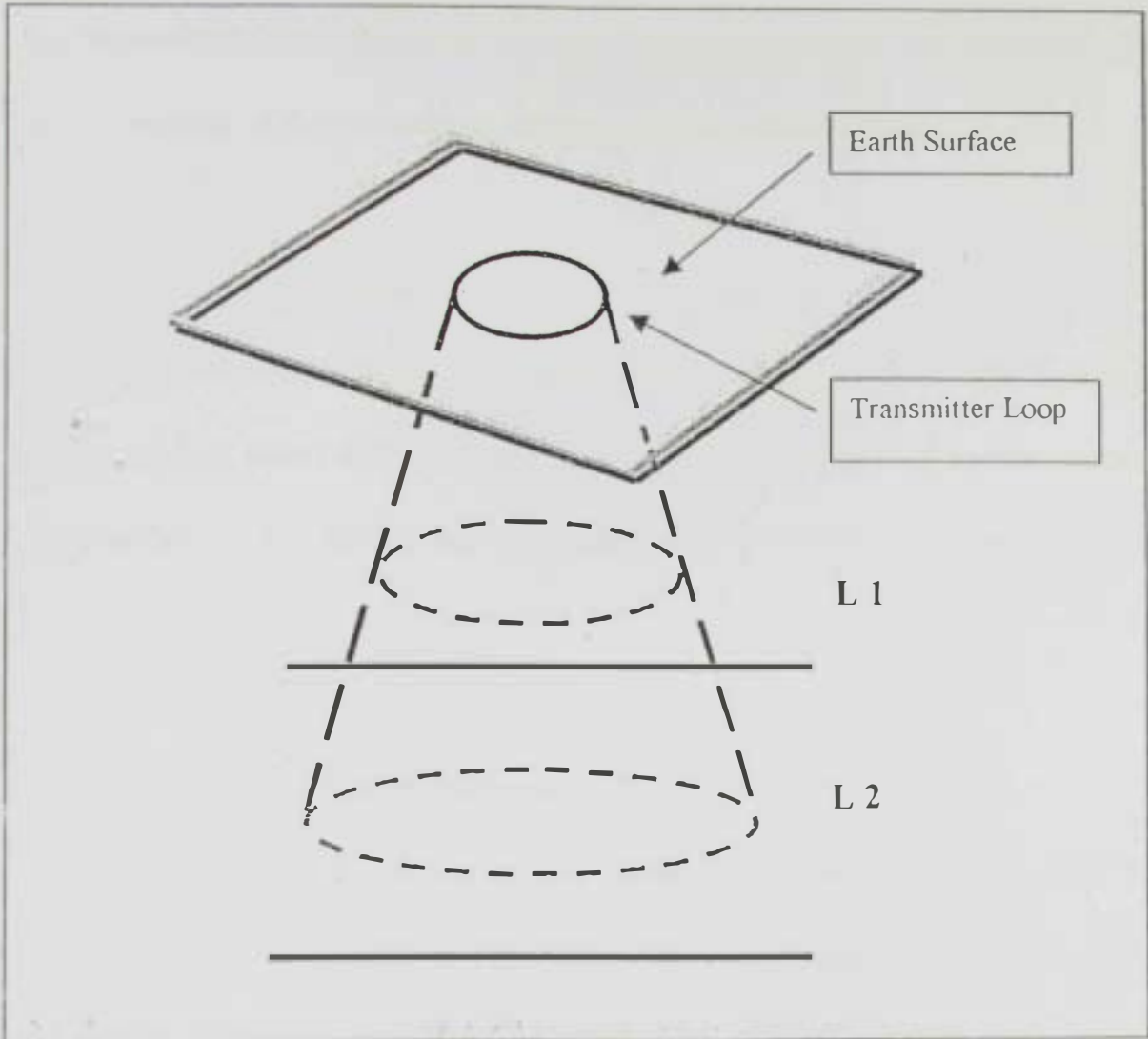


Fig. 3.4. Schematic representation of the propagation of electromagnetic waves.

magnetic field and the instrument noise to be measurable. To increase the late time signal strength and study the resistivity of deep layers, the transmitter moment must be increased. This can be achieved by increasing of the transmitter current, the loop area or both.

3.2.1.2.2 TDEM Survey

A TDEM survey has been conducted in the Al-Dhaid plain, covering an area of about 850 km³. Selection of TDEM measuring device, station positioning and measurement configuration were the main targets of that stage.

3.2.1.2.2.1 The TDEM Instrument

The TDEM survey of the study area was conducted with an instrument manufactured by the Geonics Company (Canada). Two transmitters/receiver (EM 47 and EM 57) of higher and lower frequencies, respectively, were used to acquire resistivity information of shallow and deep layers with the needed accuracy. By combining the measurements made from both transmitters, the shallow and deep earth layers were adequately mapped.

The receiver, a PROTEM 57 (C) unit, samples the coil response at a series of time intervals that are delayed by a prescribed amount from each

turn-off of the loop current. There are 20 geometrically spaced gates on channel positions in each time range.

3.2.1.2.2 Measurement Layout

The initial field trials led to an optimum loop size of 50x50 m to allow a high production rate while maintaining a high signal level and data quality. At each sounding location, a number of measurements were recorded at different gain settings to enhance data from greater depths.

3.2.1.2.3 Stations Positioning

A total of 131 stations were occupied. At each sounding location north and east coordinates were recorded using a Global Positioning System (GPS) navigator. The accurate position was obtained by averaging several hundreds of GPS measurements. The measurements were later corrected by post processing software, using a fixed reference GPS at the base in the Al Dhaid city.

3.2.1.2.3 TDEM Data Processing and Interpretation

3.2.1.2.3.1 TDEM Data Processing

The field data analysis procedure requires prior processing by transient electromagnetic interpretation software using interactive forward and

inverse modelling techniques. In the first step, the delay voltages for each gate were transformed into apparent resistivity values. The apparent resistivities ϑ_a (Ohm.m) are given as a function of time (t) by the following equation:

$$\vartheta_a = (\mu / 4 P t_c) * (2 \mu M / 5 t_c (dB / dt))^{2/3}$$

where

μ is the magnetic permeability ($4\pi \times 10^{-7}$ H/m),

t_c is the gate mean time in seconds,

M is the transmitter moment (Loop area m^2 x current A), and

$(dB / dt) = (V_o * 19200) / (E * 2^n)$ in (nV / m^2).

V_o is the voltages (mV),

E is the receiver moment (m^2),

n is the amplified gain, and

t is the time.

However, an automatic one dimensional inversion technique was used to generate resistivity models composed of up to 8 layers. The models attempt to produce the actual values recorded in the field. As with all geoelectric models, one of the principle assumptions is that the earth can be represented by a series of horizontal layers of constant lateral resistivities and thicknesses. Data points that fall outside of the predicted line demonstrate the departure from this generalisation. The

electromagnetic noise effects were masked as much as possible prior to final processing.

3.2.1.2.3.2 Interpretation of TDEM Data

The TDEM soundings that were acquired and processed by IWACO (1986) have been interpreted in the present work and the results are given in terms of resistivity, thickness, and total dissolved salts distribution in each geoelectric layer.

3.2.1.3 Geoelectrical Interpretation of Resistivity Profiles:

3.2.1.3.1 First Layer

The resistivity contour map of the first layer (Fig. 3.5) indicates that its resistivity increases from the southwestern part of the study area towards north. A zone of high resistivity occupies the northern part and strikes in the NW-SE direction. The high resistivity values in the south are less than 500 Ohm.m, while the resistivity values increase to reach more than 2000 Ohm.m at the northwestern corner of the study area.

3.2.1.3.2 Second Layer

The resistivity contour map of second layer (Fig. 3.6) delineates an increase in resistivity from the south to the north. The lowest resistivity

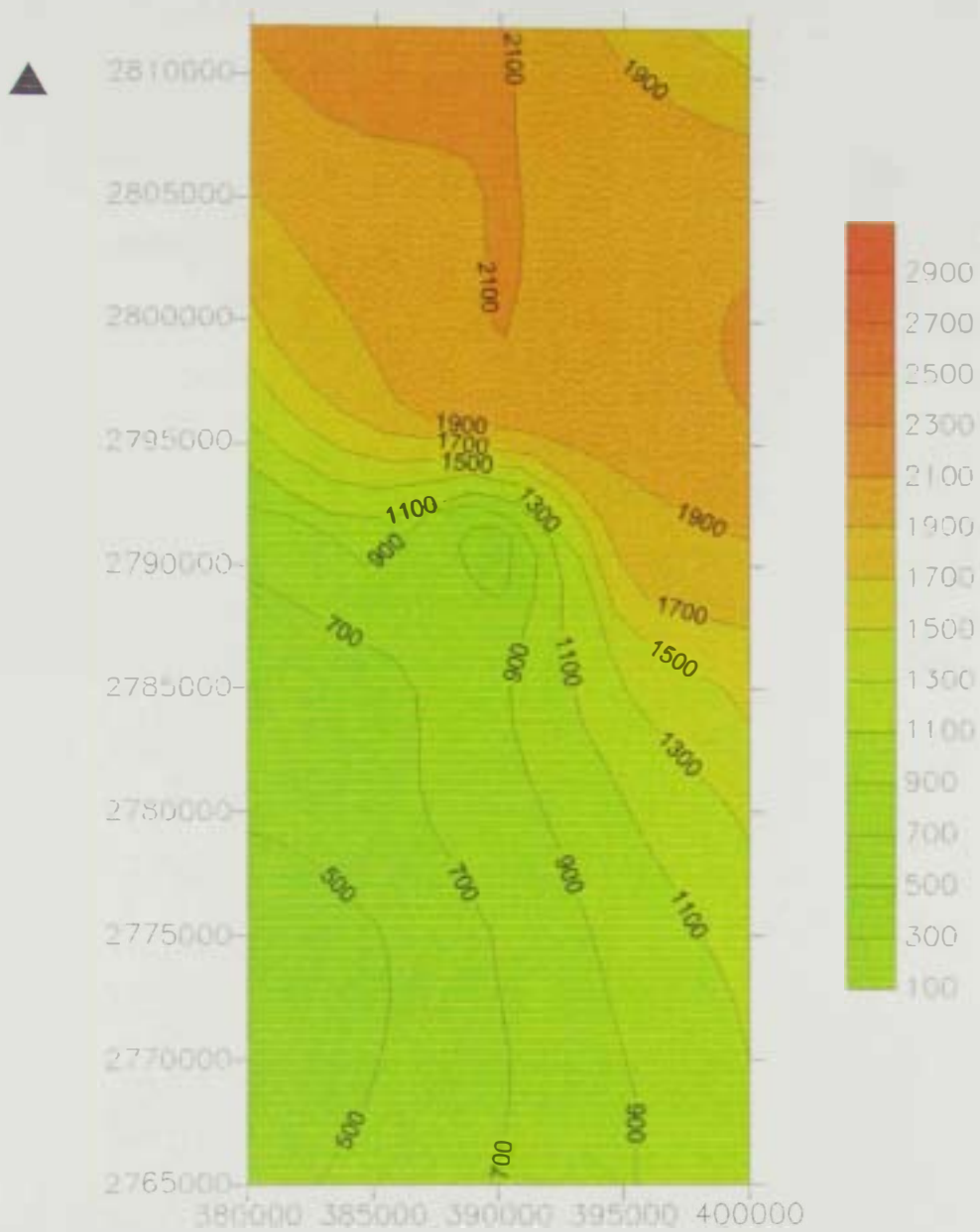


Figure 3.5. Resistivity distribution (Ohm.m) in the first geoelectric layer

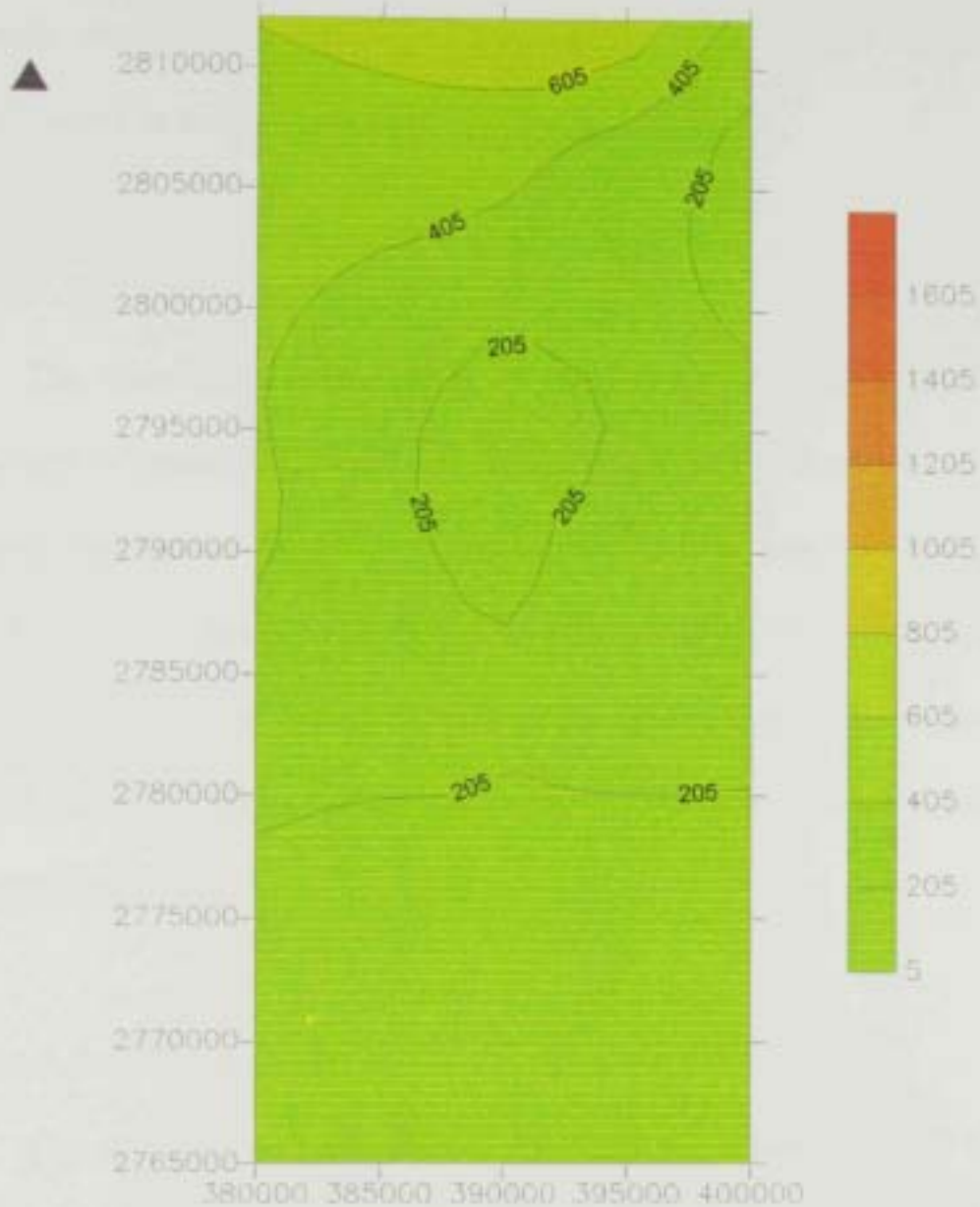


Figure 3.6. Resistivity distribution (Ohm.m) in the second geoelectric layer.

value of about 205 Ohm.m and was found in the southern part of the study area, whereas the highest resistivity value of 605 Ohm.m was calculated in the northern part.

3.2.1.3.3 Third Layer

The resistivity contour map of third layer (Fig. 3.7) delineates a pattern of resistivity increase from the northwestern corner of the study area towards the east. Resistivity values of less than 10 Ohm.m were calculated for this layer at the northwestern corner, while values of more than 1000 Ohm.m were calculated in the central zone. The southwestern part shows a gradual decrease of resistivity, reaching values smaller than 200 Ohm.m.

3.2.1.3.4 Fourth Layer

The resistivity contour map of fourth layer shows (Fig. 3.8) a simple pattern of resistivity increase from the northwestern corner of survey area towards the east and southeast. The high resistivity values at the northwestern corner are very low (<2 Ohm.m), where the values increase to reach about 100 Ohm.m at the northeastern corner and about 80 Ohm.m at the southeastern corner.

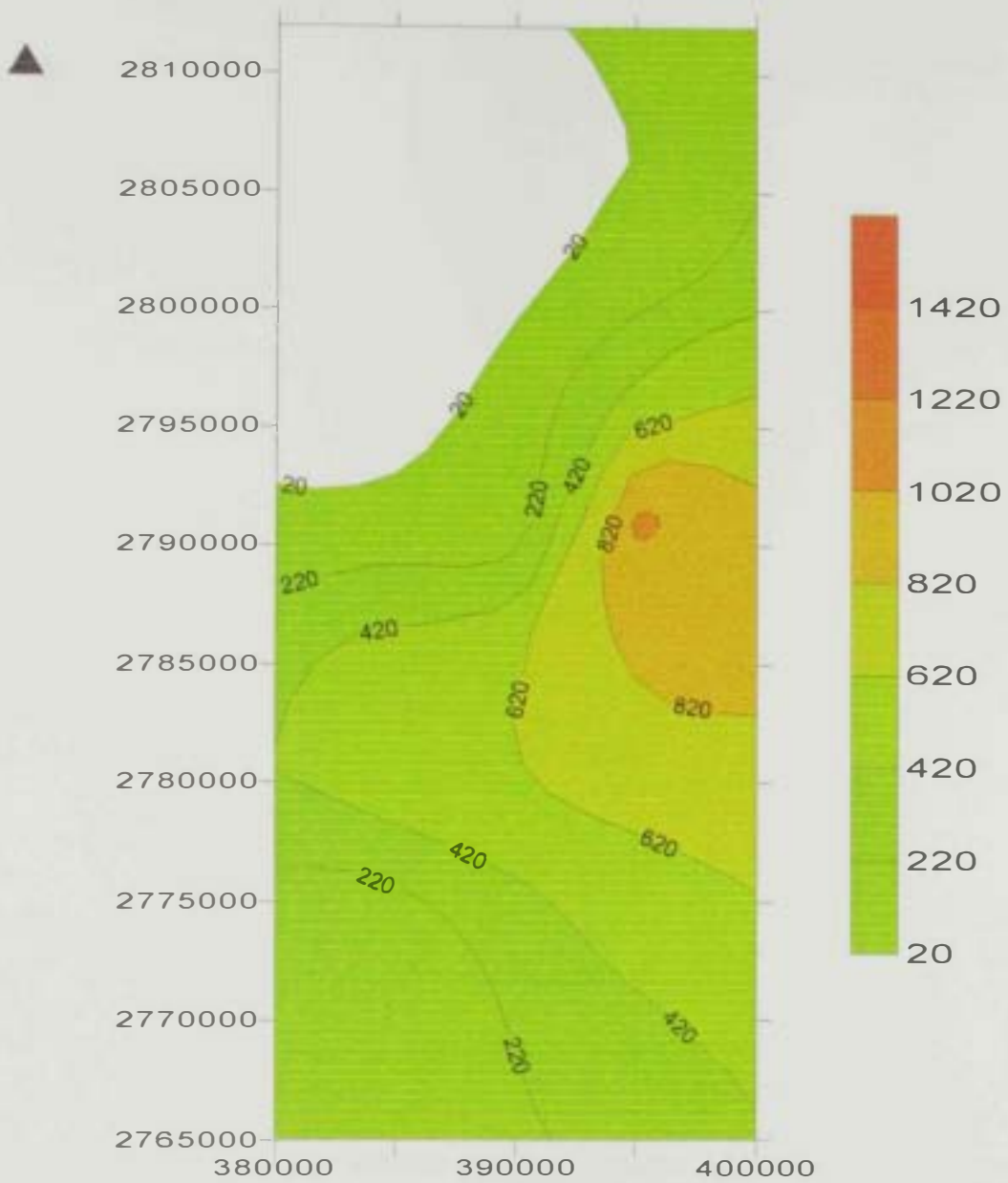


Figure 3.7. Resistivity distribution (Ohm.m) in the third geoelectric layer.

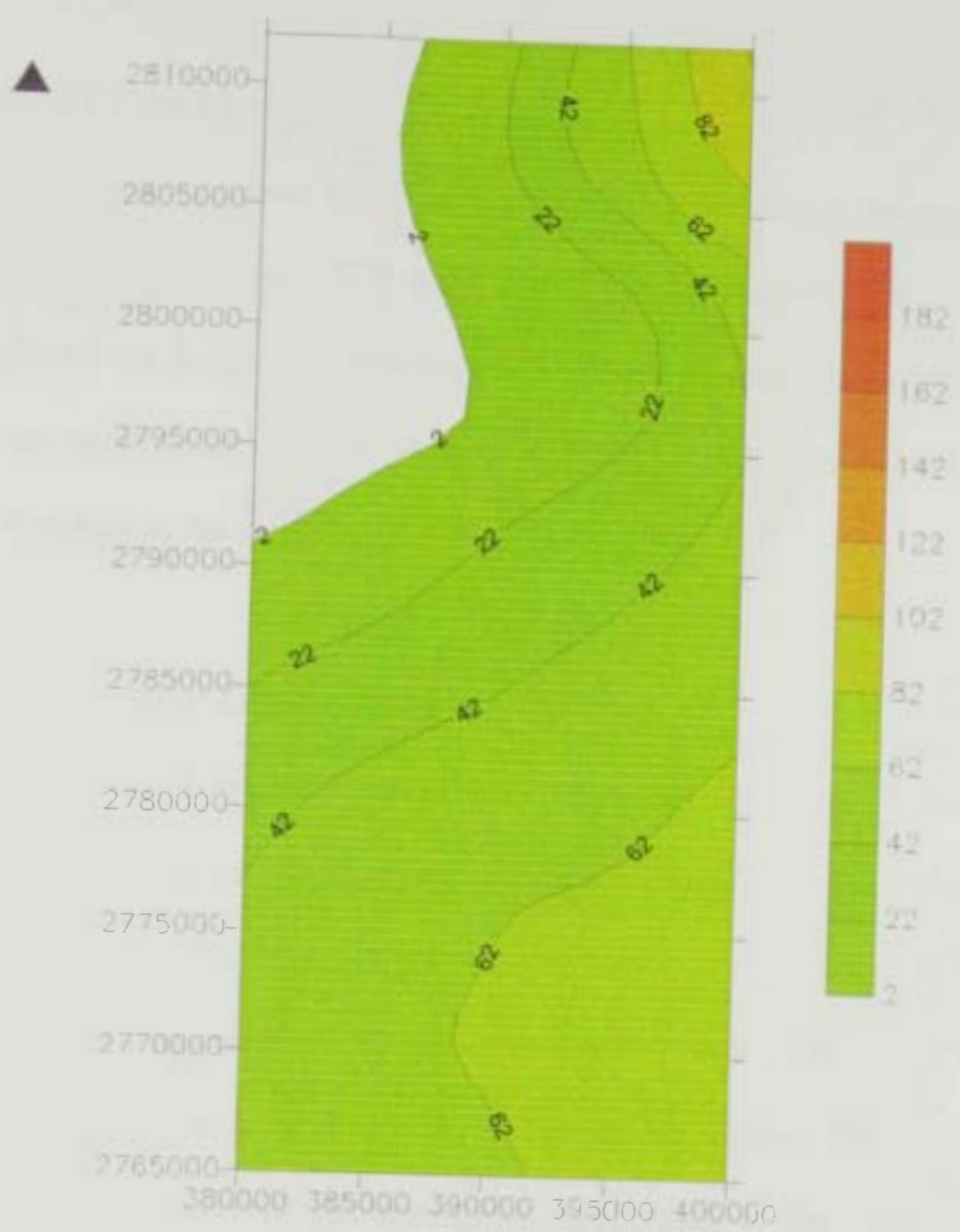


Figure 3.8. Resistivity distribution (Ohm.m) in the fourth geoelectric layer.

3.2.1.4 Total Dissolved Salts (TDS) Distribution Maps

3.2.1.4.1 First Layer

The total dissolved salts (TDS) were calculated from the resistivity values in the first layer. TDS map (Fig. 3.9) illustrates an increase of TDS content from the northeastern corner (less than 10 ppm) of the study area to the southwestern corner (less than 50 ppm) with anomalously high TDS values in the central part.

3.2.1.4.2 Second Layer

The total dissolved salts (TDS) that were calculated from the resistivity values in this layer are depicted in (Fig. 3.10). An increase of TDS content was distinctly noticed from northeastern corner of the layer to the southern corner of it, with anomalously high TDS values in the central part of the layer. The TDS values varied between 200 ppm at the northeastern corner of the layer and >2000 ppm at the southwestern corner of the layer. The TDS values in the central part reached about 1000 ppm.

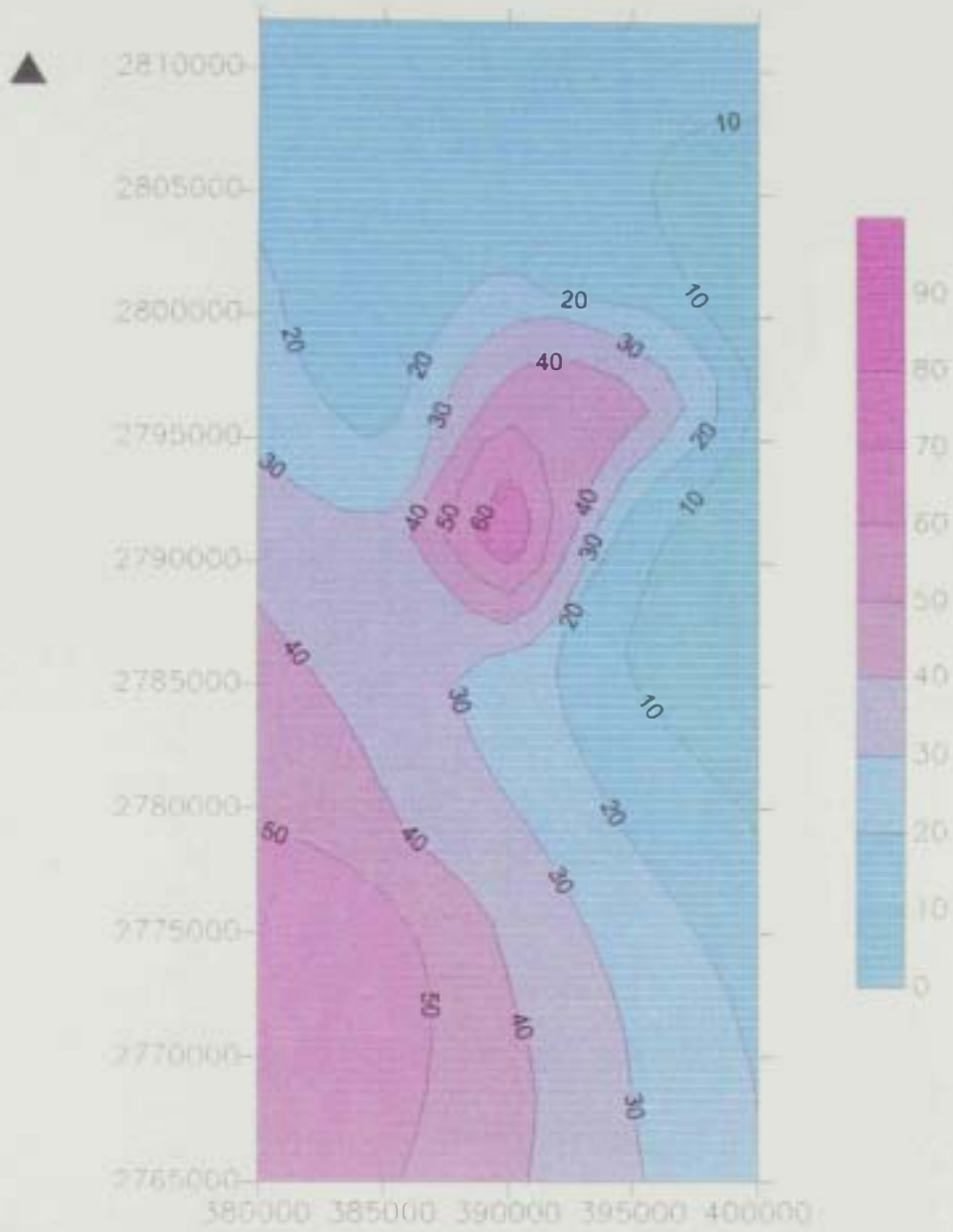


Figure 3.9. Distribution of Total Dissolved Salts (ppm) in the first geoelectric layer.

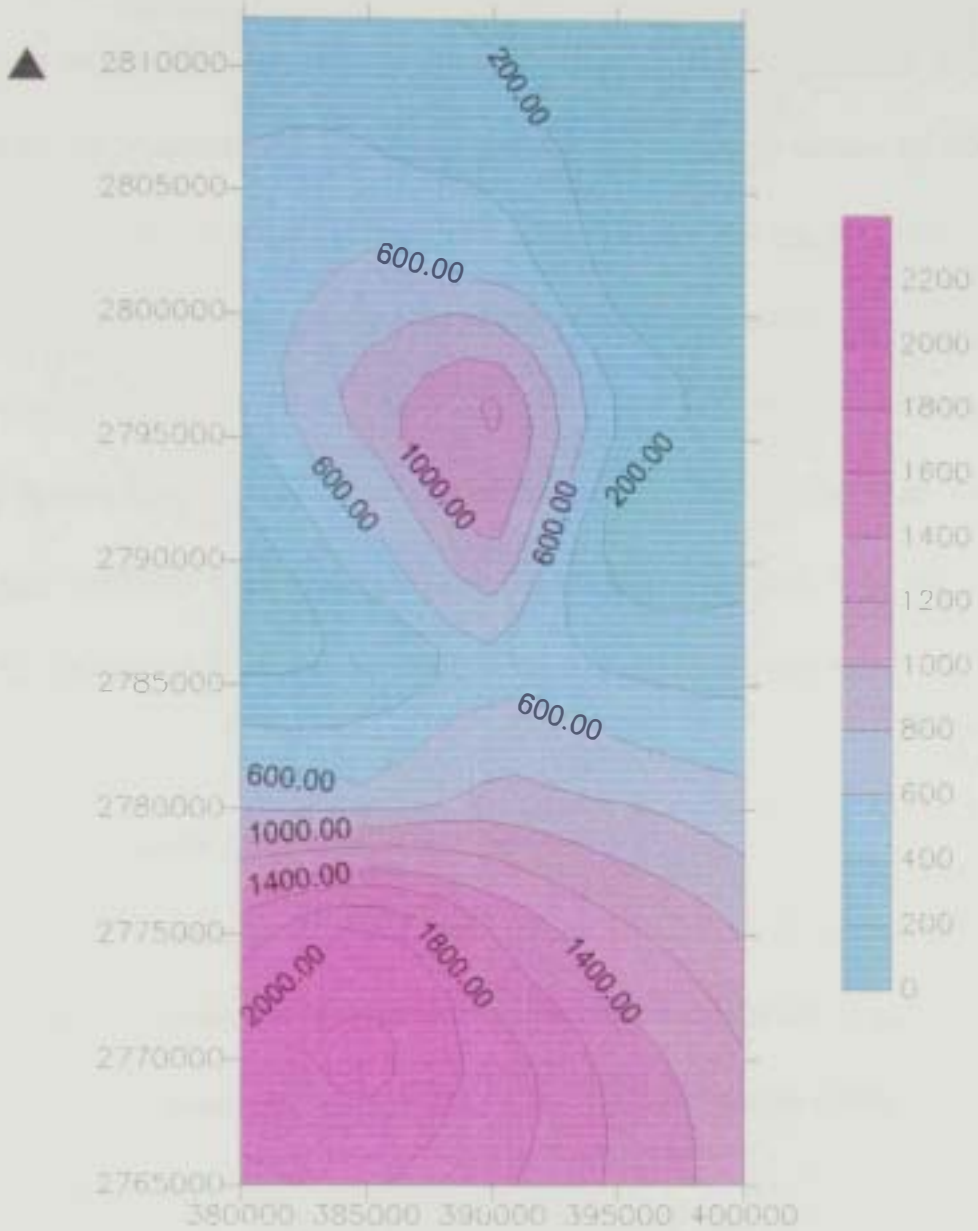


Figure 3.10. Distribution of Total Dissolved Salts (ppm) p in the second geoelectric layer.

3.2.1.4.3 Third Layer

The TDS calculated from the resistivity values in the third layer are shown as a contour map (Fig. 3.11). Generally, the TDS values increased in the northeastern and southwestern direction, where values of 900 ppm were calculated. In the central area, especially at the eastern edge, a nose of smaller resistivity values was observed through the middle part of the survey layer. The lowest values of TDS at the eastern corner were about 100 ppm where it shows a westward increase to reach more than 300 ppm at the western end. This TDS distribution indicates that the aquifer recharge occurs through the eastern border of the survey area.

3.2.1.4.4 Fourth Layer

The TDS values in the fourth layer exhibit a sharp increase from southeastern corner of the layer to northwestern corner (Fig. 3.12). The TDS values varied between < 100 ppm at southeastern corner and >7500 ppm at the northwestern part of the layer.

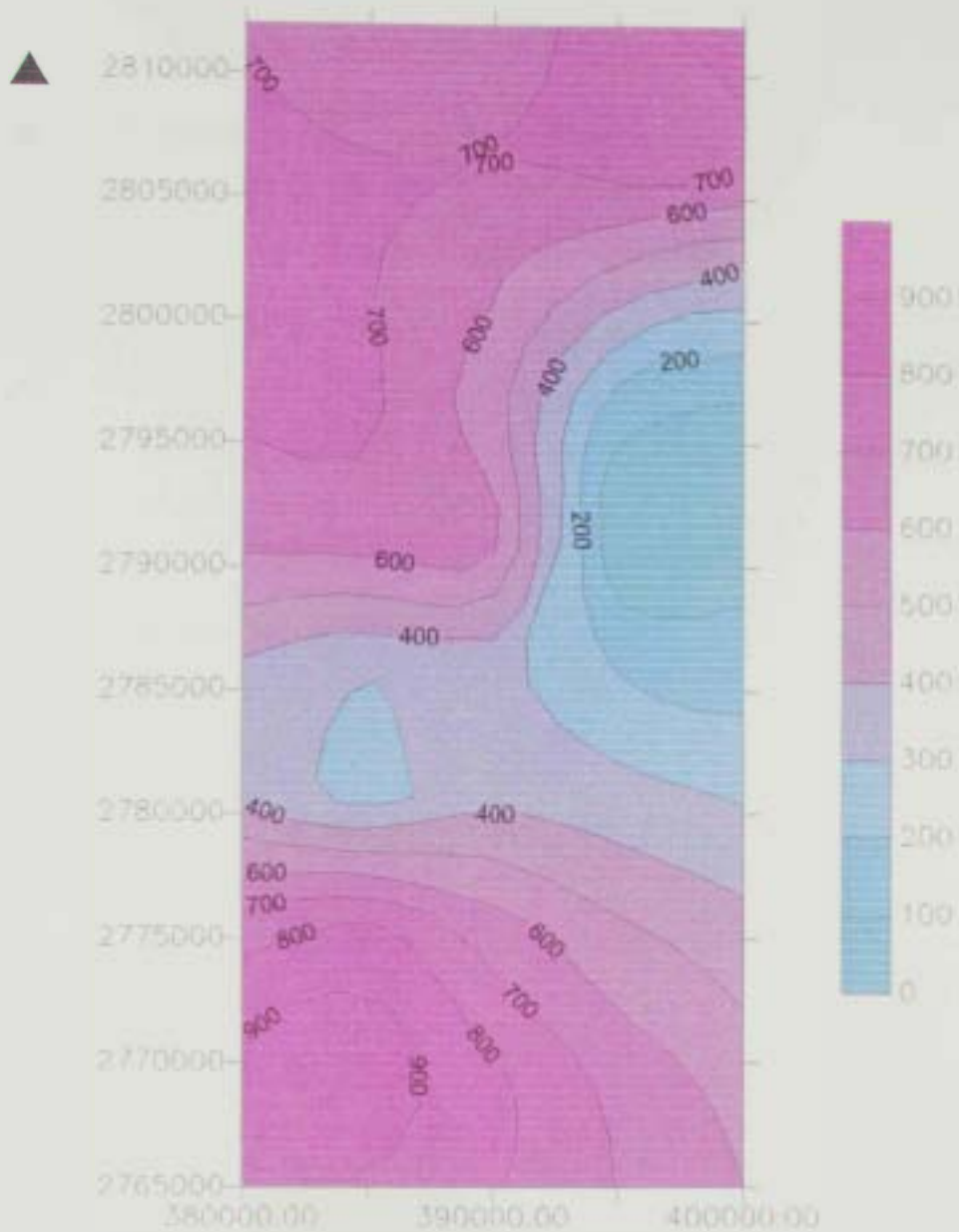


Figure 3.11. Distribution of Total Dissolved Salts (ppm) in the third geoelectric layer.

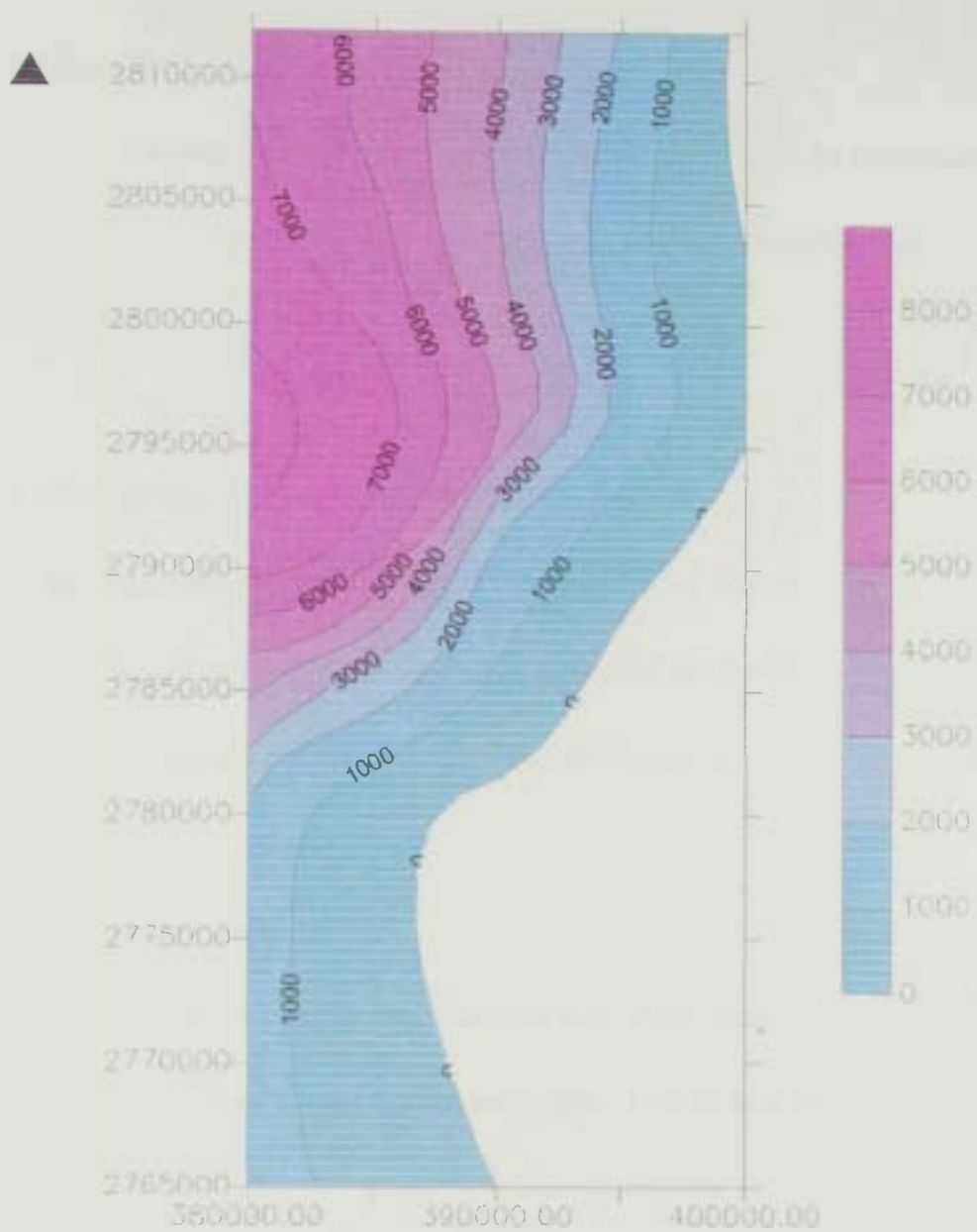


Figure 3.12. Distribution of Total Dissolved Salts (ppm) in the fourth geoelectric layer.

3.2.1.5 Thickness Distribution Maps of the Geoelectrical Layers

3.2.1.5.1 First Layer

The thickness of the first geoelectrical layer (Fig. 3.13) increases from 1.5 m at the northeastern and southeastern corners to more than 5 m at the western part of the layer.

3.2.1.5.2 Second Layer

The thickness of the second geoelectrical layer (Fig. 3.14) varies between less than 5 m at the southern part of the layer to more than 15 m in the central and northern parts of the study area.

3.2.1.5.3 Third Layer

The thickness of the third geoelectrical layer (Fig. 3.15) increases from 28 m at the southeastern part to more than 150 m at its northern part.

3.2.1.5.4 Forth Layer

The thickness of the fourth geoelectrical layer (Fig. 3.16) varies between <80 m at the western part of the layer to about 450 m at the northern corner of the survey area. The thickness distribution suggests that the deposition took place on an uneven surface, where two east-west

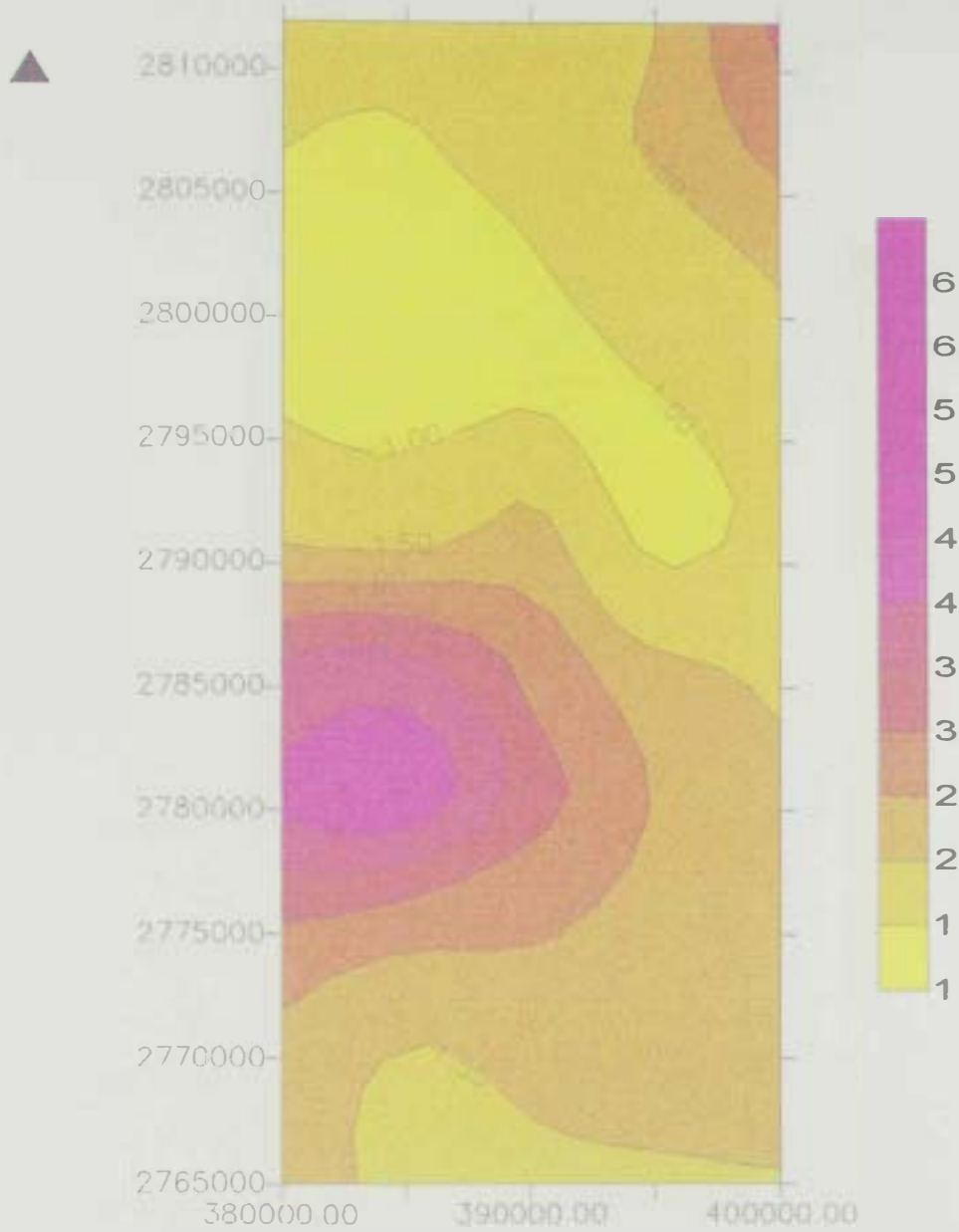


Figure 3.13. Thickness distribution (m) in the first geoelectric layer.

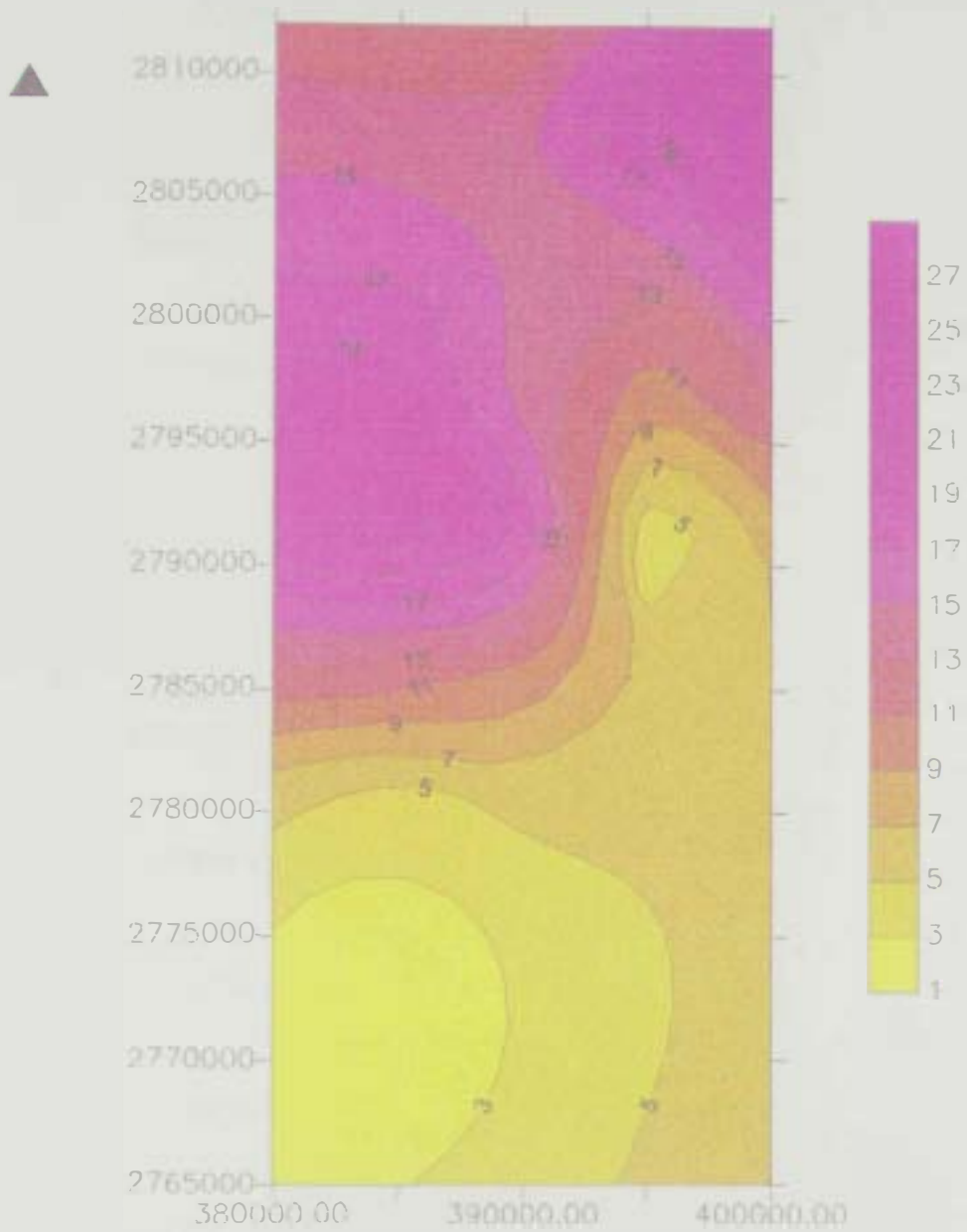


Figure 3.14. Thickness distribution (m) in the second geoelectric layer.

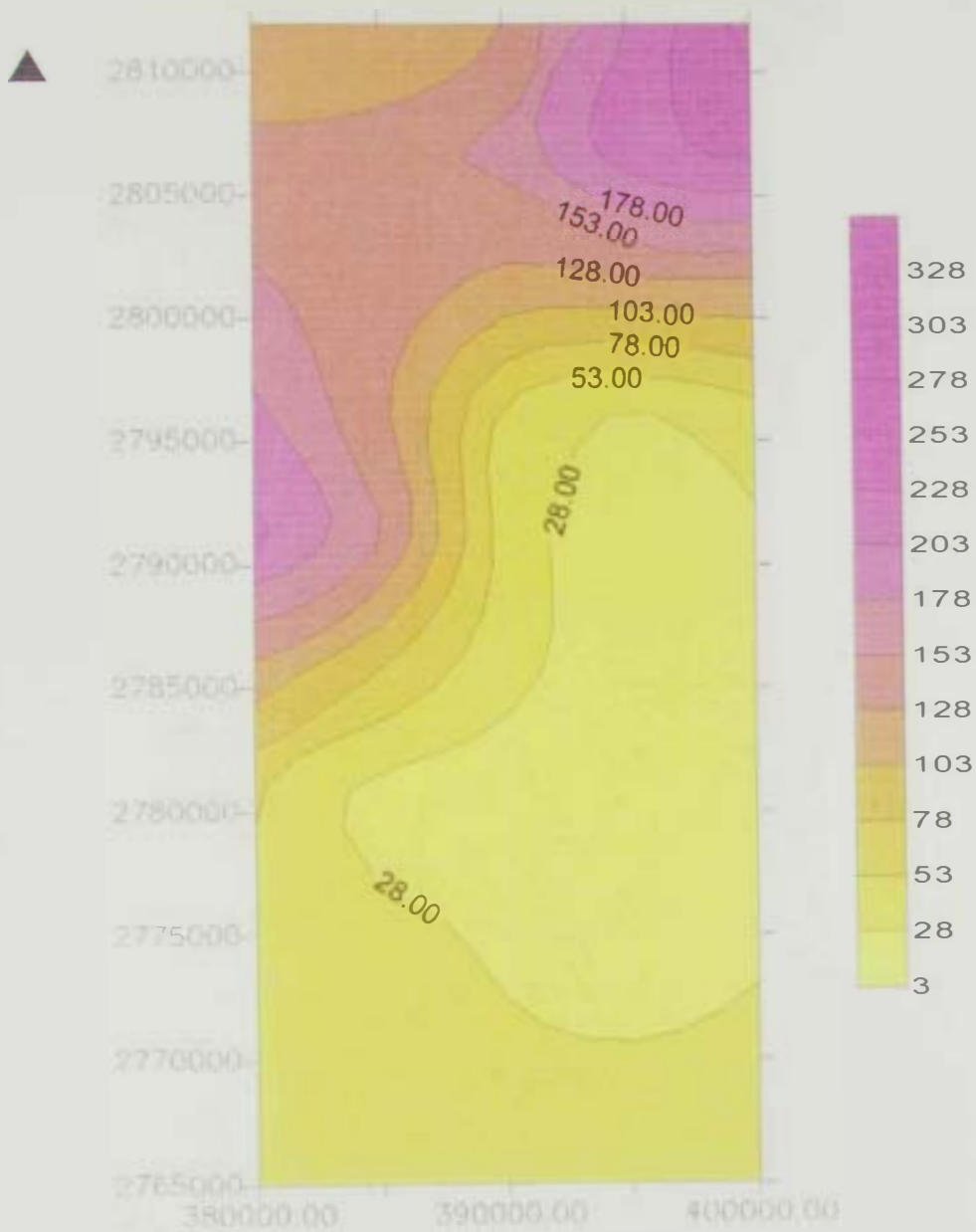


Figure 3.15. Thickness distribution (m) in the third geoelectric layer.

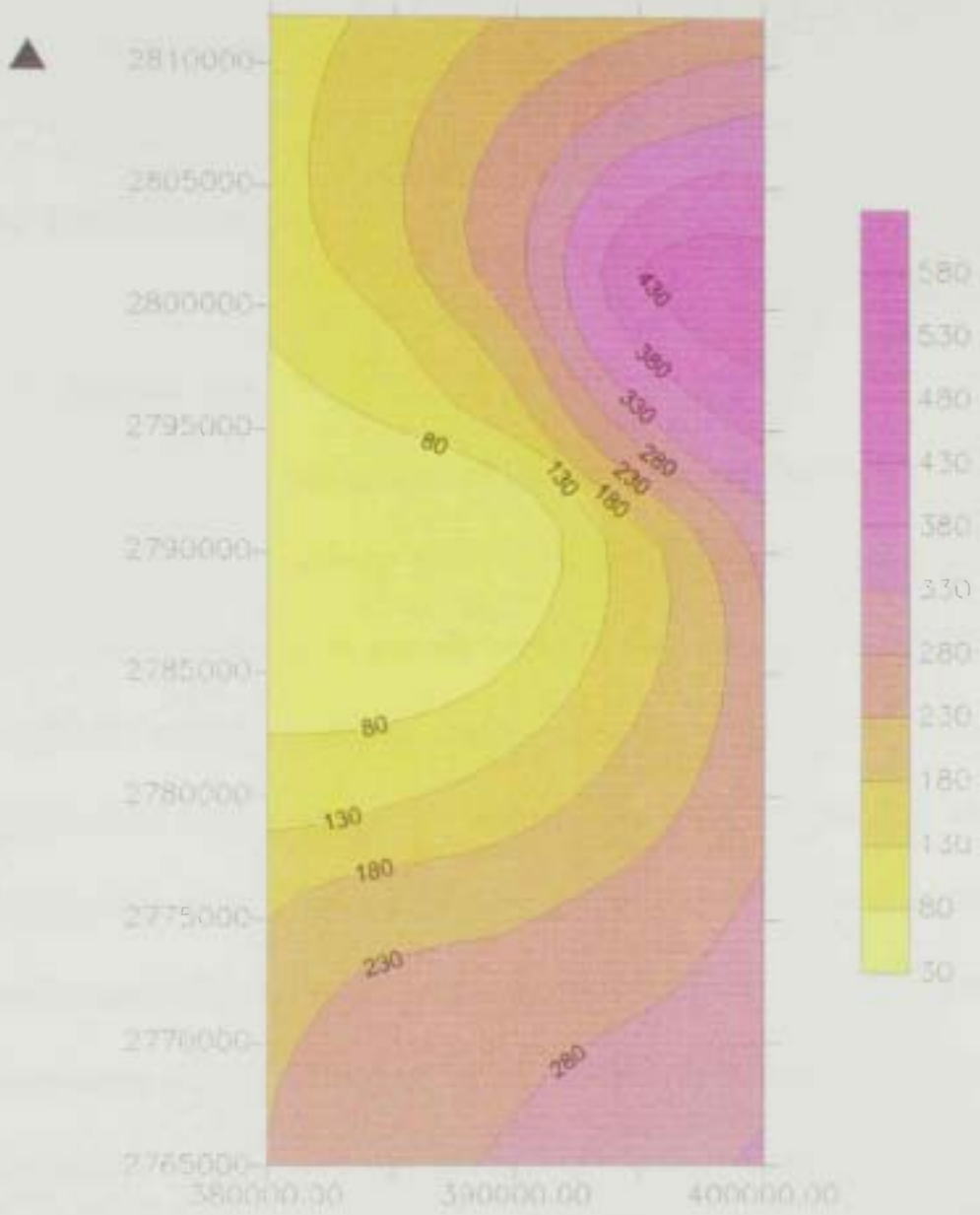


Figure 3.16. Thickness distribution (m) in the fourth geoelectric layer.

grabens separated by a central horst existed in this area. The northern graben was deeper than the southern one and hence the sediments are thicker in the north.

3.3 Borehole Logging

3.3.1 Introduction

The electrical properties of the rocks are essential tools for interpretation of resistivity data as the velocity in the interpretation of seismic data, density in gravity surveys and magnetic susceptibility in magnetic surveys (Keller and FrischKnecht, 1979). Generally, geophysical well logging is conducted to gain information about the sedimentary sequence penetrated by the logged well. The most important applications of well logs is defining rock contacts and providing means of correlating geologic information of different boreholes. The most useful and widely applied geophysical logging techniques are based on electrical resistivity, electromagnetic induction, self-potential, natural and induced radioactivity, sonic velocity and temperature logging. Besides, the well logs are considered a basic source of information about porosity, permeability, water saturation, temperature and conductivity.

The lithology of the penetrated rocks and the rock contacts are normally determined by comparison of well logs. The most useful logs for this purpose are the resistivity, self-potential (SP) and sonic velocity. Caliper log also provides information on the lithologies present in a borehole. Formation porosity, on the other hand, is usually estimated from resistivity, sonic velocity and radioactivity logs. In addition, porosity estimates may be obtained by gamma ray density logging and neutron-gamma-ray logging. The permeability and water saturation percentage are derived from resistivity measurements. Water inflow and/or outflow can be interpreted from temperature logs. The quality of groundwater and its chemical characteristics are obtained from conductivity and hydrochemistry logs.

3.3.2 Geophysical Logs

The geophysical well logs were conducted in several wells during two different phases. The first phase was carried out in (1985) by IWACO where resistivity, caliper and SP logs have been performed. The second phase (JICA 1996) included two boreholes in which caliper, gamma ray, resistivity, neutron, density, sonic, temperature, conductivity and hydro-chemistry logs were made (Figures 3.17 and 3.18).

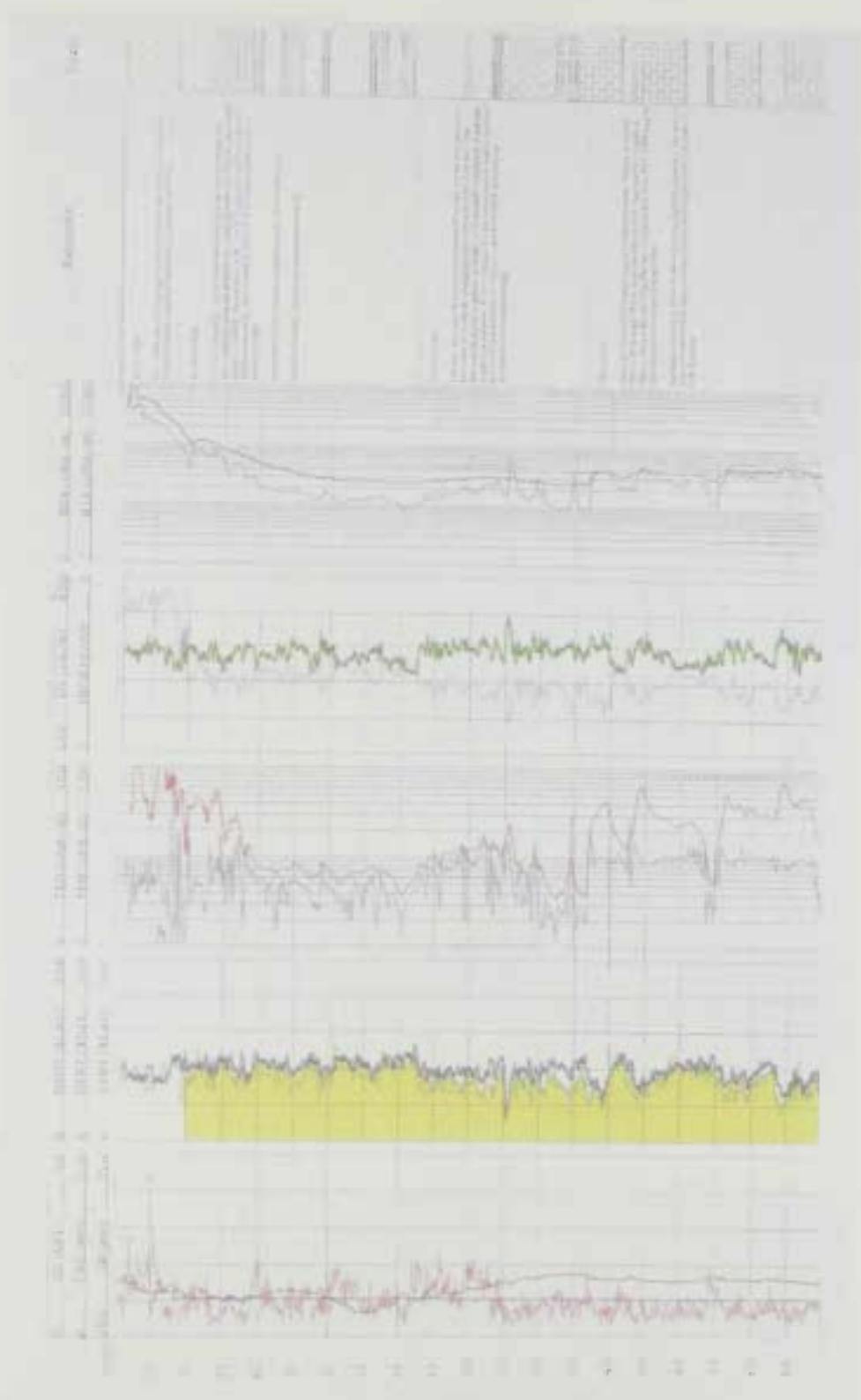


Fig.3.17.a. Well log and lithologic interpretations in well No(1)

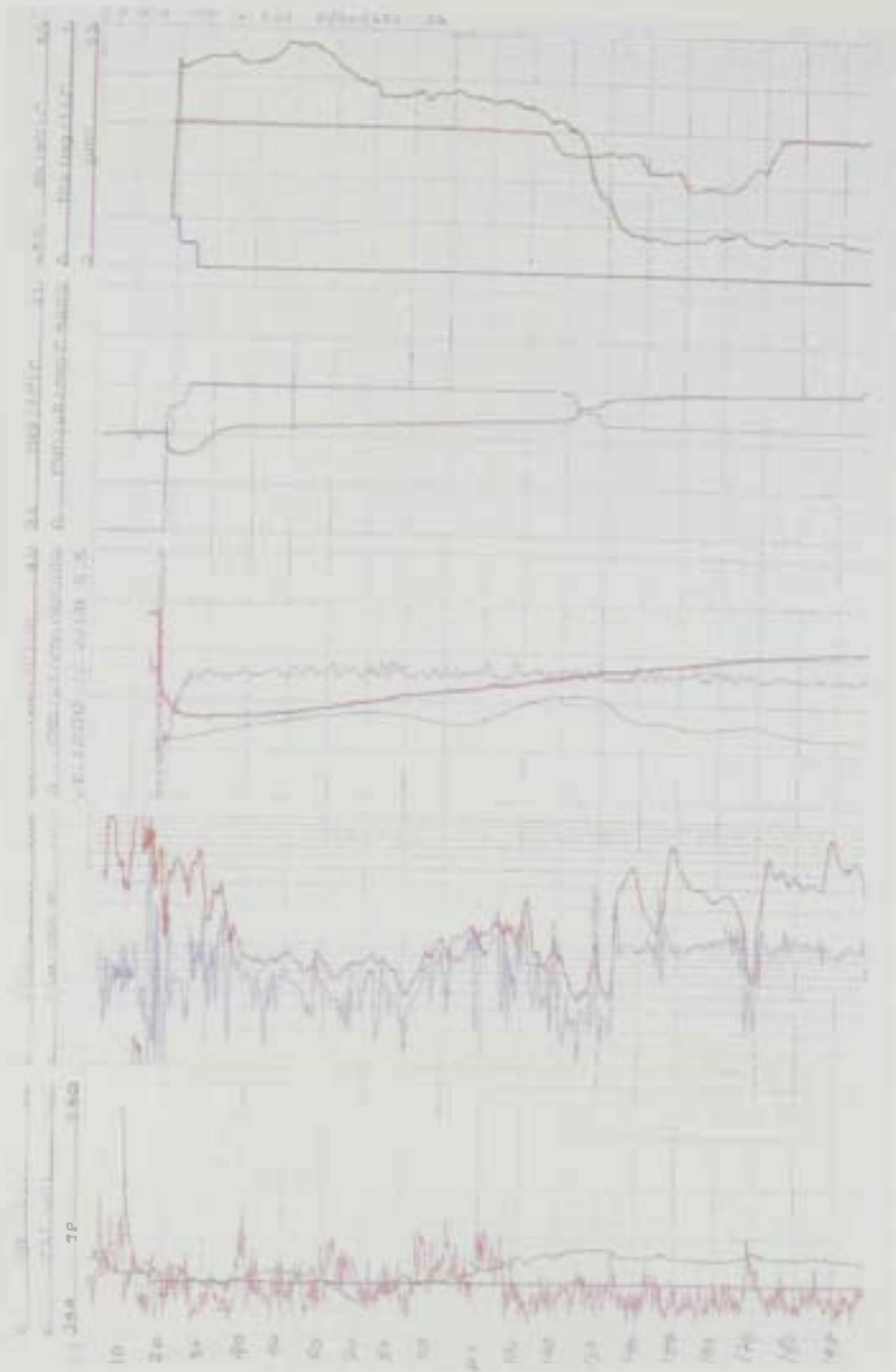


Fig.3.17.b. Fluid characteristic well log in well No.(1)

3.3.3 Interpretation of Well Logs

The geophysical logs can be interpreted in terms of lithology and fluid (Bassiouni, 1994). The following paragraphs include a brief description of the formation lithologies and petrophysical properties such as rock type, thickness, porosity (primary or secondary), fluid characteristics, groundwater quality and hydrodynamic regime in the area.

3.3.3.1 Interpretation of Well Logs In Borehole (1)

3.3.3.1.1 Formation Lithology Characteristics

Sonic log successfully distinguishes primary porosity from secondary porosity. Sonic log has a tendency to measure primary porosity whereas both the density and neutron porosity logs measure total porosity. Subsequently, the difference between the two logs provides a measure of the secondary porosity.

The alluvial gravel sediments were identified from the ground level to 16.5 m deep, which corresponds to formation porosity of 35 % Lst. Gamma peaks mark intervals of >10 m thick clays intercalations within the alluvial gravel. The overall clay content of the alluvial gravels is low.

Clays intercalates dolomitic limestone succession extending between 16.5 m and 84.5 m. Gamma activity remained low and whilst

the formation resistivity ranged from 3.9 ohm.m to 9 ohm.m throughout the interval, the lower density porosity compared to the neutron porosity represents dolomite rather than clay. The average formation porosity recorded is 40% Lst. The primary porosity is indicated in the limestone when sonic porosity records similar value to that of density and neutron porosity.

The depth between 84.5 and 133 m indicated dolomite, where the density porosity was typically some (5% Lst) lower than the neutron porosity. The average formation porosity decreased to (36% Lst) with a corresponding increase in formation density (an average of 2.3 g/cm^3). Thin, hard, low porosity limestone was identified at depth of 110.5 m. Increased gamma values between 84.5 m and 109.5 m correlated well with the formation resistivity (23 ohm-m). The high gamma is unlikely to be associated with clays. A thin-fissured zone was identified by the caliper log at a depth of 124 m. In dolomite beds, sonic porosity was lower than both the density and neutron porosity values, which indicated the presence of secondary porosity. The low formation resistivity values between depths 122 m and 133 m correlated with a large amount of secondary porosity and the highly fractured nature noted in the core.

Carbonates were interpreted at the depth range from 133 m to 200 m where gamma activity decreased to an average of 4 API. The limestone was identified as being dolomitic in places and has variable porosity;

between (20% Lst) and (47% Lst). Gamma peaks and lower formation resistivity identify a number of clay streaks. A slight development of secondary porosity is indicated between depth of 169 m and 190 m.

3.3.3.1.2 Fluid Characteristics

The environment of a well logging is the polymer mud filling borehole and inside casing after well development, in which temperature and conductivity logs were performed.

In the polymer mud filled borehole, a positive fluid temperature gradient was recorded below a depth of 24 m and reached a bottom hole temperature (BHT) of 37.3°C. This feature indicated absence of vertical fluid movement. A number of slight changes in the fluid temperature gradient were noted at a depth of 74 m, between 101 m and 108 m and from 130 m to 139 m which suggests inflow of groundwater into the polymer mud filled open hole at these depths. The fluid conductivity range measured in the open hole varied between 1200 $\mu\text{S}/\text{cm}$ and 2150 $\mu\text{S}/\text{cm}$ and the slight decrease in fluid conductivity close to depth of 74 m and 130 m, respectively, would tend to confirm the inflow of fresher groundwater into the borehole.

The groundwater table was identified by higher sonic transit time above 17m. Also increased formation resistivity above 35 m, where no

significant change in clay content or formation porosity is noted, would suggesting partially saturated formation.

For the majority of the logged section increased formation resistivity correlates to lower porosity, limestone/dolomite horizons and low fluid content in the pores. There was a significant increase in the formation resistivity bellow 133 m, which does not appear to correlate with any significant change in either formation porosity and/or clay content. It was therefore most likely to be related to a more resistive and higher water quality in the formation. However, between 122 m and 133 m, low formation resistivity was recorded within an interval of interpreted secondary porosity and joints/fractures recorded in the core. The low formation resistivity is most likely related to the water filled nature of the joints/fractures. This interval also correlates with interpreted groundwater flow from the fluid temperature, conductivity and hydrochemistry logs.

3.3.3.2 Interpretation of Well Logs In Borehole (2)

3.3.3.2.1 Formation Lithology Characteristics

Alluvial gravels were interpreted from well logging in the interval from the ground surface to 29 m, where a slight increase in gamma activity was noted. Limestone dominated matrix and/or chaotic were

indicated by the overlaying density and neutron porosity logs. Gamma activity reached a maximum of 13 API above 10 m. Formation porosity records ranged from (32% Lst) to (58% Lst).

Limestone with thin interbedded dolomite was interpreted between 29 m and 101 m where gamma activity averages 4 API and for the majority of the logged section the density and neutron porosity logs recorded the same values. The caliper log at depths of 33 m and 39 m identifies thin fissures. The sonic porosity logs indicated the dominance of primary porosity in the carbonate formation, with the exception of a limited development of secondary porosity between 60 m and 219 m deep.

The average formation porosity is 40% Lst. Primary porosity is present in the formation as indicated by the sonic porosity values being similar to that of the density and neutron porosity values. Sandstone horizons were recorded also in the core over this interval. The typical geophysical signature for sandstone was not recorded due to its fine-grained nature.

Below 219 m, the formation becomes increasingly clay rich where gamma activity reaches a maximum of 14 API. The average formation porosity is 32% Lst, decreasing to less than 20 % Lst in places. The caliper log identified highly fissured and non-compacted horizons.

3.3.3.2.2 Fluid Characteristics

In the mud filled borehole, a positive fluid temperature gradient was recorded below 60 m and reached a bottom hole temperature (BHT) of 39.1 °C. This feature indicated absence of vertical fluid movement. From the mud level to 60 m, the fluid temperature decreased slightly with depth, suggesting that the inflow of groundwater from the formation was occurring at the time of logging. Throughout the well logging process the fluid conductivity value (2550 $\mu\text{S}/\text{cm}$) was lower than the mud pit value. The lower fluid conductivity can be explained by either a dilution by groundwater flowing into the borehole or by the dilution from water pumped in from the surface during logging to allow formation logs to be recorded to the surface.

In cased wells, the fluid logs identified three distinct water bodies: a slightly poor quality water from the groundwater level to 230 m deep where the fluid conductivity fluctuates between 1700 $\mu\text{S}/\text{cm}$ and 2000 $\mu\text{S}/\text{cm}$. Inflexions on both the fluid temperature and fluid conductivity logs between 69 m and 71 m and from 113 m to 122 m infer inflow of groundwater.

3.4 Water Salinity Distribution

The distribution of water salinity with depth in borehole (1) is illustrated in (Fig. 3.19). This figure shows a continuous increase of TDS content from <500 mg / l close to the surface to about 780 mg / l at a depth of 65 m. A decrease of water salinity was distinctly noticed starting gradually from a depth of 70 m to 105 m. A minimum water salinity of (693 mg / l) was calculated at a depth of 95 m. The low water salinity in this layer is attributed to the water inflow through the fissure systems caused by geologic structures affecting the area. The depth range from 105 m to 130 m is represented by a gradual increase of water salinity to reach a value of 930 mg / l at a depth of 130 m. The water salinity in the underlying formation gradually decreased to reach its minimum value of 530 mg / l at a depth of 155 m. This also suggested a groundwater inflow in this zone. However, the temperature difference data indicated water inflow at depths of 75 m and 130 m, which confirmed the results of water salinity distribution in the well.

Water Salinity in mg/l

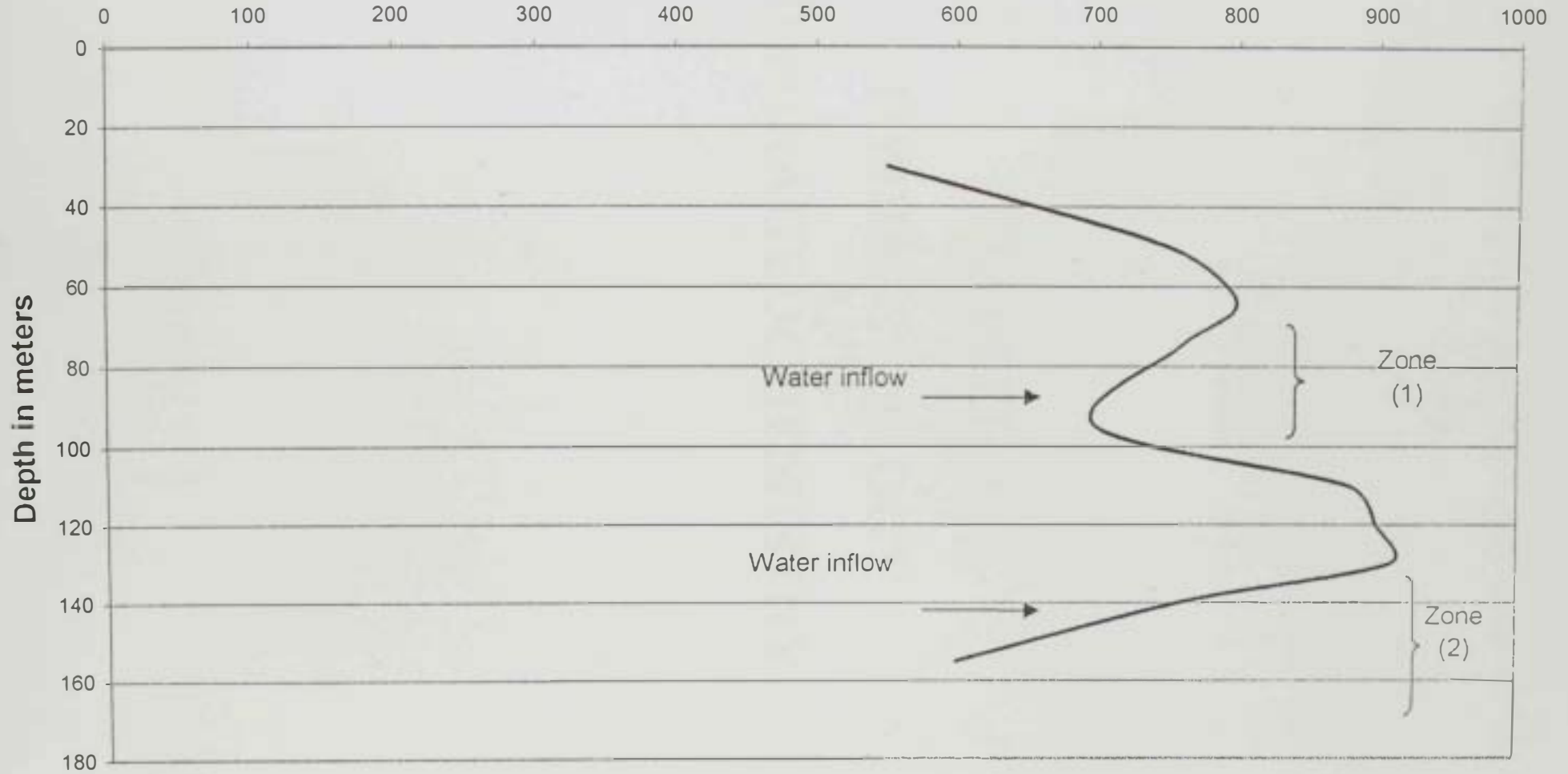


Fig.3.19. Water Salinity distribution versus Depth in Borehole (1)

CHAPTER 4

**HYDROGEOLOGY
AND
HYDRAGEOCHEMISTRY**

CHAPTER 4

HYDROGEOLOGY AND HYDRAGEOCHEMISTRY

The Al Dhaid is one of the most extensively developed agricultural regions in UAE. Therefore, large amounts of groundwater were pumped to meet irrigation demands. As a result, the area has witnessed several groundwater-related problems such as: (1) depletion of shallow and deep aquifer systems, (2) deterioration of groundwater quality and (3) saline-water intrusion. During 1995 and 1996, the Japan International Cooperation Agency (JICA) has conducted a master plan study on the groundwater resources of the Al Dhaid area. As a staff of the Ministry of Agriculture and Fisheries (MAF) in UAE, the student has participated in all fields, lab and modeling activities achieved by JICA on the study area.

Because of the dynamic nature of hydrogeologic systems, it was necessary to follow up the work of the JICA on the Al Dhaid area after 1996, taking into account: (1) the continuous decline in hydraulic heads of shallow and deep aquifers, (2) increasing groundwater salinity, (3) expansion of farming activities and (4) wide use of chemical fertilizers in agriculture.

The objectives of this chapter are to summarize the results of field measurements of hydraulic heads and lab analyses of water-dissolved

ions during the 1996-1999 period. Discussion of these results can provide answers for the questions on aquifer depletion and groundwater-quality deterioration.

To achieve the objectives of this study, the student has measured water levels in observation boreholes at the Al Dhaid area during the period-1996-1999. The results of chemical analysis of water samples collected from about 100 wells in 1995-1996, in addition to 1999 analyses of some of these wells were also used. Figure 4.1 shows the location of observations wells used to measure the hydraulic head at the Al Dhaid area during the period 1996-1999, while the locations of water wells sampled for chemical analyses are illustrated in the hydrogeochemistry section (Fig. 4.13).

4.1 Climatic Conditions

The UAE has a hot desert climate with high temperatures and infrequent, irregular, low rainfall. The summer is long (April-November) and dry, with very high temperatures, and the winter is short (December-March) and has mild to warm temperatures and a slight to moderate rainfall. The summer mean temperature across the country is 35°C in July, while the average monthly rainfall in the same month is 2 mm. January is the coolest month with an average temperature of 18°C, whereas February is the wettest month with an average monthly rainfall

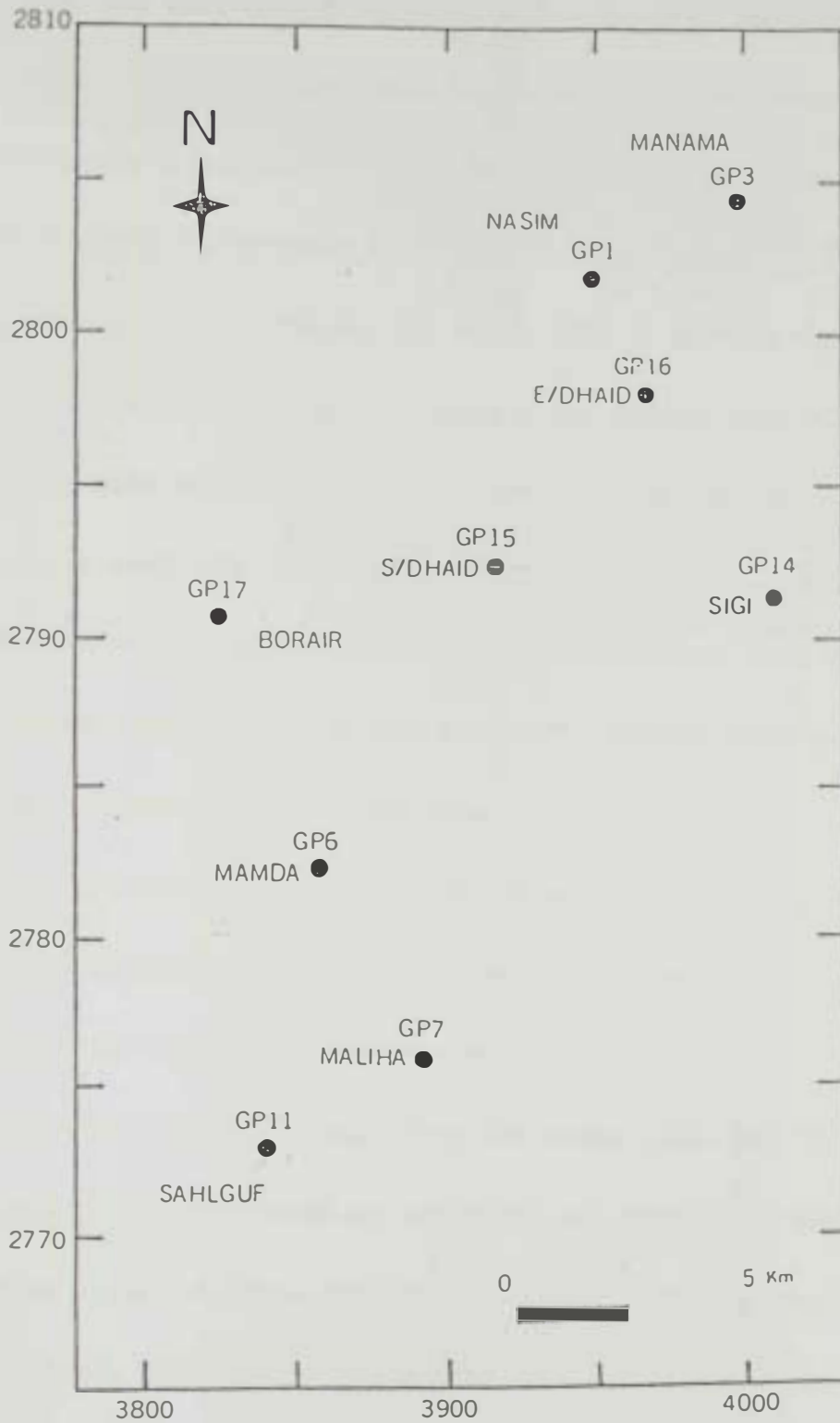


Figure 4.1. Location of the Ministry of Agriculture and Fisheries observation wells in the Al Dhaid area, United Arab Emirates.

of 42 mm. The following discussion on the climate of the study area is based on the analysis of the climatological records of 42 meteorological stations in central and northern UAE, including the Al Dhaid station.

The minimum temperature in UAE does not go below 0°C in winter, but the maximum temperature may reach 50°C in summer during July. The mean annual temperatures are more or less uniform with slight local variations, most noticeably in the mountains to the east. High altitudes result in a relatively low mean temperature of 27°C. The coolest temperatures occur in Ras Al Khaimah, north of the study area, where the winter mean minimum can be less than 10°C. Interior areas experience the biggest diurnal range in temperature.

The mean maximum sunshine hours appear in May, with 11.5 hours and a mean minimum of 8.4 hours occurring in December. The skies are relatively cloud-free throughout the year.

The relative humidity is high along the eastern plain and the Arabian Gulf coast and decrease south and eastwards and over the Northern Oman Mountains in the east. The mean annual relative humidity exceeds 60% in the east coast, decreasing to less than 45% in Al Ain. The diurnal variation in relative humidity is extremely high and ranges from 100% in early morning to 2% in late afternoon.

The winds tend to be light or light-to-moderate and the mean annual wind speed is less than 10 knots. There is a tendency for winds to be stronger between March and August. The predominant wind directions are from the northwest and south or southeast. The strongest winds are felt along the Gulf of Oman, followed by mountain region, the Arabian Gulf coast, and desert foreland, including the study area. Lighter winds affect the internal parts of UAE.

The average annual rainfall in UAE is 119 mm, which is highly variable from a year to another. For example, for the year 1982, the annual mean rainfall was 282 mm while in the mountain region the rainfall was over 450 mm in some parts. On the other hand, the year 1984 had an annual mean rainfall of only 24 mm and recorded a level of only 1.6 mm in Abu Dhabi (Al Shamesi, 1993). Rainfall distribution is lowest in the west and south of UAE, increasing towards the north and east over the gravel plains and foothills of the Northern Oman Mountains. The highest annual rain, regardless of whether it is a wet or a dry year, falls over the Northern Oman Mountains where the annual rainfall rises to 160 mm compared to less than 40 mm in Liwa. Almost 90% of annual rainfall occur during the winter and spring and the wettest months are usually February and March where 60% of the rainfall is recorded. Summer witnesses only a few monsoon rain events.

The evaporation rates exceed rainfall all over UAE. For example, in Al Ain evaporation rates peak in July at over 13 mm per day, falling to around 4 mm per day in December and January. Mean annual evaporation is 3322 mm against a mean annual rainfall of 119 mm (Garamoon, 1996).

4.2 Hydrogeology

The core samples obtained from eight test wells drilled to 200 and 300 m deep confirmed the results of 130 transient electromagnetic soundings (TEM) and indicated the presence of three hydrogeologic units in the Al Dhaid area. Figure 4.1 shows the locations of the MAF observation wells used in this study area. The student used the lithologic logs of these wells, in addition to new information obtained from JICA's (1996) study, to investigate the hydrogeologic conditions of the study area.

4.2.1 Hydrogeologic Units

Three hydrogeologic units identified in the Al Dhaid area include an upper aquifer, an aquiclude and a lower aquifer. The following is a brief description of these units:

4.2.1.1 The upper aquifer

The upper part of this aquifer is composed of Holocene semi-consolidated, well-graded silt to gravel particles with a maximum

thickness of 50 m and an average thickness of 20 m. The lower part is made up of Pleistocene-Neogene alternating consolidated gravel, sand and calcareous layer with a maximum thickness of 200 m and an average thickness of 80 m. The Holocene sediments has an average resistivity of 100 ohm-m, while the Pleistocene-Neogene layer has an average resistivity of 50 ohm-m. Figure 4.2 shows that the aquifer thickness varies between 60 m at the foothills of the Northern Oman Mountains and 160 m east of GP-15 and south of GP-16 (Figure 4.1) in a trough of a NW-SE direction. This trough possibly coincides with Wadi Ham structural trend. The aquifer thickness decreases to the west (70 m in GP-6 and GP-11), north (80 m in GWR-2) and south (70 m in GP-7).

4.2.1.2 The aquiclude

The Paleogene sediments, consisting of an impervious layer of shale, marl, claystone and dolomite, act as an aquiclude for the lower aquifer. This layer has an average thickness of 50 m and an average resistivity of <10 ohm-m. The aquiclude has a low hydraulic conductivity of 10^{-5} to 10^{-7} cm/sec (JICA, 1996). The maximum thickness of this layer is 300 m north of Flaj Al Mualla, whereas the minimum thickness (50 m) is encountered along a NW-SE direction passing by the observation wells GP-15 and GWR-4 (Figure 4.3). This direction coincides with the Wadi Ham structural trend.

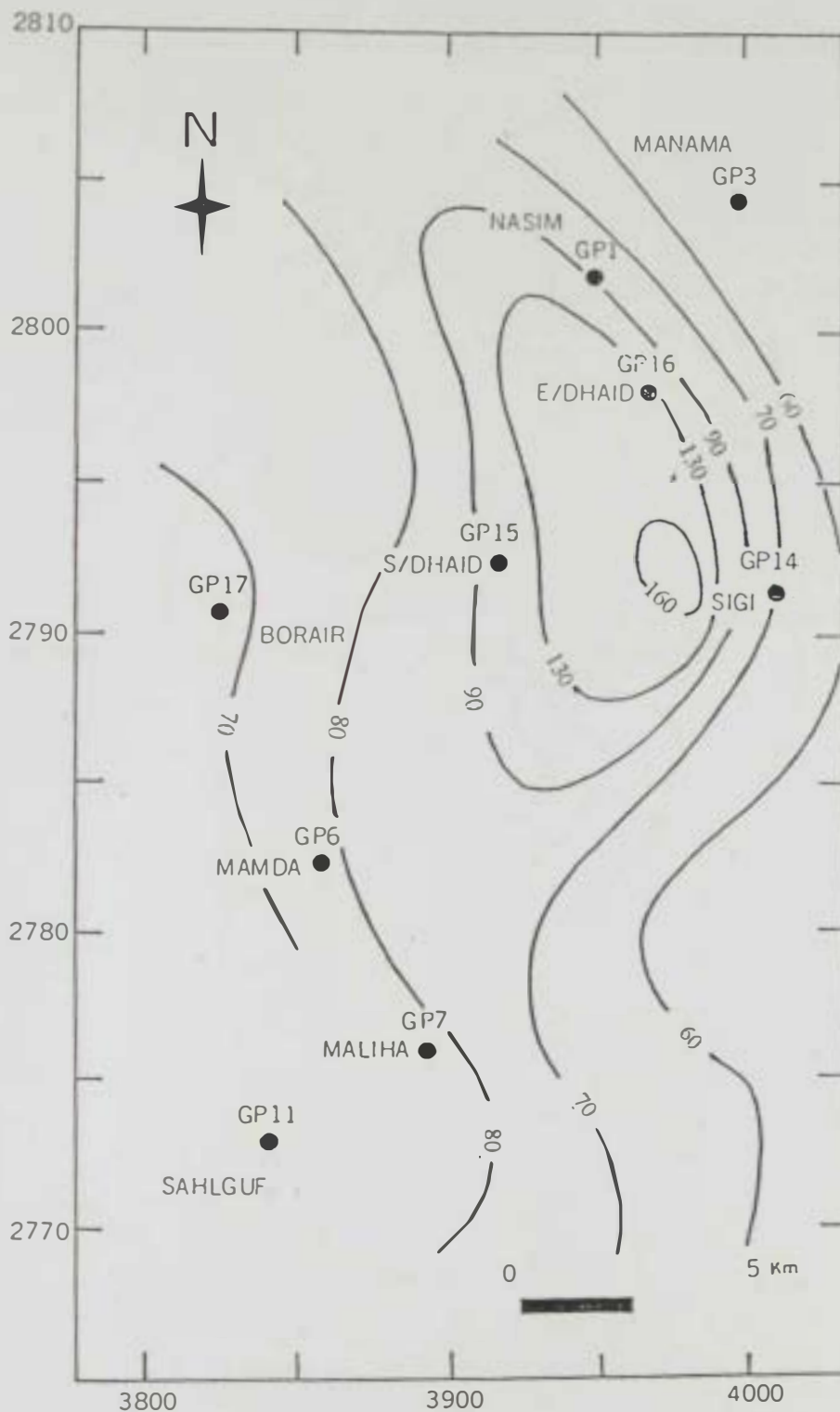


Figure 4.2 Isopach map of the upper aquifer (the Holocene-Pleistocene aquifer) in the Al Dhaid area, in meters above mean sea level (Based on data from the MAF and JICA, 1996).

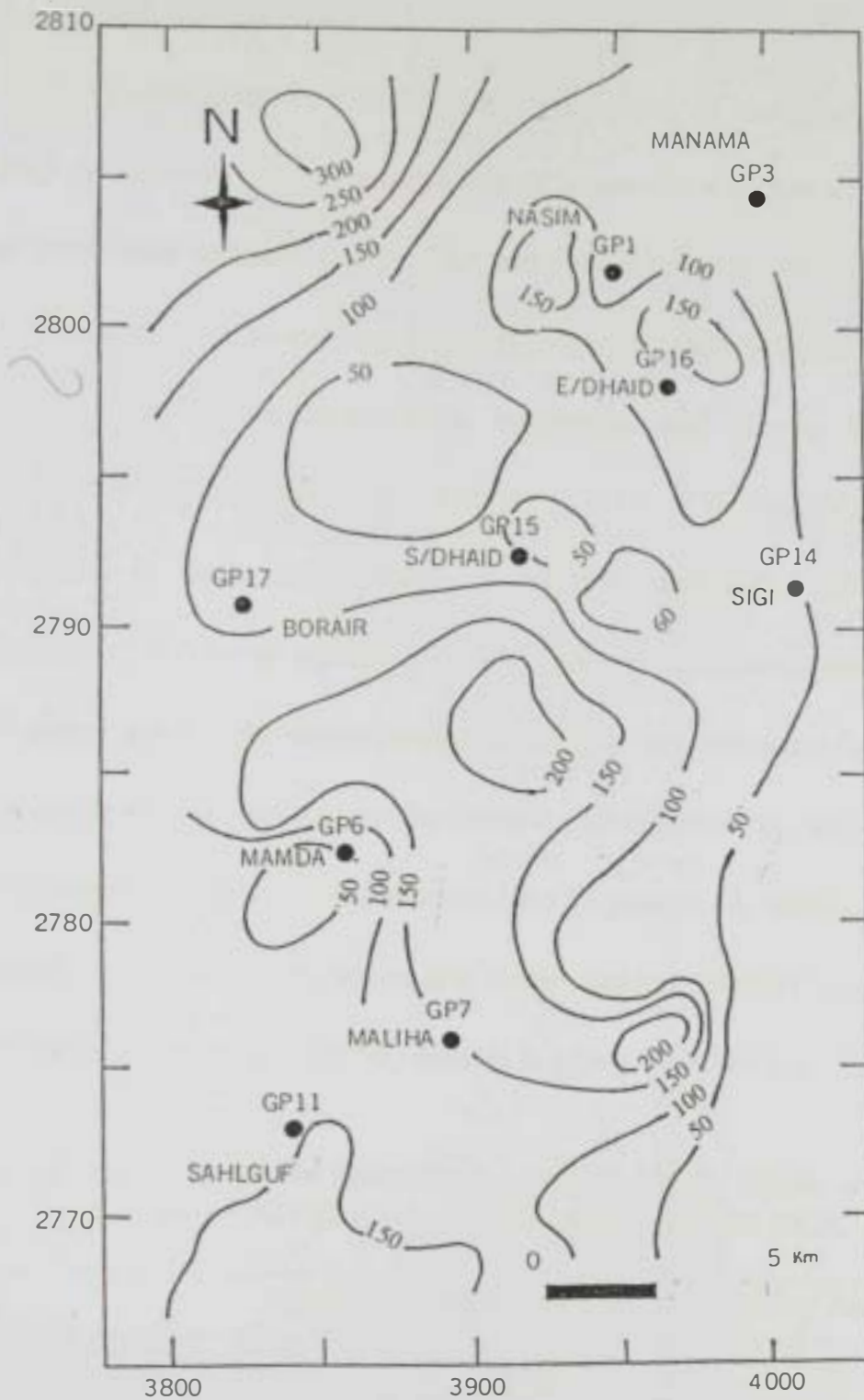


Figure 4.3 Isopach map of the Paleocene aquiclude in the Al Dhaid area, in meters (Based on data from the MAF and JICA, 1996).

4.2.1.3 The lower aquifer

The Maastrichtian to Cenomanian formations in the study area are poorly productive with the exceptions of intersection points of the major structural lines and fault zones. The natural gamma ray survey indicated the presence of 50 anomalies, possibly coincide with vertical structures affecting this aquifer. Equivalent carbonate and clastic facies has appropriate property for a productive aquifer. This aquifer is more productive in three zones along a NE-SW direction. The average resistivity of the lower aquifer is 20 ohm-m. The conglomerate layers of well-sorted gravel interbedded among limestone and dolomite facies form the most productive section in the lower aquifer. However, the thickness of this layer does not exceed several tens of meters. A summary of the hydraulic properties of the upper and lower aquifers within the study area as extracted from JICA's (1996) reports is given in Table 4.1.

Table 4.1 A summary of hydraulic properties of the upper and lower aquifers in the Al Dhaid area, UAE (compiled from JICA, 1996).

Aquifer	Upper Aquifer	Lower Aquifer
Hydraulic property		
Average thickness (m)	100	175
Average resistivity (ohm-m)	75	20
Transmissivity (m^2/day)	85	51
Storage coefficient	0.004	0.0028
Specific capacity ($m^3/hr/m$)	3	2
Porosity (%)	40	30
Static water level (m-amsl)	19	23

Both the IWACO (1986) and JICA (1996) studies indicated the presence of a fissured aquifer in the Al Dhaid area. Despite the high transmissivity ($776 \text{ m}^2/\text{day}$) and storativity (0.24) of this aquifer, little is known about its distribution, thickness and mode of recharge. The natural gamma ray survey conducted by the Japanese company JICA indicated the presence of 50 anomalies, possibly coincide with vertical structures affecting the fissured aquifer. The hydrogeologic condition of this aquifer needs further investigations in the future.

4.2.2 Hydraulic Heads

The depth to groundwater at the Al Dhaid area ranges from 40 to 100 meters below the ground surface. Several water wells in the area are now abandoned because they went dry as a result of heavy groundwater pumping during the last three decades. The hydraulic head maps of the upper and lower aquifers for the years 1984 and 1999 (Figures 4.4, 4.5 and 4.6) show the following features:

1. The hydraulic head decreases from 230 m at Well GP-14 in east to 95 m at Well GP-17 in the west, indicating that the regional groundwater flow directions are from the east (the Northern Oman Mountains in UAE) towards the west and northwest (the Arabian Gulf).

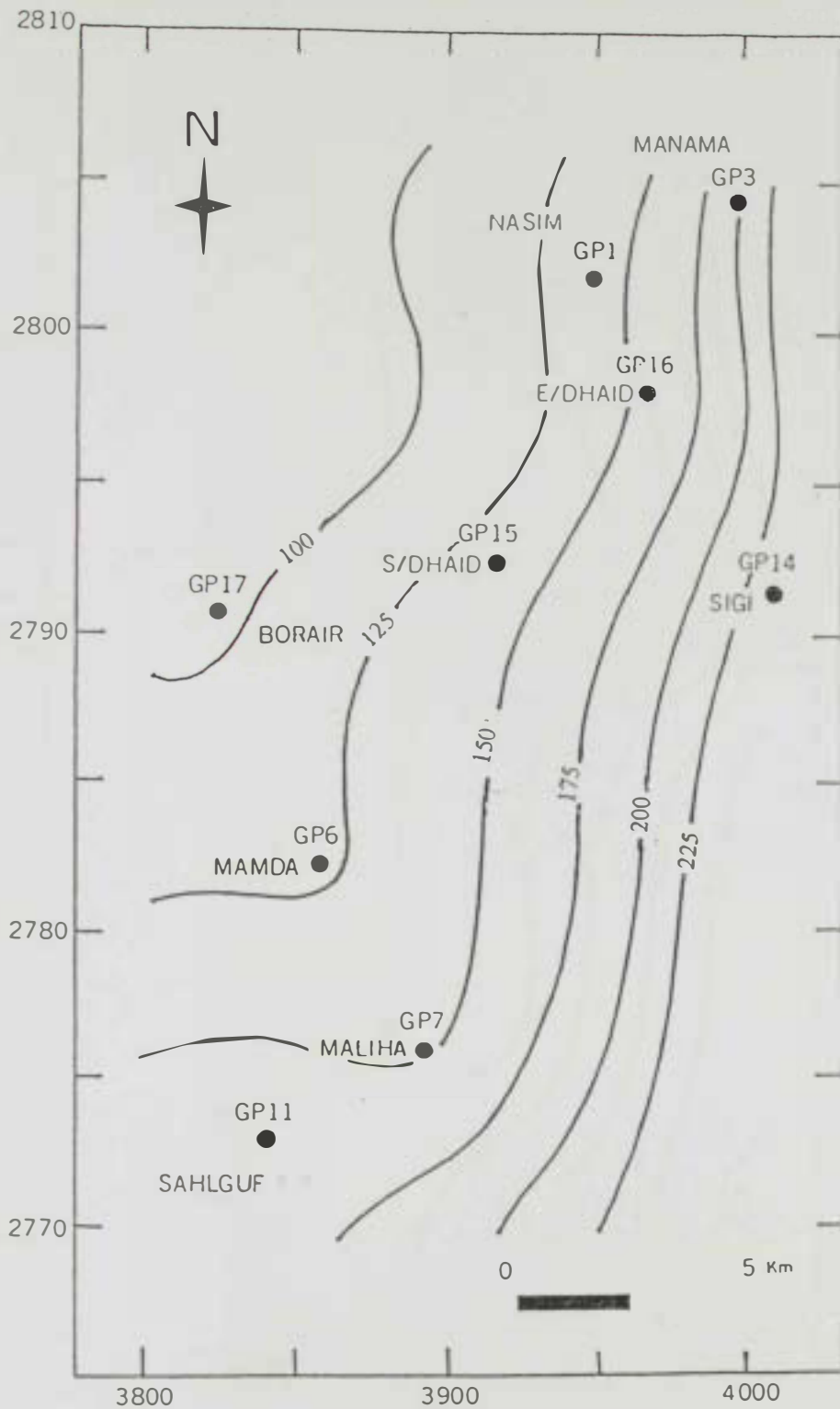


Figure 4.4 Hydraulic head contour map of the upper aquifer in the Al Dhaid area, in meters above sea level, in 1984.



Figure 4.5 Hydraulic head contour map of the upper aquifer in the Al Dhaid area, in meters above sea level, in 1999.

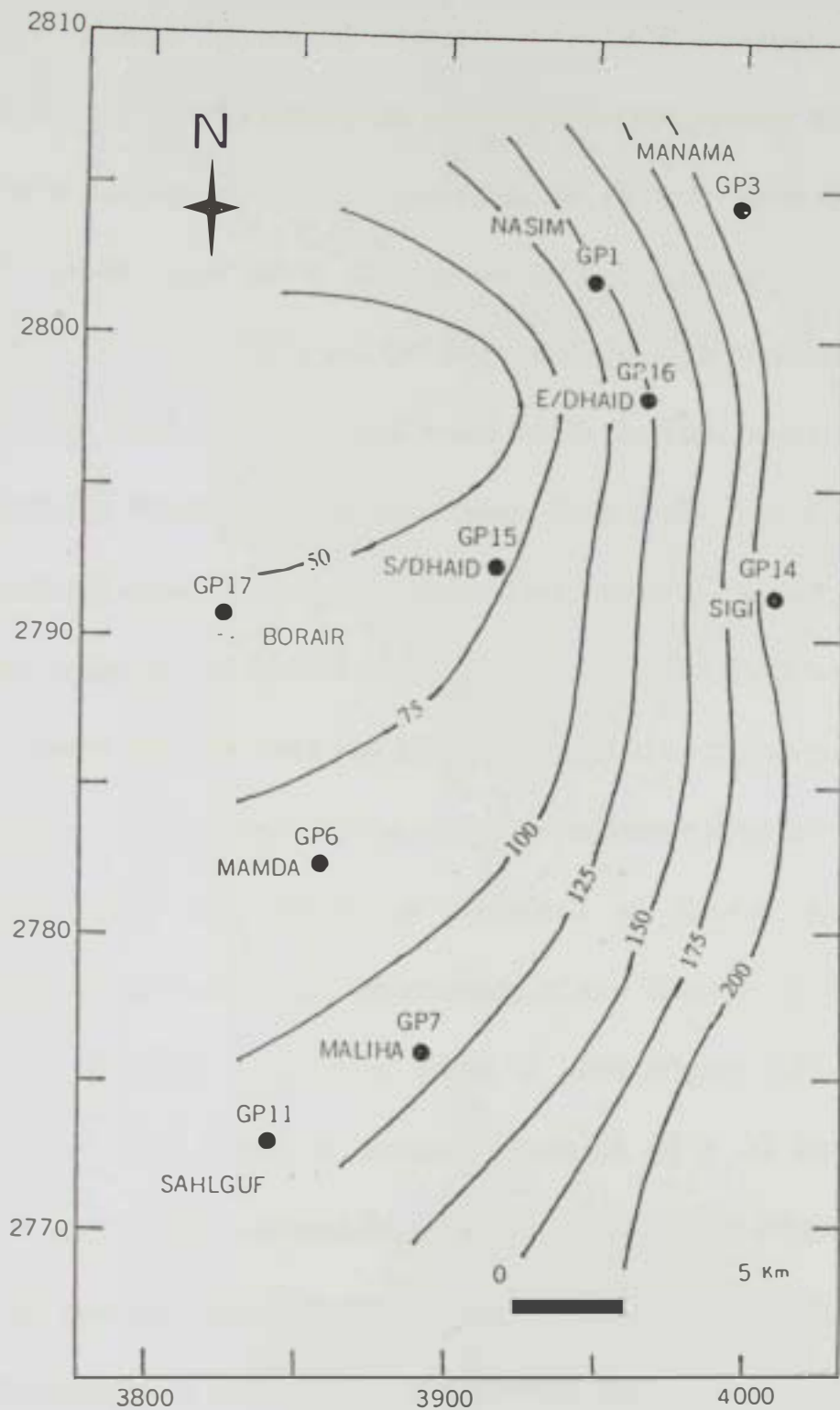


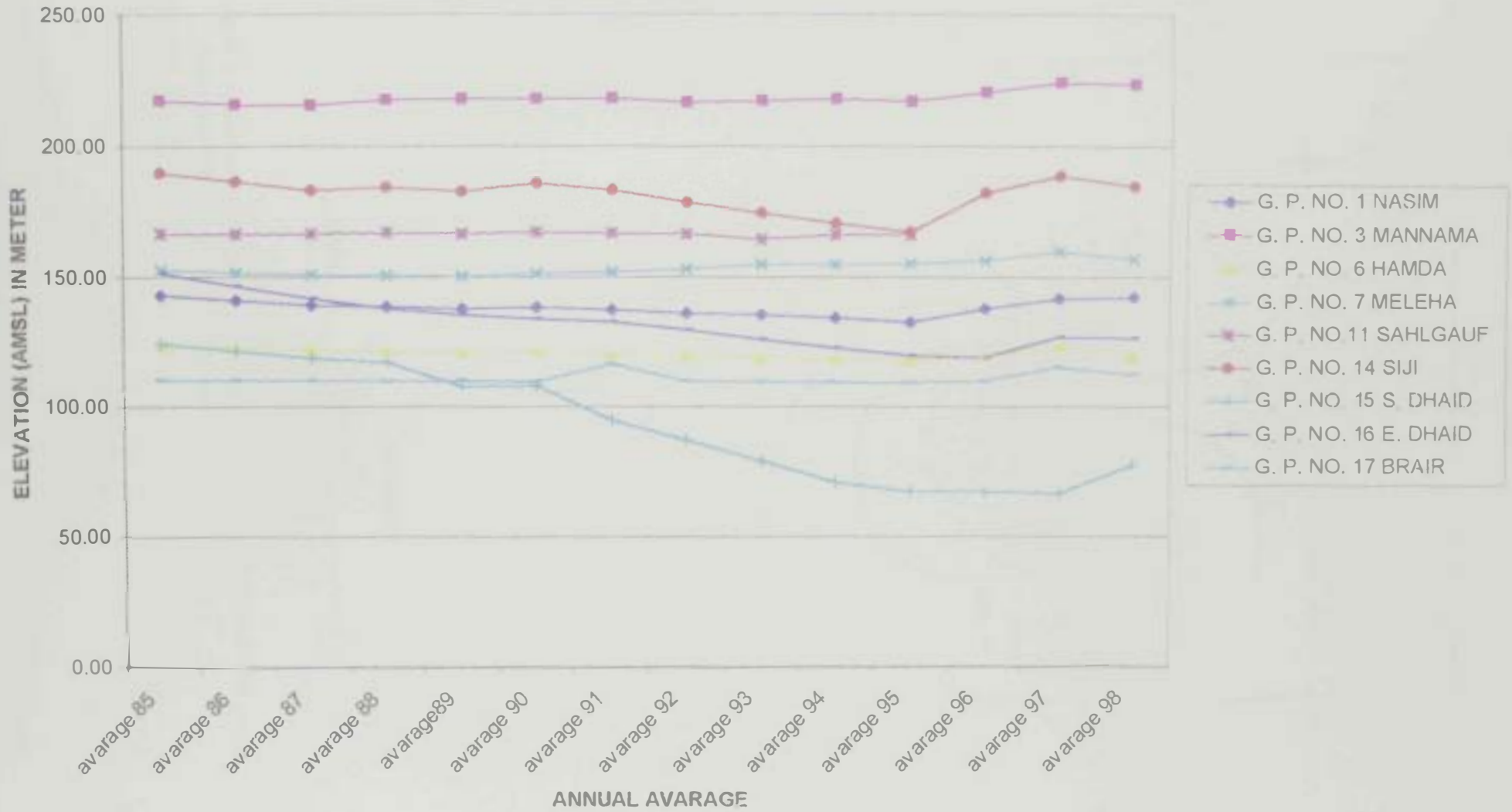
Figure 4.6 Hydraulic head contour map of the lower aquifer in the Al Dhaid area, in meters above sea level, in 1999.

2. The change in annual average water-table elevations of nine observations wells during the period 1985-1998 reveals three trends (Table 4.2; Figure 4.7): (a) water-table rise, (b) water-table decline and (c) steady water table. The limited rise in groundwater level of observation wells GP-1 and GP-14 is related to their location along the NW-SE Wadi Ham structural trend which facilitate aquifer recharge from the Northern Oman Mountains. Both wells may also tap the fractured aquifer that is characterized high hydraulic conductivity and fast recharge. The decline of groundwater level in GP-15, estimated at 55 meters between 1984 and 1999, is a result of excessive groundwater pumping for all purposes. The steady groundwater level in observation wells GP-7 and GP-17 is attributed to limited groundwater development and banning construction of new farms since 1980's.
3. The difference in hydraulic heads in 1984 (Figure 4.4) and 1999 (Figure 4.5) reveals a cone-of-depression of a 20 km average diameter centered around the observation well GP-15 (Figure 4.8).
4. The average hydraulic gradients are 0.025 along the eastern front of the study area and 0.005 in the western parts (Figures 4.4, 4.5 and 4.6).

Table 4.2 Water-table elevations, in meters above sea level, at nine observation wells in the Al Dhaid area, UAE, for the period 1985-1998.

Recorder & Location	Av. 85	Av. 86	Av. 87	Av. 88	Av. 89	Av. 90	Av. 91	Av. 92	Av. 93	Av. 94	Av. 95	Av. 96	Av. 97	Av. 98	Total Average
GP-1NASIM	142.80	140.82	139.14	138.46	137.74	138.36	137.26	136.04	135.42	134.19	132.52	137.68	141.58	142.30	138.16
GP-3 MANNAMA	217.23	215.49	215.42	217.24	217.82	217.73	217.94	216.30	217.03	217.78	216.76	220.24	224.02	223.35	218.17
GP-6 HAMDA	123.15	122.23	121.61	121.56	120.74	121.20	119.98	119.24	118.61	118.05	117.65	119.33	123.43	118.82	120.40
GP-7 MELEHA	152.75	151.53	150.80	150.71	150.14	151.37	152.07	153.02	154.90	154.70	155.15	156.36	159.82	156.83	153.58
GP-11 SAHLGAUF	166.44	166.34	166.41	166.87	166.53	167.14	166.66	166.43	164.38	166.11	166.06				166.30
GP-14 SIJI	189.58	186.22	182.92	184.11	182.59	185.17	182.70	177.97	174.21	170.39	167.08	181.84	188.30	184.40	181.25
GP-15 South DHAID	124.26	121.33	118.57	117.00	107.54	107.99	94.62	87.09	78.95	70.78	67.32	67.28	66.43	77.47	93.33
GP-16 East DHAID	151.32	146.37	141.63	137.73	135.37	133.80	132.55	129.52	125.70	122.44	119.52	118.67	126.72	126.40	131.98
GP-17 BRAIR	110.18	110.02	109.85	109.80	109.97	109.61	116.30	109.71	109.55	109.32	109.13	109.80	115.11	112.19	110.75

Figure 4.7. Change in the annual average groundwater elevation at nine observation wells in the study area, in meters above sea level, during the period 1985-1998.



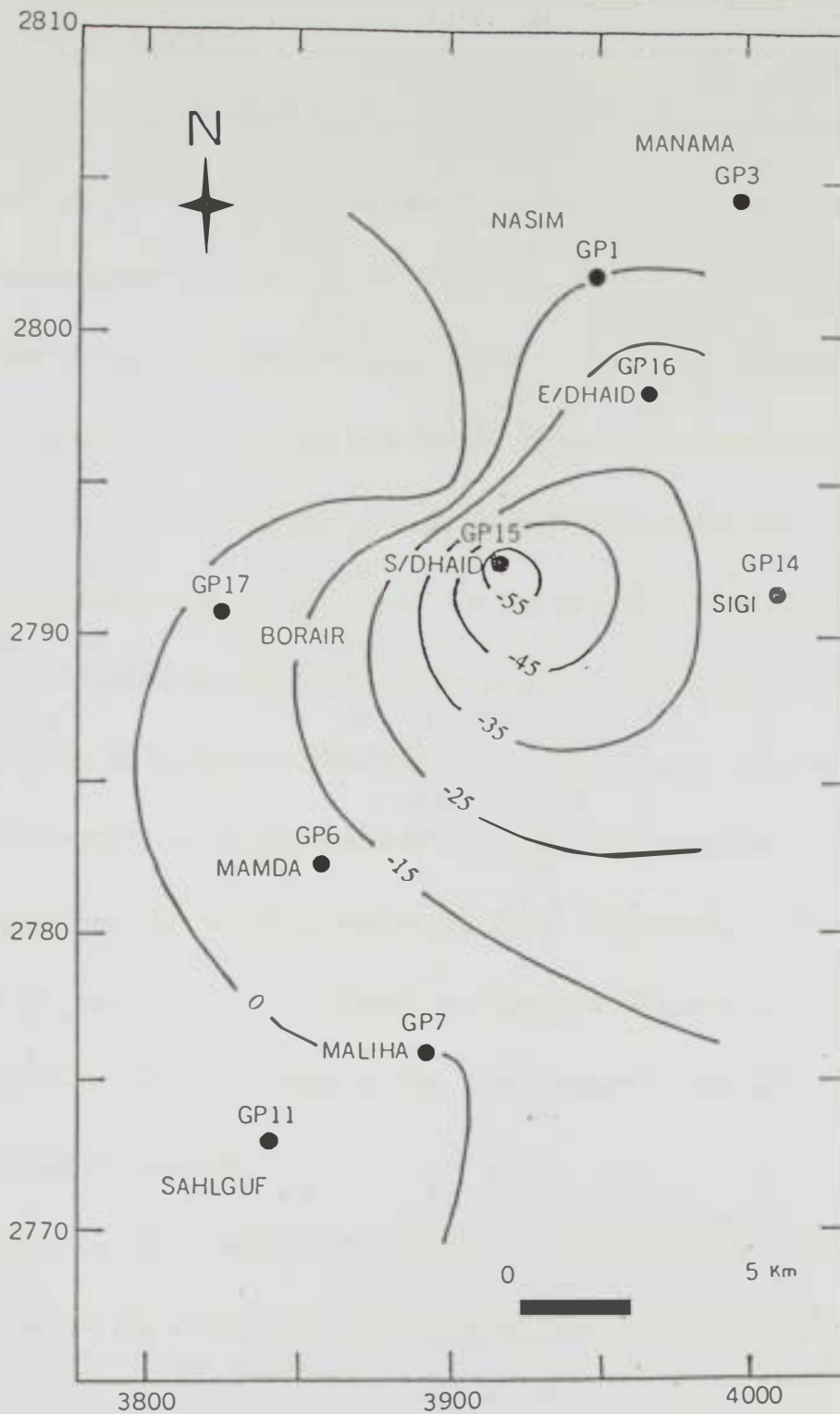


Figure 4.8 Contour map showing the cone-of-depression associated with groundwater extraction between 1984-1999 in the Al Dhaid area.

4.2.3 Water Balance

The study area suffers from a highly negative water balance caused by natural constraints and human-related activities. The natural constraints are represented by low rainfall (average annual = 155 mm) and an extremely high potential evapotranspiration (PET = 3700 mm/yr). JICA (1996) reached a conclusion that the groundwater abstraction is more than double the natural recharge for groundwater in the study area.

The flood records by the MAF for the period 1975-1998 shows that the mean annual runoff generated from all the mountain wadis in the Al Dhaid area is 11 MCM. However, these records also illustrate that the runoff amounts are highly variable from one year to another (Figure 4.9).

Inspection of rainfall-groundwater level relationship reflects a good (Siji) to poor to fair (Al Dhaid) correlations (Figures 4.10 and 4.11). Figure 4.10 also indicates a lag time between rainfall events and groundwater recharge.

Based on the results of a numerical modeling study, JICA (1996) summarized the water balance in the Al Dhaid area in Figure 4.12.

4.3 Hydrogeochemistry

Aquifers can be looked at as chemical reactors in which reactions occur between water and aquifer matrix, which results in a continuous change

Figure 4.9. Annual runoff volume (x 1000 m³) of five major wadies in the study area during the period 1975-1998 (Based on records of the MAF).

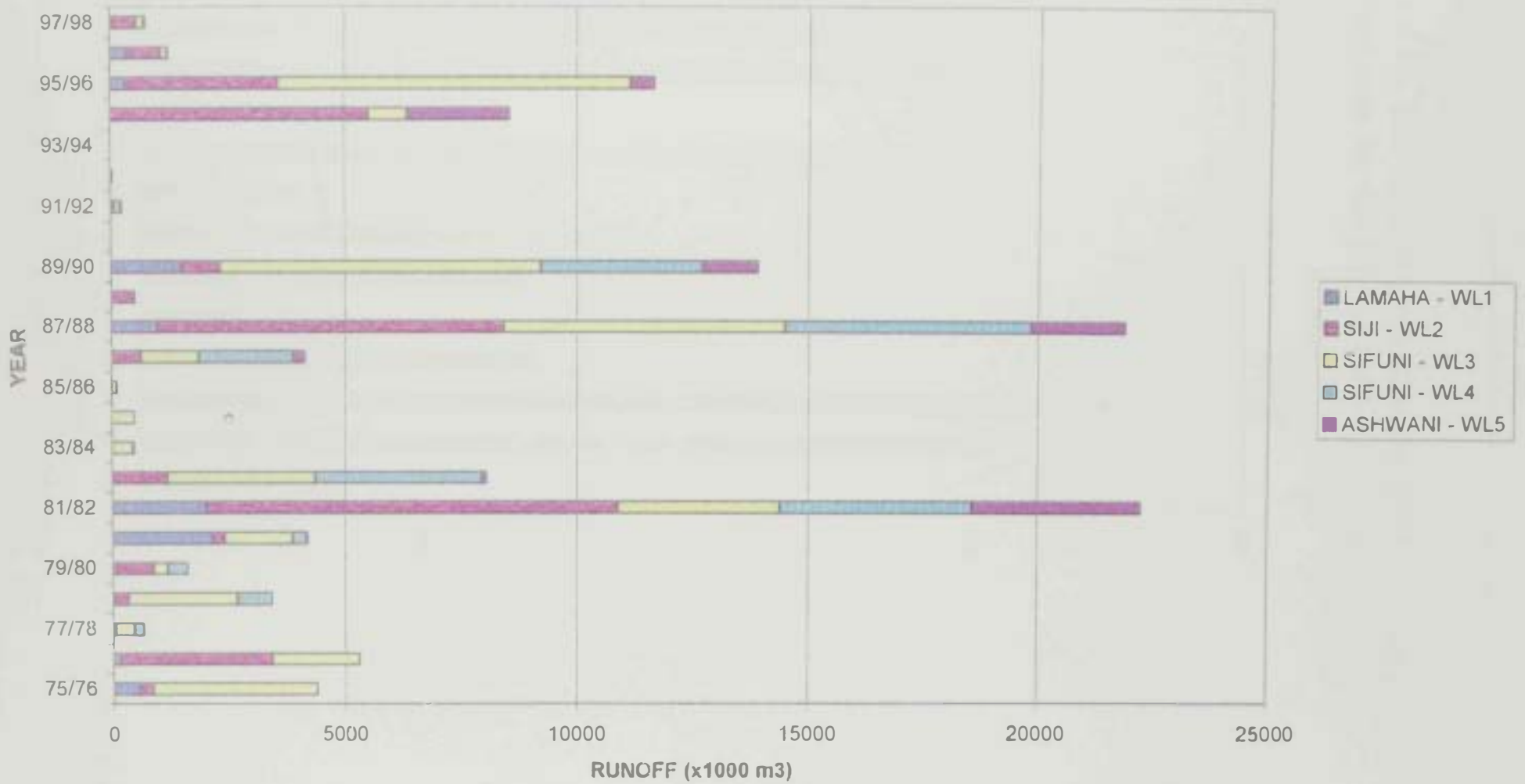


Figure 4.10. The rainfall-groundwater level relationship of the Siji area for the period 1985-1998 (Based on records of MAF)

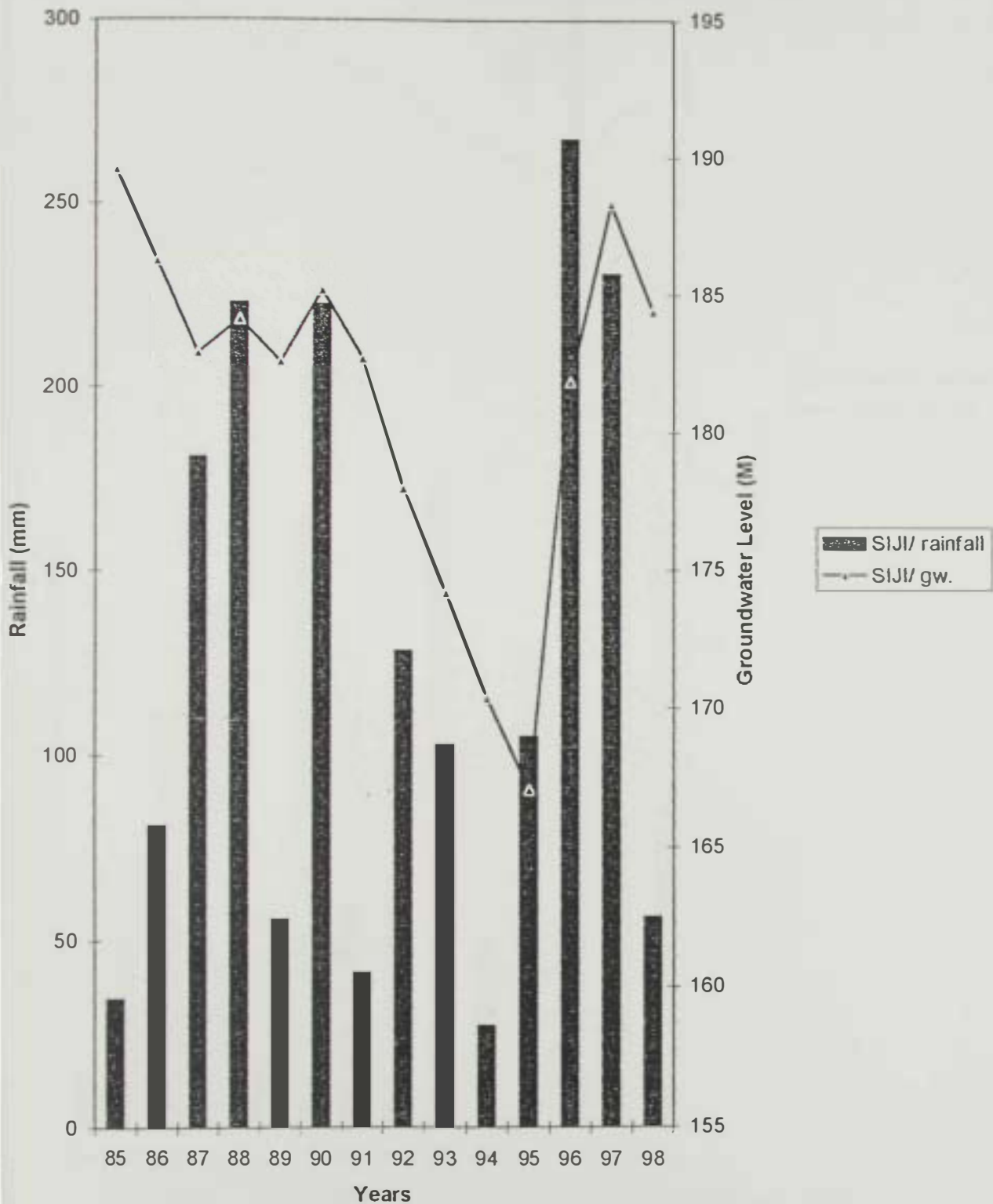
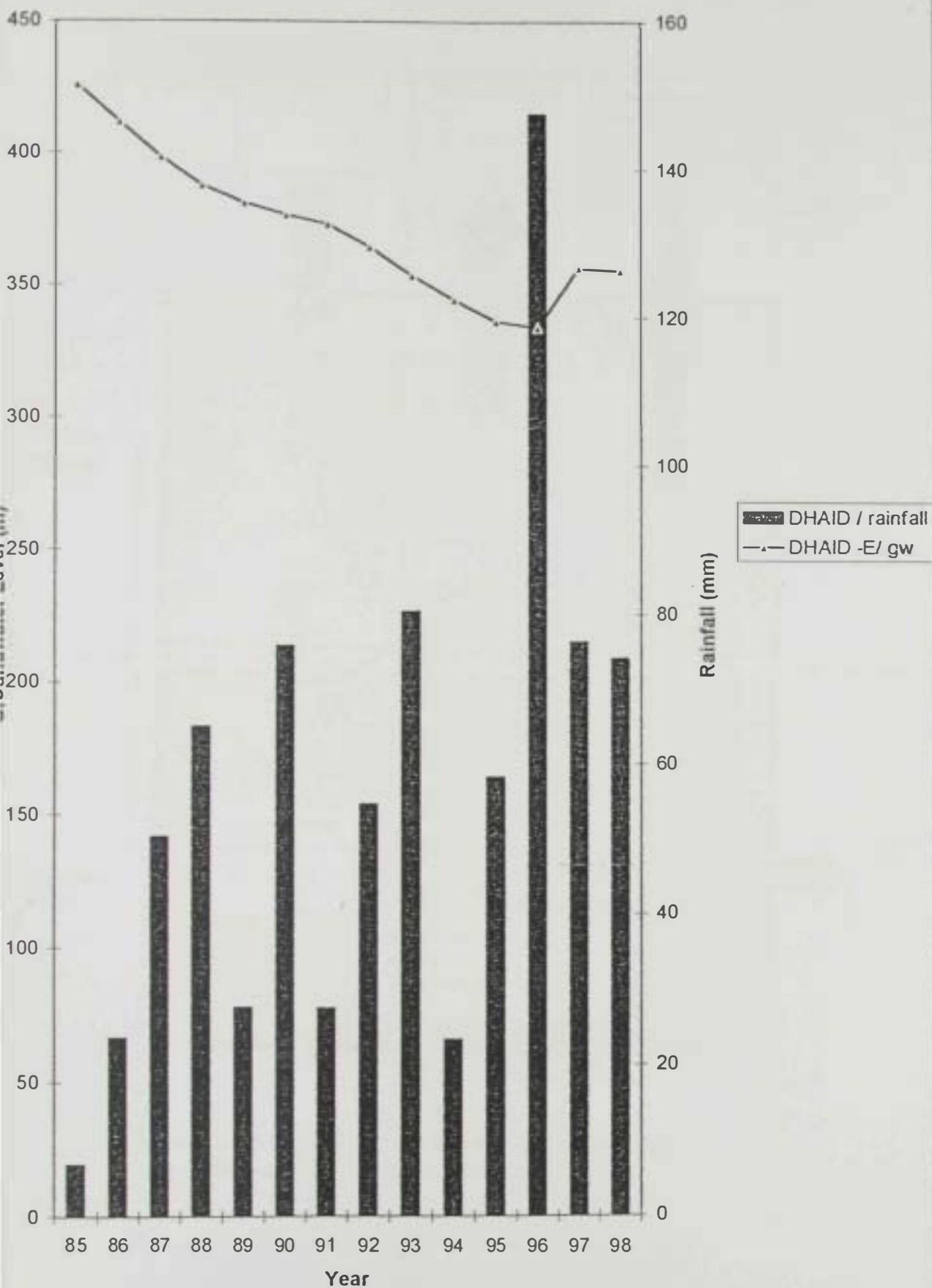


Figure 4.11. The rainfall-groundwater level relationship of the Al Dhaid area for the period 1985-1998 (Based on records of MAF)



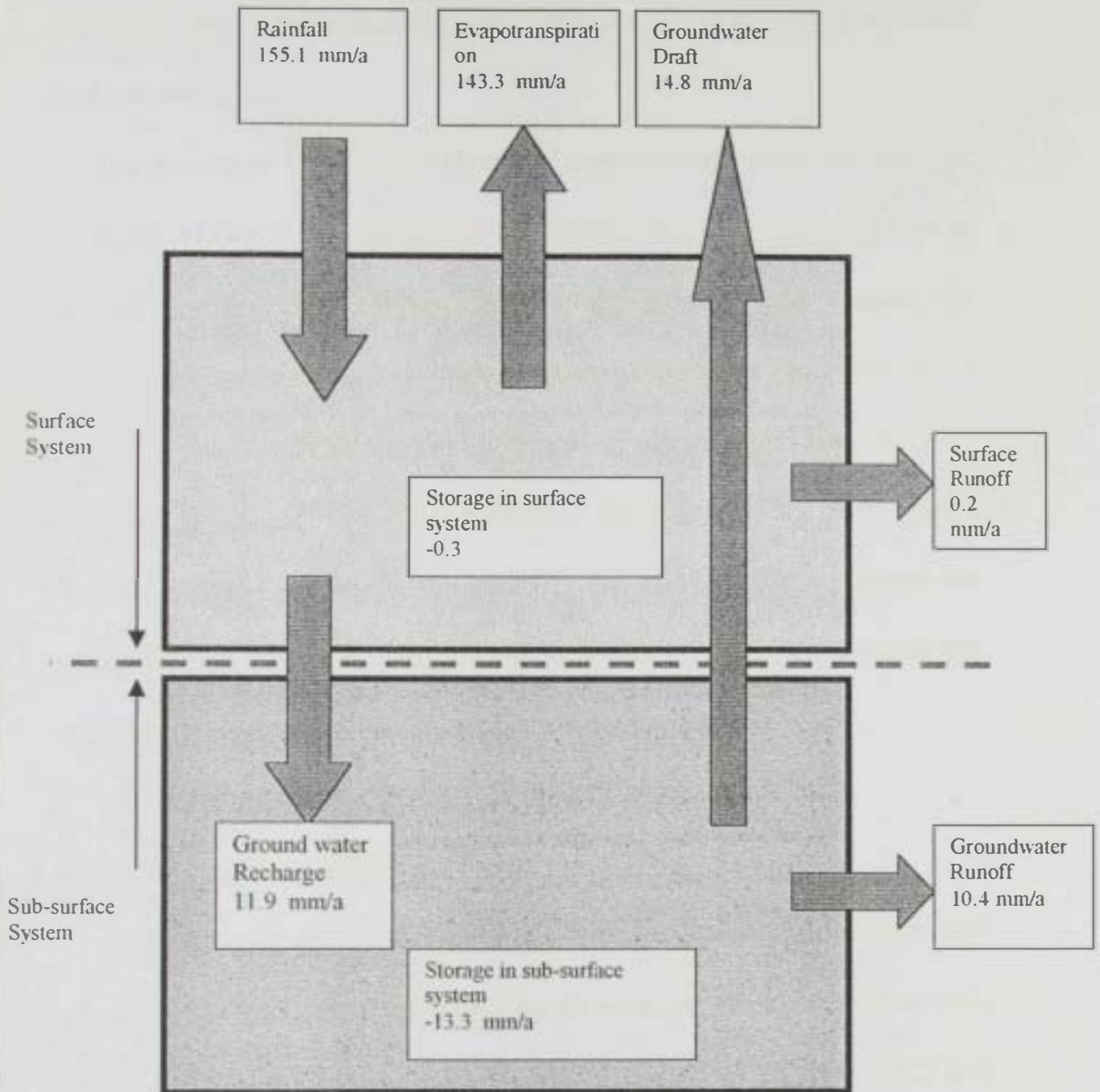


Figure 4.12. A summary of the water balance in the study area for the period 1977 - 1995 (JICA, 1996)

in the physical properties of groundwater and its host rock. These reactions cause continuous changes in the nature and chemistry of water and containing rock.

The results of chemical analyses of over hundred samples collected from the Al Dhaid aquifers during the 1996-1999 period are used here to identify the chemical characteristics of groundwater and evaluate its quality. Figure 4.13 shows the locations of water wells sampled for chemical analysis major and minor chemical constituents. Samples were analyzed in the MAF central laboratories for major cations (Ca^{2+} , Mg^{2+} , Na^+ and K^+) and anions (HCO_3^- , CO_3^{2-} , SO_4^{2-} and Cl^-). The hydrogen-ion concentration (pH) and total dissolved solids (TDS) in milligrams per liter (mg/l) were directly measured in the field.

4.3.1 Physical Properties

Usually, the reactions between the ion-depleted rain water and aquifer's solid matrix is controlled by different physical parameters such as the hydrogen-ion concentration (pH), electrical conductivity (EC) and temperature (T).

The iso-temperature contour map (Figure 4.14) shows that the highest temperature groundwater (39°C) was measured around GP-15, which coincides with the center of the cone-of-depression (see Figure 4.8)

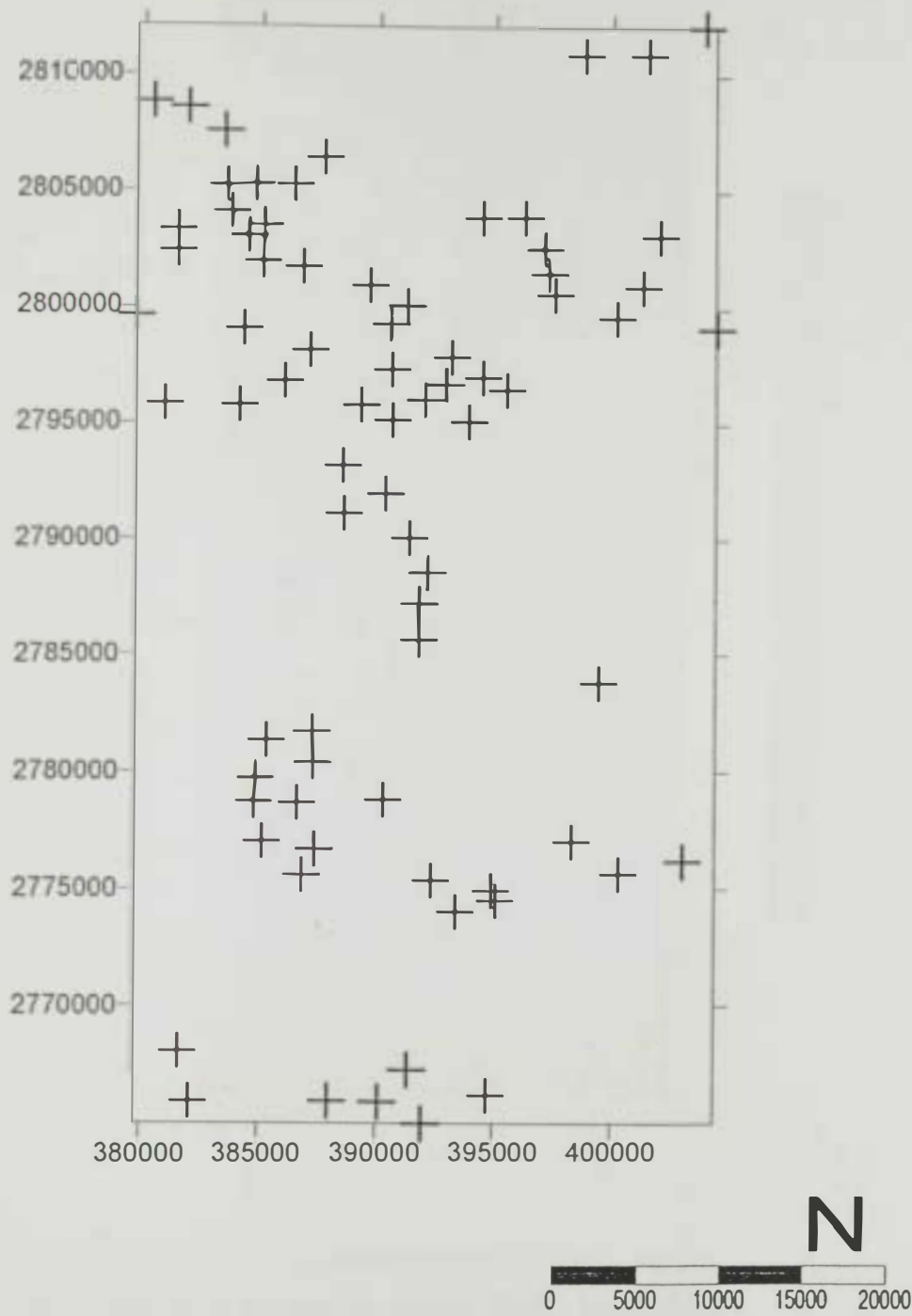


Figure 4.14. Location map of water wells sampled for chemical analyses from the study area during the period 1996-1999.

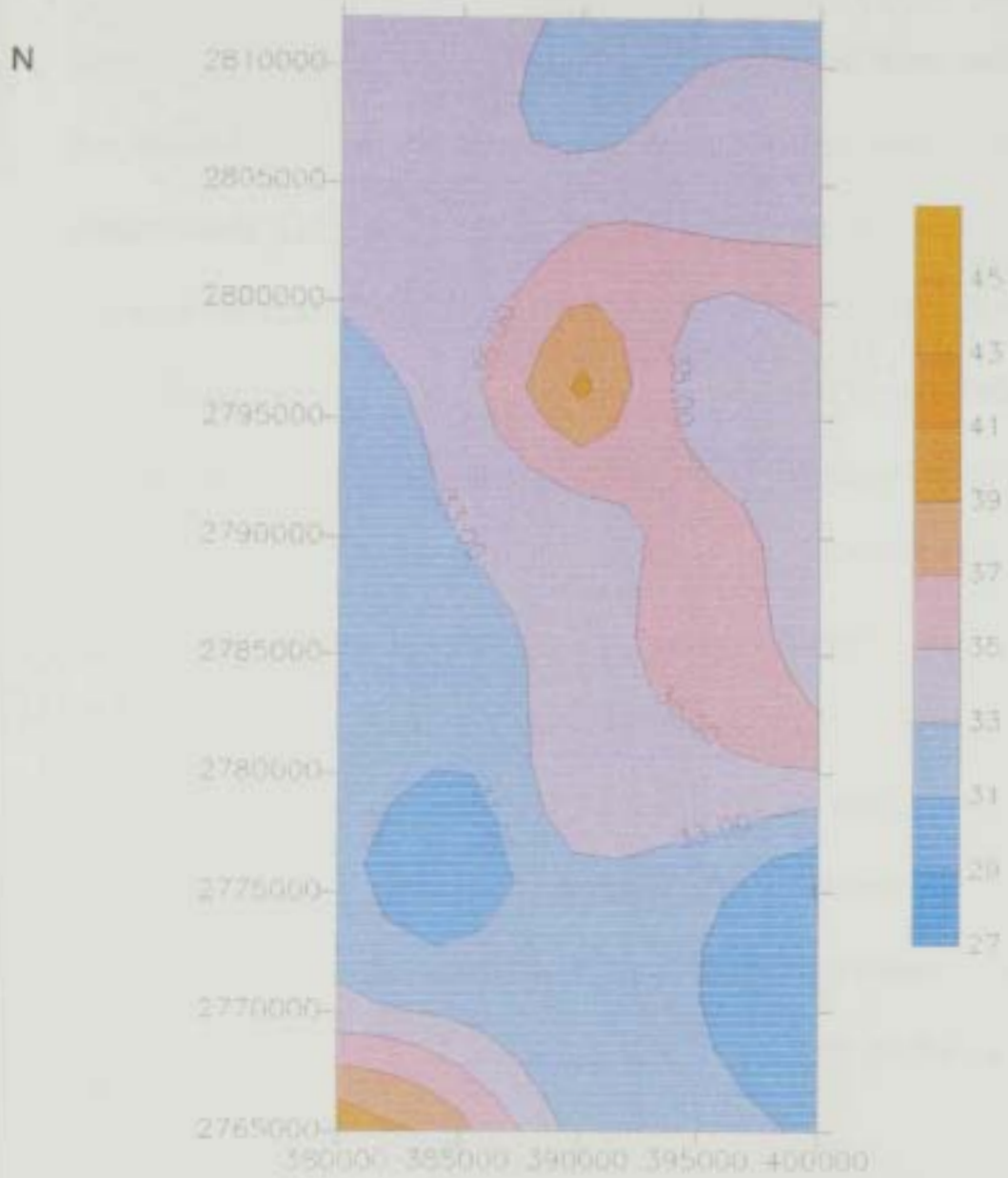


Figure 4.14. Iso-temperature ($^{\circ}\text{C}$) contour map of ground water samples collected from the study area, during the period 1995 - 1996.

resulting from excessive groundwater pumping within and around the Al Dhaid city. It seems that the relatively higher temperature, more saline water moving upward (through upconing) causes this temperature anomaly. In contrast, groundwater samples collected from wells within the courses of Wadi Al Dhaid and Wadi Hamdah show much lower temperatures (32°C). These wells possibly intercept relatively cooler recharge water as it moves from the eastern mountains towards west.

Hydrogen-ion concentration (pH) of groundwater is controlled by the amount of dissolved carbon dioxide (CO_2), carbonates (CO_3^{2-}) and bicarbonates (HCO_3^-) (Domenico and Schwartz, 1990). Figure 4.15 is an iso-pH contour map of groundwater in the Al Dhaid area. It illustrates that the high pH waters are those obtained from the mafic and ultramafic ophiolitic rocks along the eastern front of the study area (pH near 11 were measured in some ophiolite-dominated areas, Warren Wood, Personal comm., 1999). On the other hand, the Al Fayah carbonate mountains in the southwestern part of the study area exert their buffering effect on groundwater's pH keeping it near neutral.

The electrical conductance (EC) of groundwater samples collected from the Al Dhaid area is low ($<1500 \mu\text{S}/\text{cm}$) in the east and along the courses of major wadis draining the Northern Oman Mountains and crossing the study area from east to west such Wadi Siji and Wadi

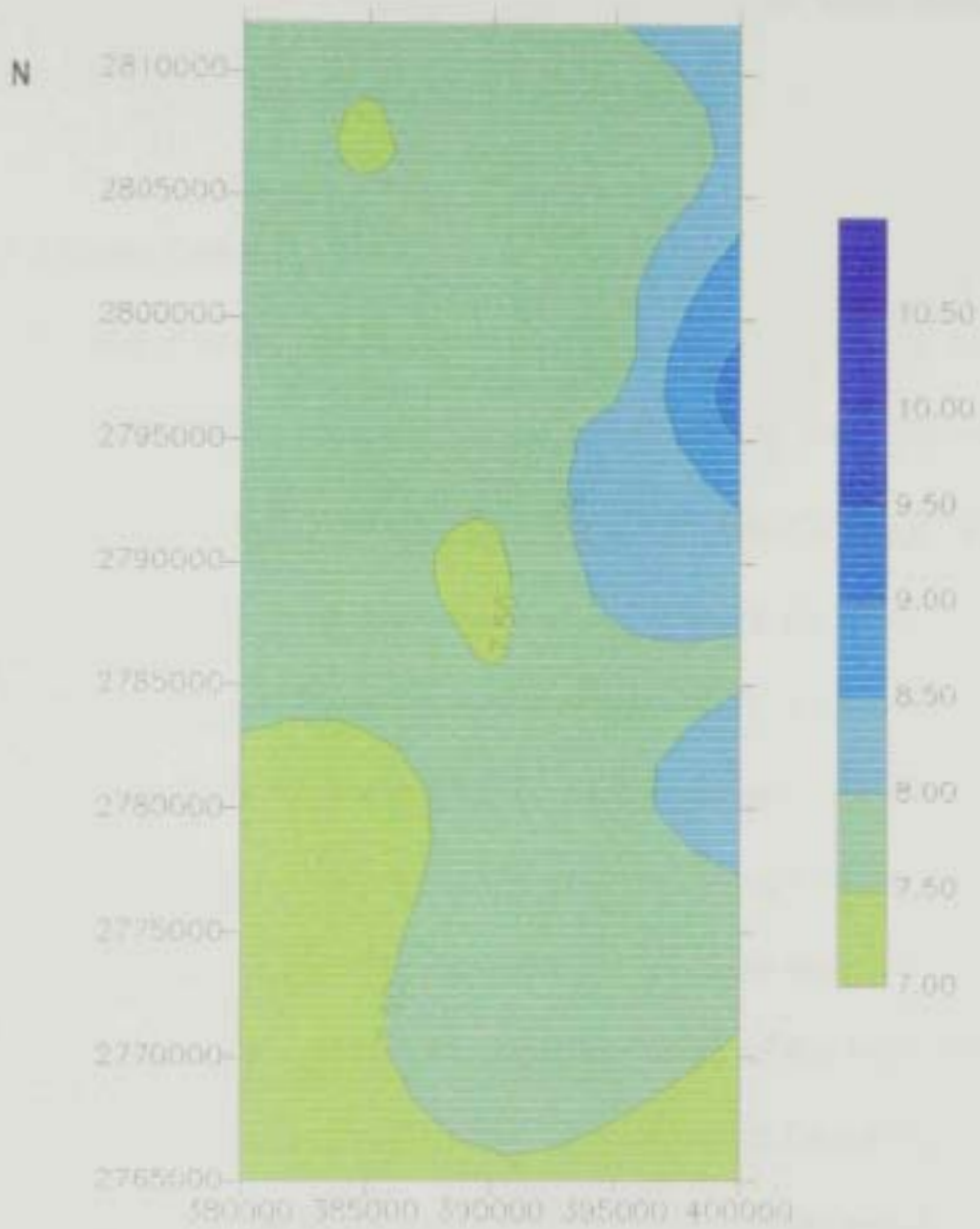


Figure 4.15. Iso-pH contour map of groundwater samples collected from the study area, during the period 1995-1996

Hamdah. The EC increases to 4500 $\mu\text{S}/\text{cm}$ in the northwest and 7500 $\mu\text{S}/\text{cm}$ in the southwest, in the directions of groundwater flow (Figure 4.16). The high EC (salinity) in the southwest can be attributed to the presence of sabkha and evaporite-rich sediments there. Upon dissolution, these deposits charge groundwater with more ions.

4.3.2 Major Cations

The sequence of cation dominance in groundwater of the Al Dhaid area has the order: $\text{Na}^+ > \text{Mg}^{2+} > \text{Ca}^{2+}$, whereas the sequence of anion dominance has the order: $\text{Cl}^- > \text{SO}_4^{2-} > \text{HCO}_3^-$. The Ca^{2+} , Mg^{2+} and Na^+ concentrations are low along the eastern front of the study area, and increase towards west and southwest (Figures 4.17, 4.18 and 4.19). The Ca^{2+} concentration increases from 20 mg/l in the east to 100 mg/l in the southwest, while the Mg^{2+} values jump from 50 mg/l to 200 mg/l along the same trend. The high Mg^{2+} in groundwater of the study area is a result of dissolution of the ultramafic ophiolitic rocks of the Northern Oman Mountains in the east. The low Mg^{2+} around the Al Dhaid city indicates that the groundwater in the upper aquifer is pumped out and that the low Mg^{2+} water represents groundwater moving upward from the lower aquifer. The Na^+ content rises from 200 mg/l in the east to 1200 mg/l in the southwest, in the direction of groundwater flow. Low cation

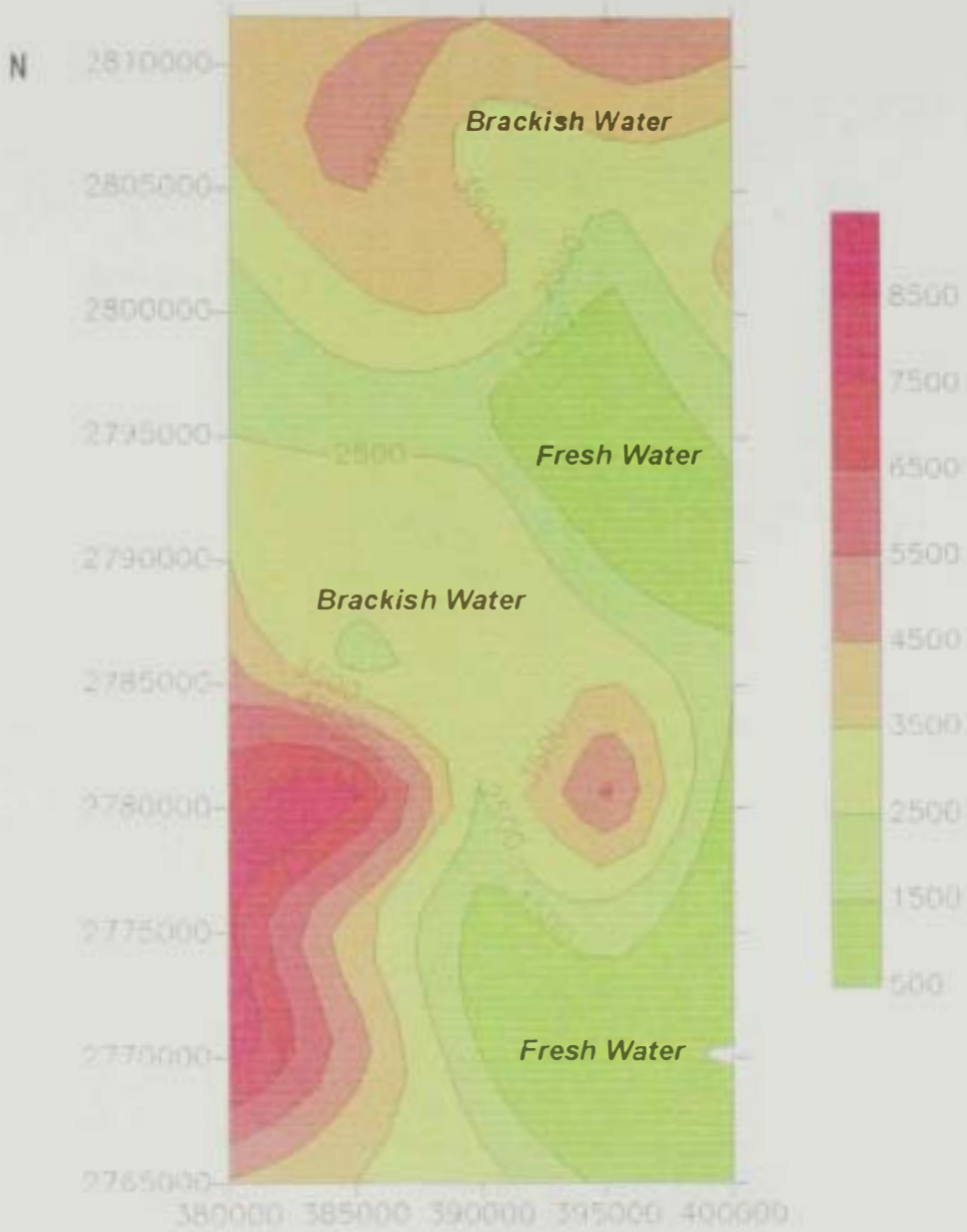


Figure 4.16 Iso-EC contour ($\mu\text{S}/\text{cm}$) map of groundwater samples collected from the study area, during the period 1995-1996.

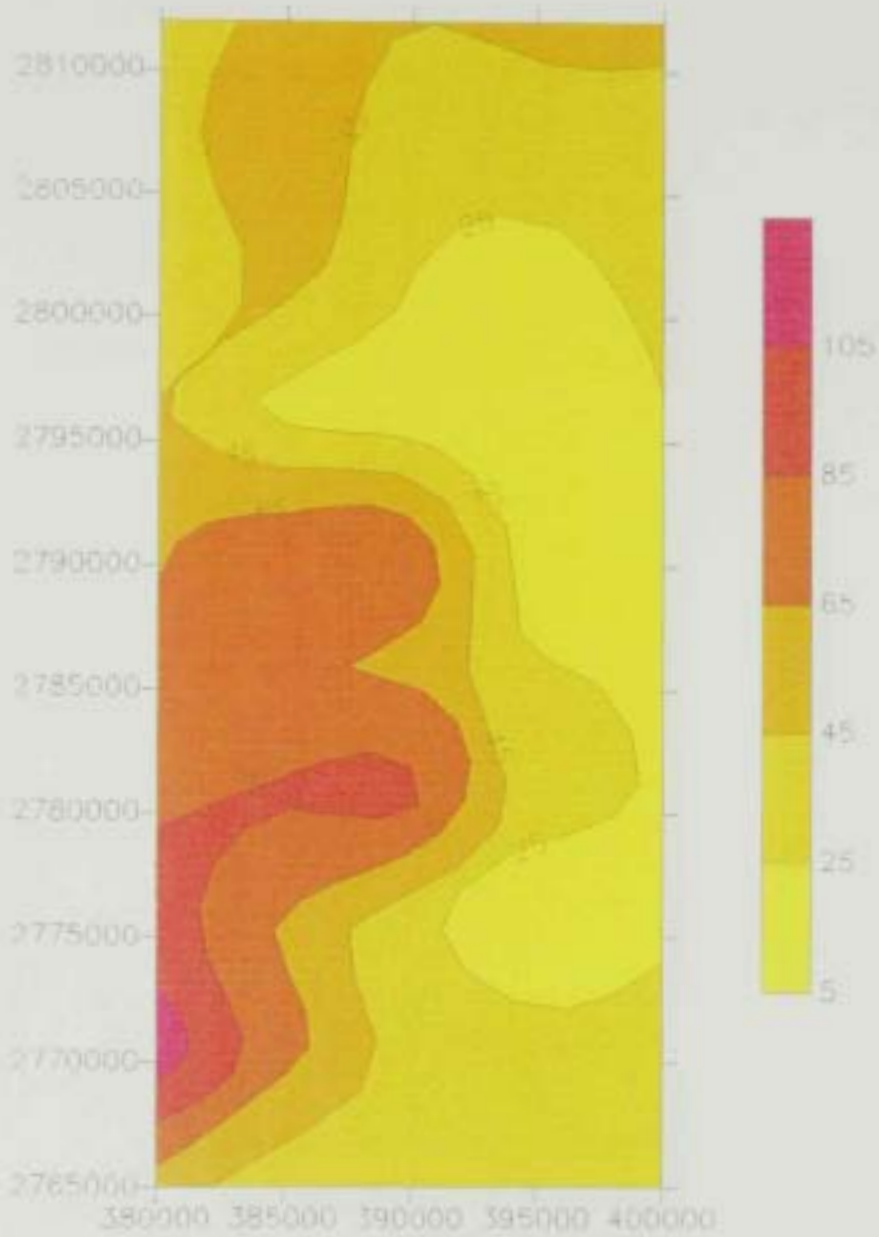


Figure 4.17. Iso-concentration contour map (mg/l) of the Ca^{2+} in groundwater of the study area, in 1996.

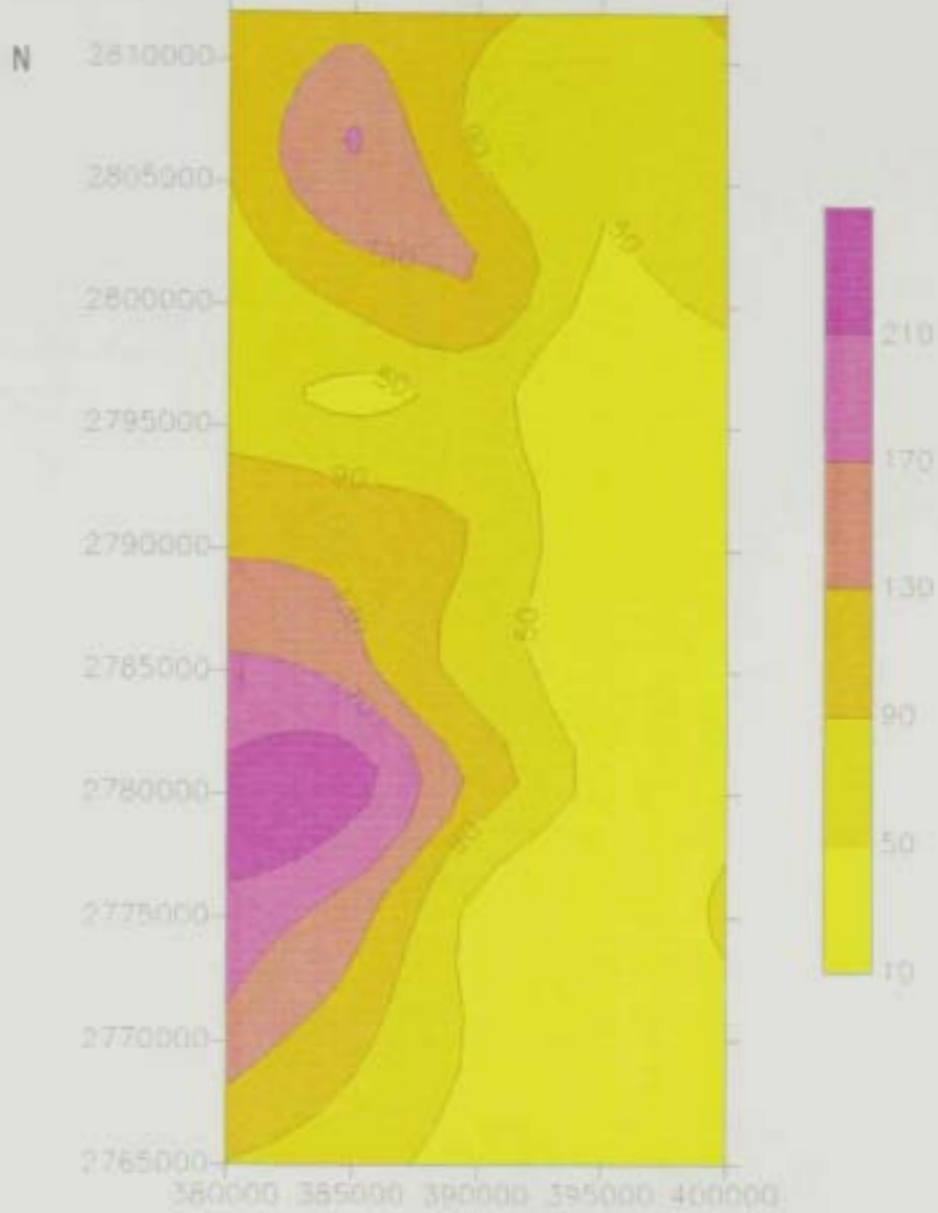


Figure 4.18. Iso-concentration contour map (mg/l) of the Mg^{2+} in the groundwater of the study area in 1996.

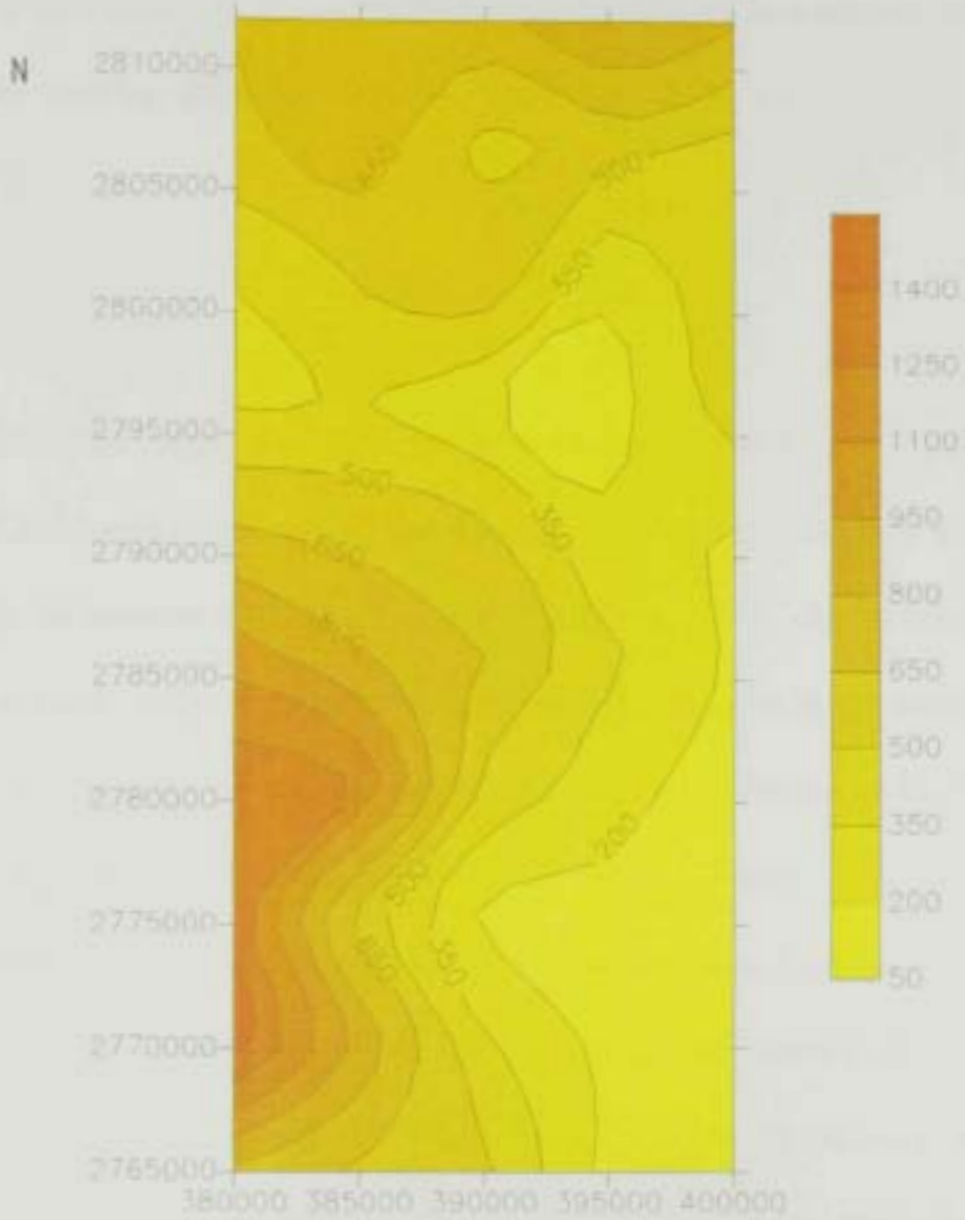


Figure 4.19. Iso-concentration contour map (mg/l) of the Na⁺ in groundwater of the study area in 1996.

concentrations also characterize groundwater samples obtained from wells located along the courses of major wadis, crossing the study area from east to west. These wadis act as conduits of low-salinity recharge water moving from the Northern Oman Mountains towards the Arabian Gulf.

4.3.3 Major Anions

Detected carbonate-ion (CO_3^{2-}) concentrations in groundwater of the Al Dhaid area occur around the Al Dhaid city, where the pH is relatively high. In contrast to most water-dissolved ions, HCO_3^- shows enrichment in recharge areas, due to dissolution of carbon dioxide in the atmosphere, and decreases in the direction of groundwater flow. However, high HCO_3^- can be also related to the carbon dioxide (CO_2) in soils or dissolution of carbonate rocks (Davis and DeWeist, 1966). Figure 4.20 shows that the HCO_3^- content decreases from 250 mg/l in the east central area to about 50 mg/l at the Al Dhaid city. From there, HCO_3^- value increases again in association with possible dissolution of carbonate rocks, especially in the Al Fayah Mountains in the southwestern part of the study area. The low HCO_3^- concentrations around the Al Dhaid city can be related to the exploitation of most of the near-surface, younger water in the shallow aquifer.

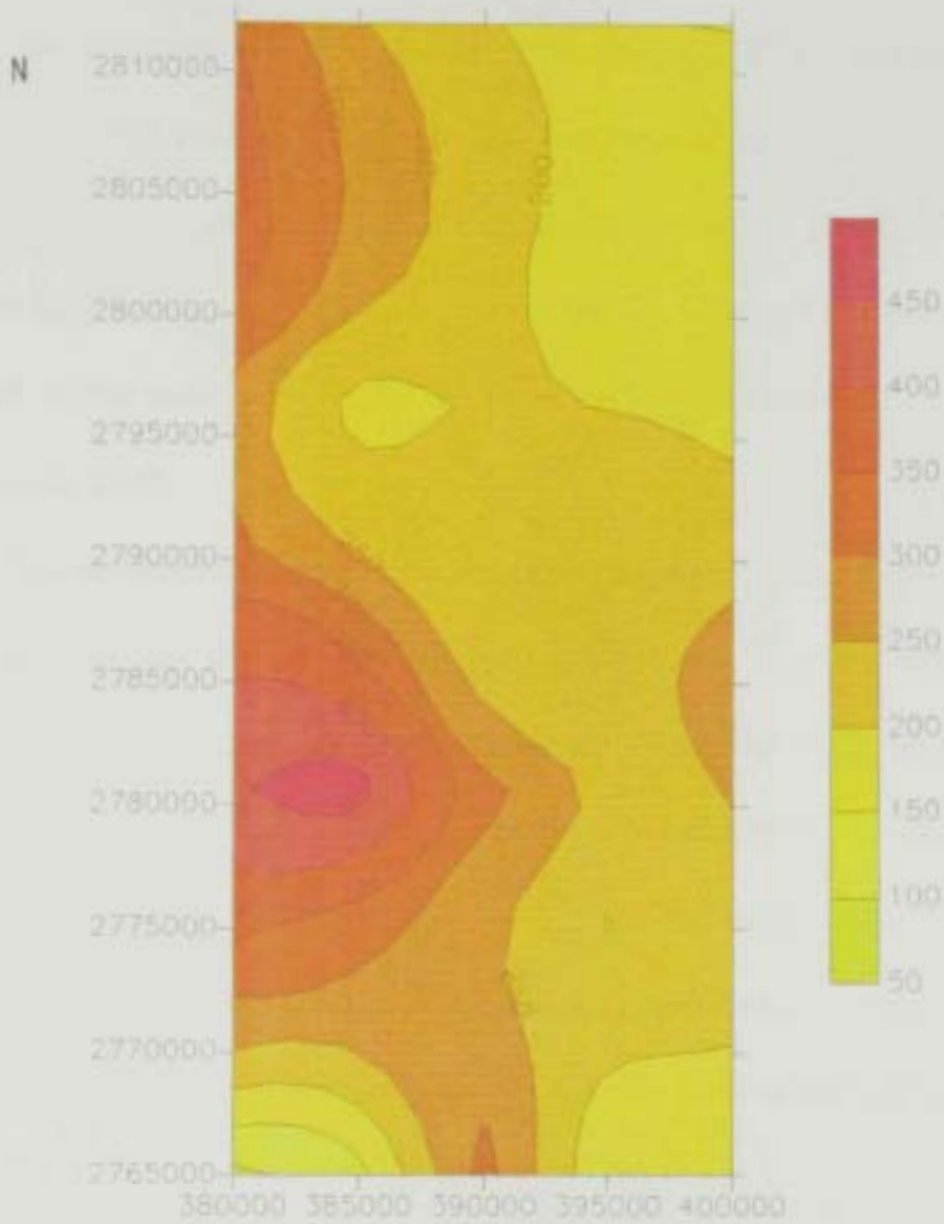


Figure 4.20. Iso-concentration contour map (mg/l) of the HCO_3^- in groundwater of the study area in 1996.

As in case of other anions, except HCO_3^- , the iso-concentration contour map shows a steady increase in SO_4^{2-} contents from east to west, in the direction of groundwater flow (Figure 4.21). Dissolution of Sabkhas and evaporite deposits are responsible for high SO_4^{2-} content (1000 mg/l) in groundwater of the southwestern part of the study area. The SO_4^{2-} concentration also increases from a 100 mg/l in the east to 400 mg/l in the northwest, along the flow path of groundwater towards the Arabian Gulf.

The distribution of chloride ion (Cl^-) in groundwater of the Al Dhaid area resembles that of SO_4^{2-} (Figure 4.22). High Cl^- concentrations are associated with dissolution of sabkhas and evaporites in the southwestern part of the study area. High Cl^- can be also related to the upconing of more-salinity water from the lower aquifer as a result of heavy groundwater pumping. The Cl^- can be also enriched in groundwater as a result of salt-water intrusion from the Arabian Gulf in the northwest.

4.3.4 Ionic Ratios

Ionic ratios expressed in equivalent per liter (epm), show the relative concentrations of various ions and can be used to indicate the predominance of a particular ion and to define locations of salt-water intrusion.

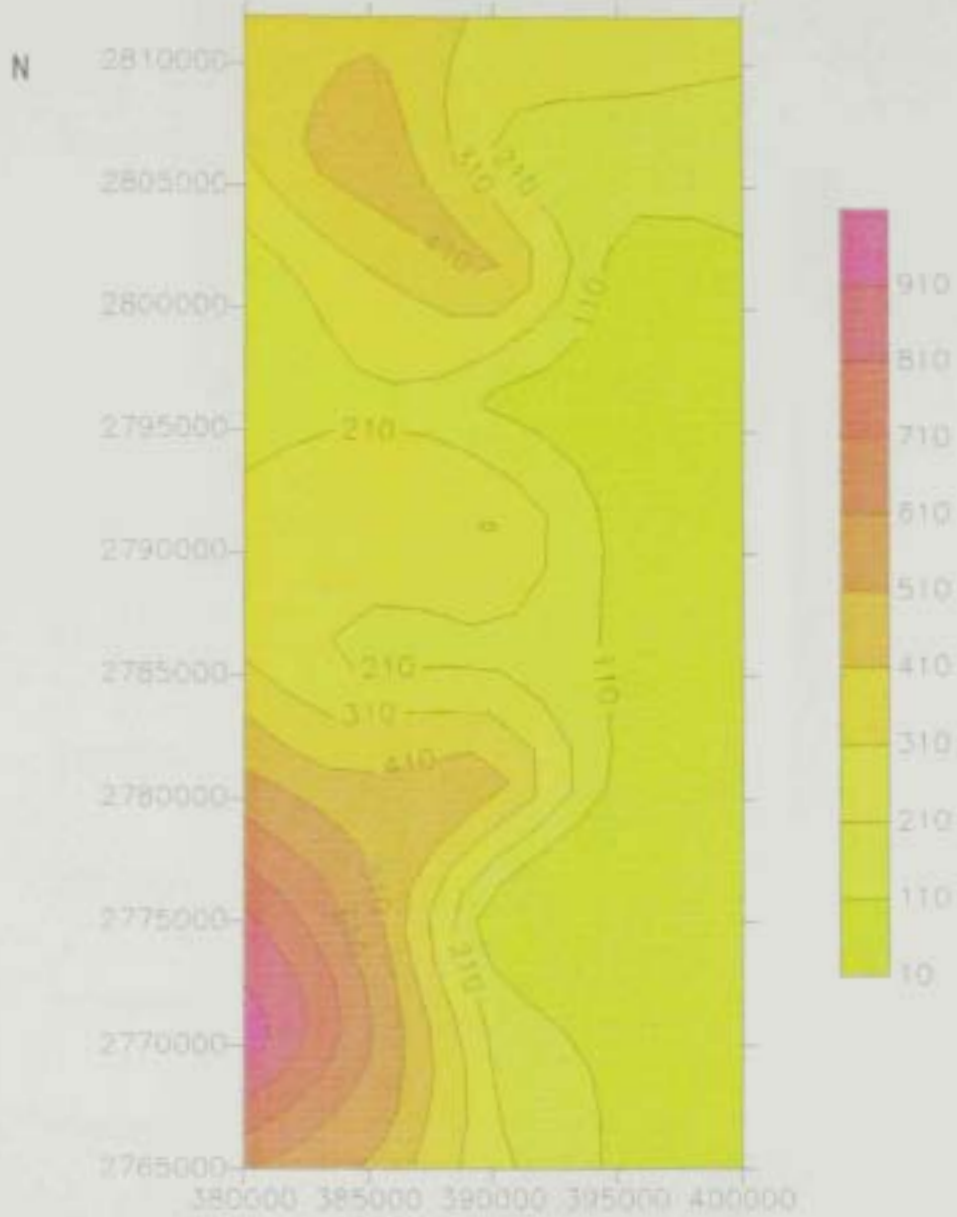


Figure 4.21. Iso-concentration contour map (mg/l) of the SO_4 in groundwater of the study area in 1996.

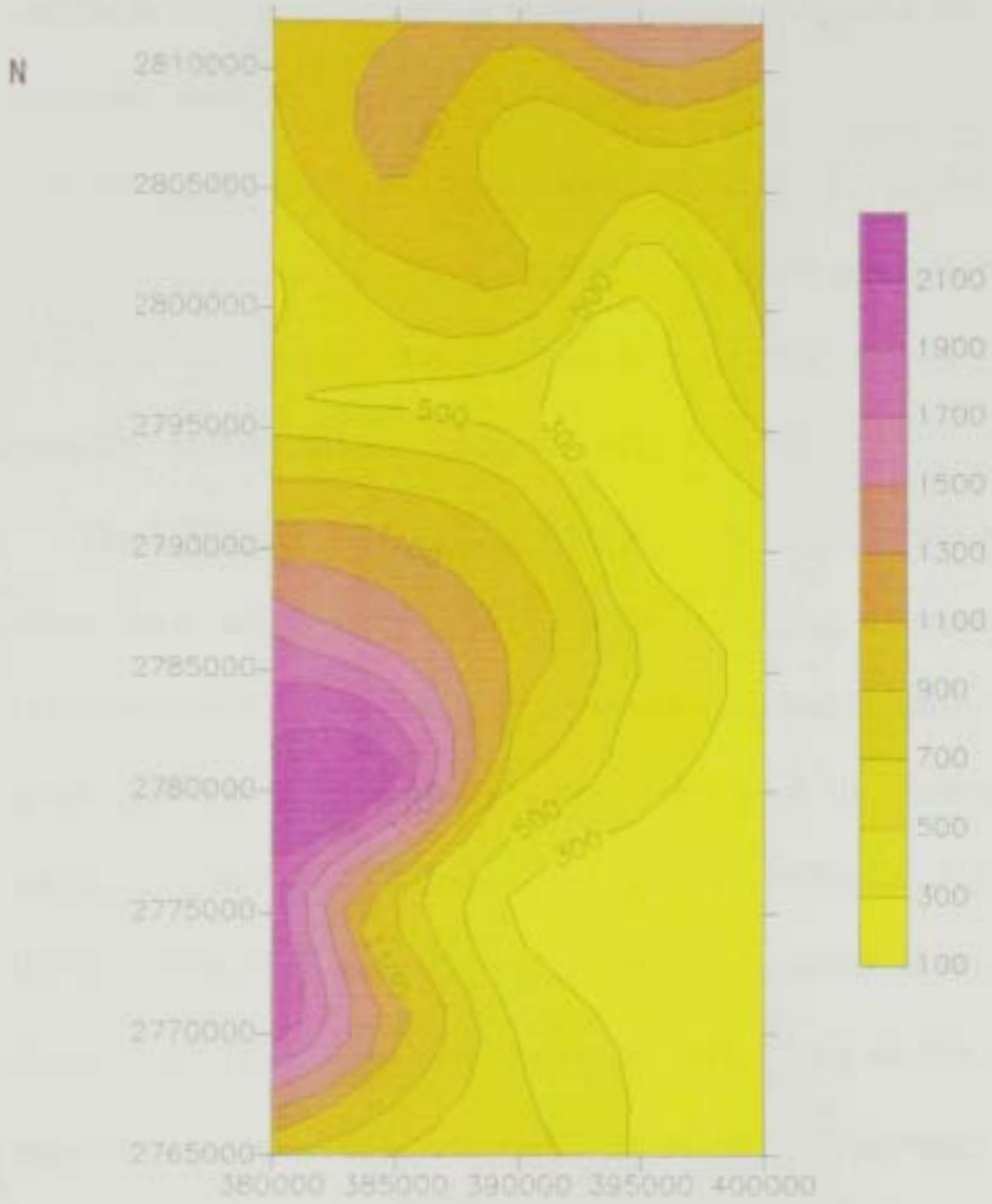


Figure 4.22 Iso-concentration contour map (mg/l) of the Cl^- in groundwater of the study area in 1996.

The Ca/Mg ratio is <1 in most groundwater samples from the study area, reflecting the influence of dissolution of Mg-rich mafic and ultramafic rocks in the Northern Oman Mountains (Figure 4.23). The ion-depleted rainwater dissolves magnesium from the ophiolitic rocks constituting the Northern Oman Mountains in UAE. This leads Mg²⁺ content higher than Ca²⁺. An exception to this is the groundwater in the Al Fayah carbonate mountains, which upon dissolution by rain releases more Ca²⁺ in groundwater and consequently a Ca/Mg ratio >1 .

The Cl/(CO₃+HCO₃) ratio is used to evaluate salt-water intrusion, either from neighboring areas or from underlying formations. The chloride-ion (Cl⁻) is a dominant anion in salt water and normally occurs in small amounts in groundwater. On the other hand, the bicarbonate-ion (HCO₃⁻) is the most abundant anion in groundwater. Figure 4.24 illustrates that, except for the eastern strip and courses of major wadis (Cl/(CO₃+HCO₃) <1), the study area is suffering from a serious salt-water intrusion problem in the north, west and southwestern parts (Cl/(CO₃+HCO₃) >1). The cause of increasing groundwater salinity can be related to upconing, dissolution of sabkhas and evaporites, or saline-water encroachment from the sea. It seems that all the three mechanisms are in effect at variable degrees within the study area.

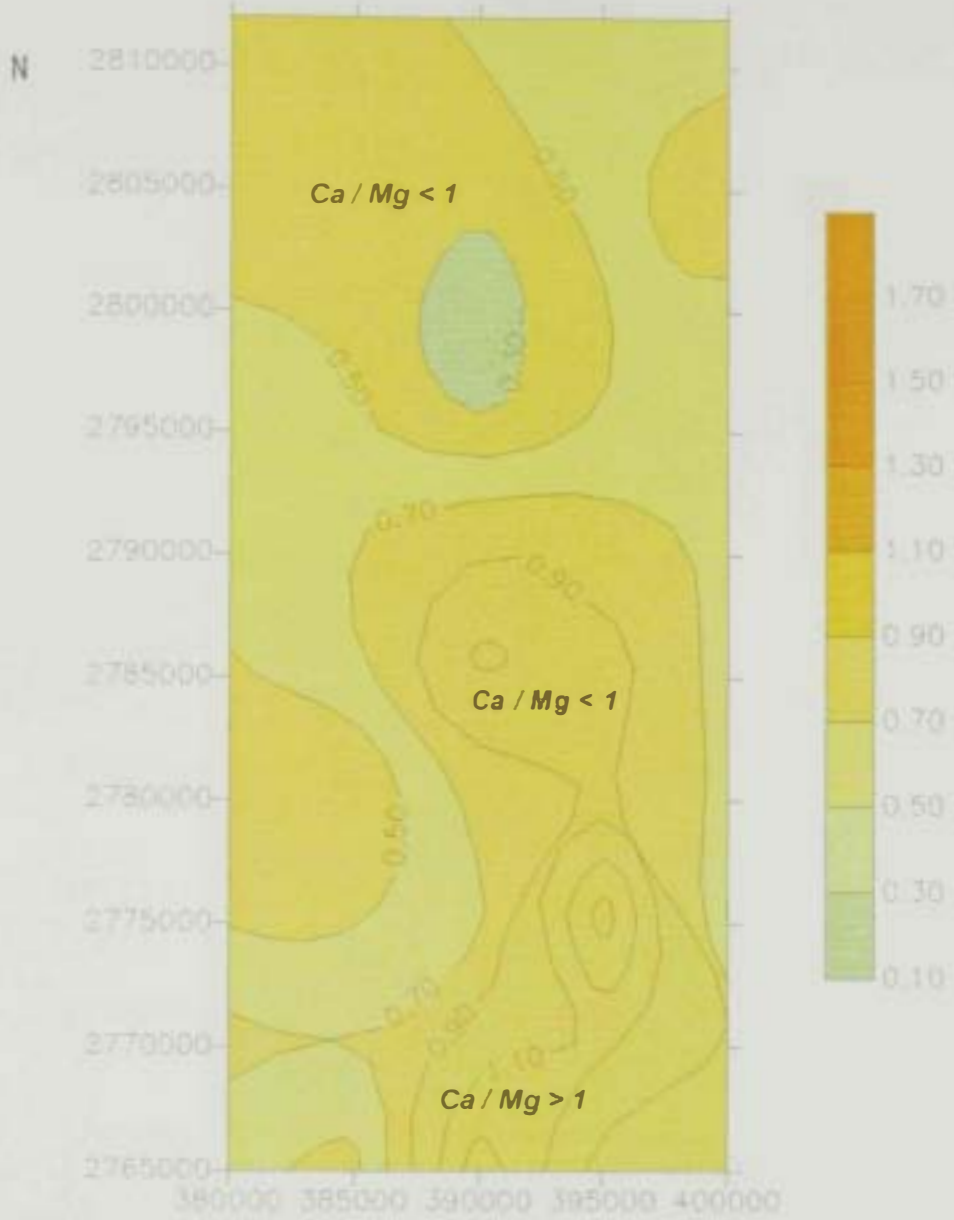


Figure 4.23. Contour map showing the distribution of $\text{Ca}^{2+}/\text{Mg}^{2+}$ ratio in groundwater of the study area.

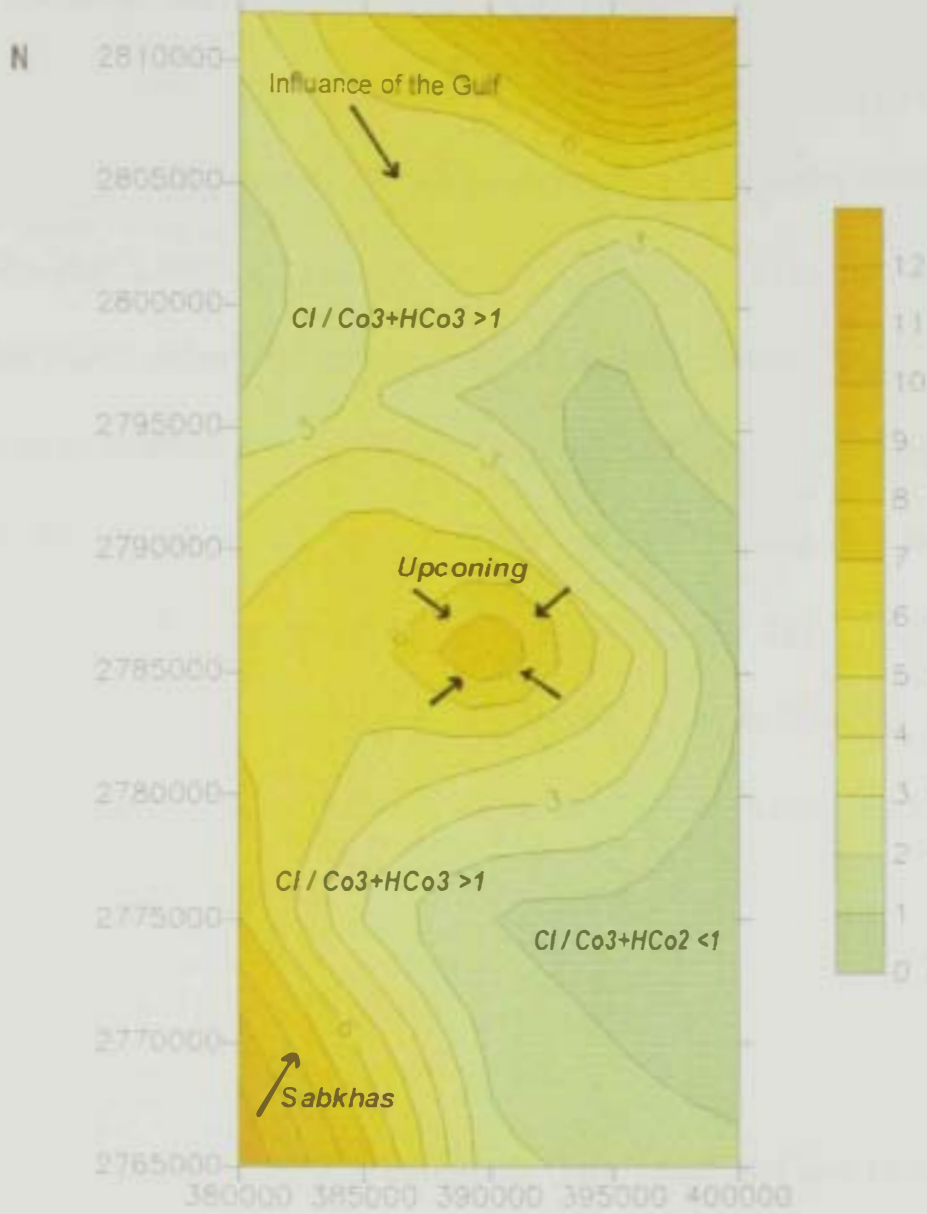


Figure 4.24. Contour map showing the distribution of $\text{Cl}^- / (\text{CO}_3^{2-} + \text{HCO}_3^-)$ ratio in groundwater of the study area.

The SO_4/Cl ratio is <1 in groundwater of most of the study area, indicating the dominance of Cl^- (Figure 4.25). In contrast, the southwestern corner of the Al Dhaid area is characterized by SO_4/Cl ratio >1 , due to the presence of sabkha and evaporite deposits in this part.

The Na/Cl ratio in seawater is less than unity (0.85), while groundwater has Na/Cl ratios greater than unity (Hounslow, 1995). Therefore, it is also used to indicate areas suffering from salt-water intrusion. The Na/Cl ratio is <1 in most of the Al Dhaid area, suggesting that the salt-water intrusion affects most of the study area (Figure 4.26). This fact supports the results obtained from the $\text{Cl}/(\text{CO}_3+\text{HCO}_3)$ ratio. Only the eastern strip of the study area, in addition to the courses of major wadis have Na/Cl ratio >1 .

4.3.5 Water Quality

The concentrations of nitrate ion (NO_3^-) and total iron (Fe), in addition to water hardness and sodium adsorption ratio (SAR), were used as quick indicators of water quality in the study area. According to Freeze and Cherry (1979), NO_3^- is the most common identified contaminant in water. The WHO (1971) recommended limits for nitrate in drinking water is 45 mg/l as nitrate (NO_3^-) and 10 mg/l as NO_3^- -N. This limit is exceeded in

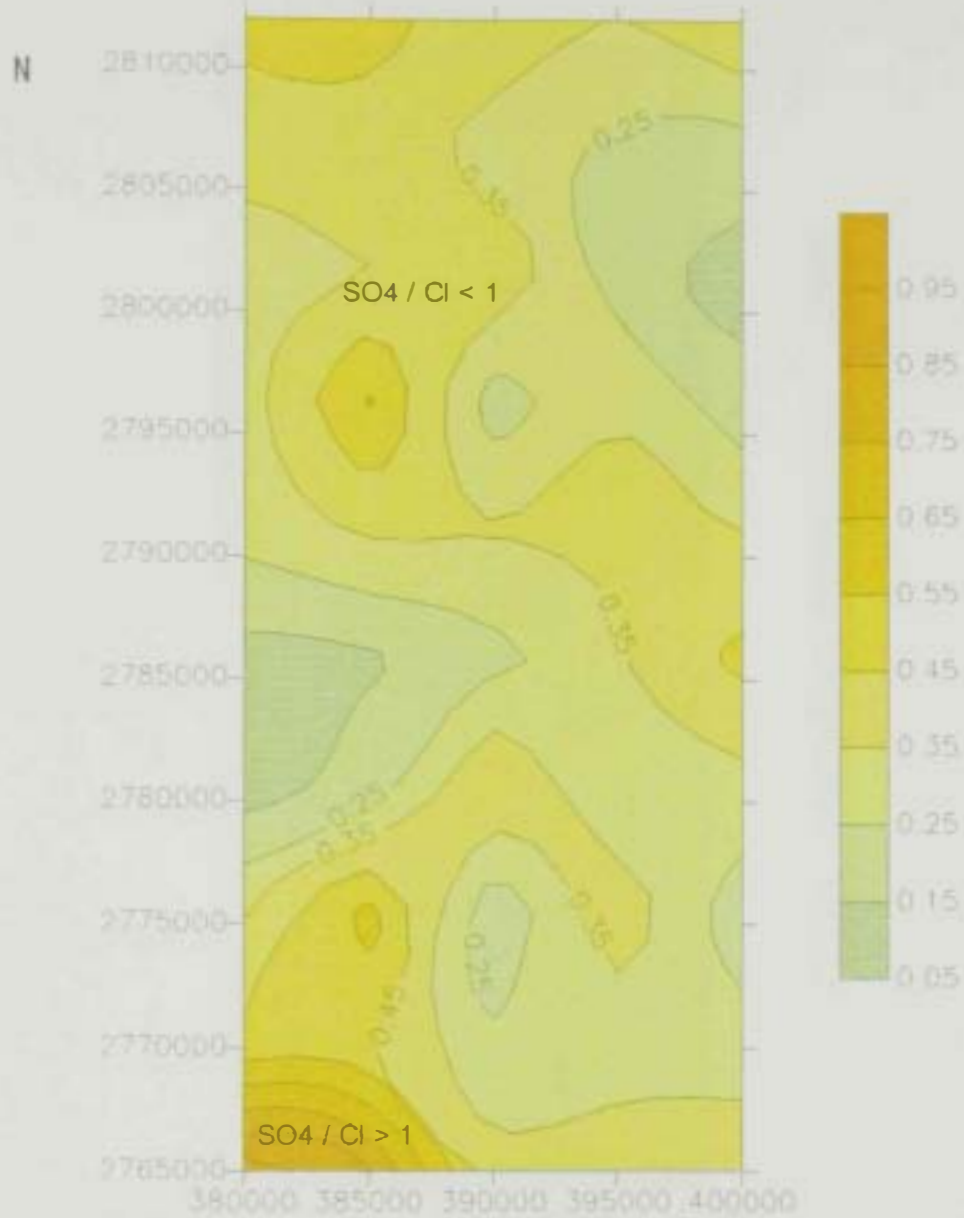


Figure 4.25. Contour map showing the distribution of SO_4 / Cl ratio in groundwater of the study area in 1996.

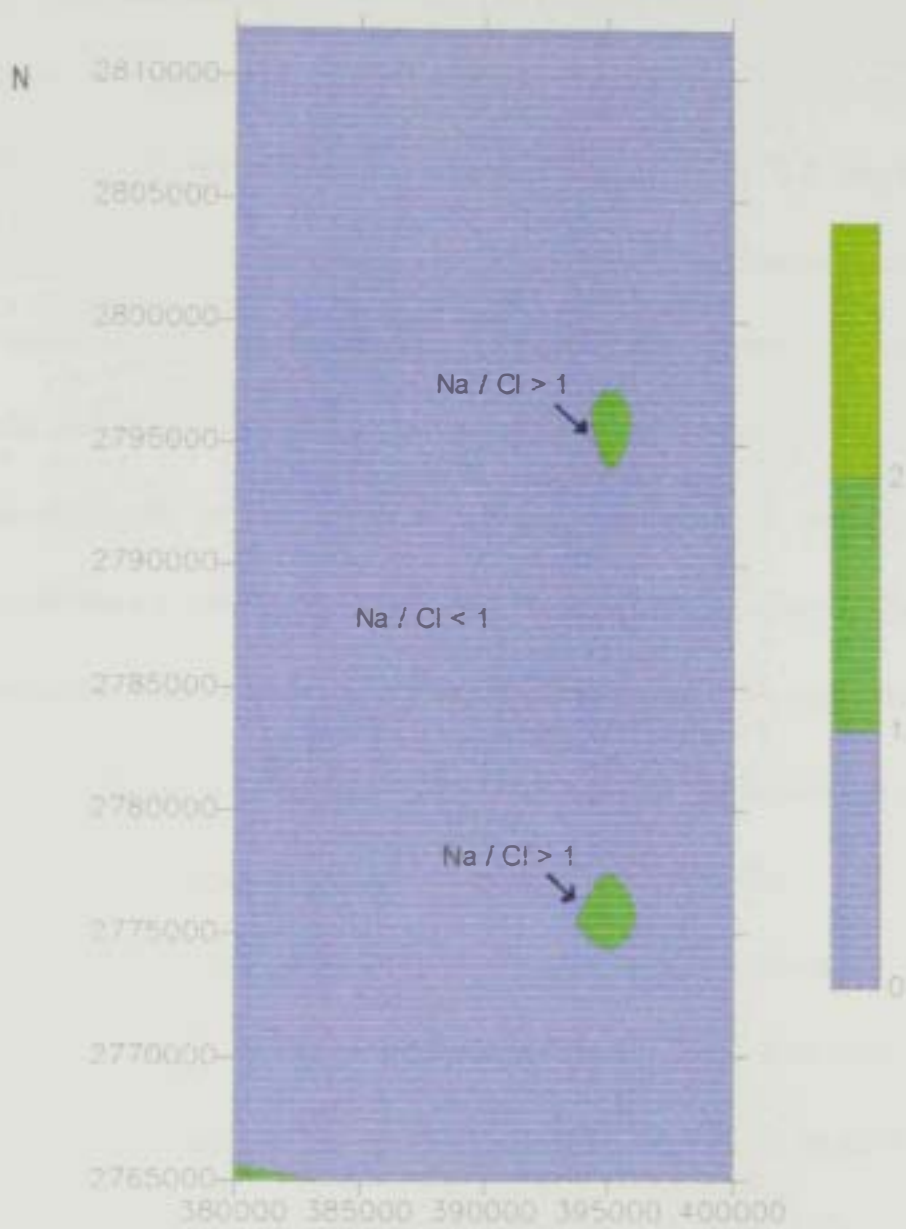


Figure 4.26. Contour map showing the distribution of $\text{Na}^+ / \text{Cl}^-$ ratio in groundwater of the study area in 1996.

the north-central and eastern parts of the study area where intensive municipal and farming activities exist (Figure 4.27).

Iron (Fe) is toxic to some aquatic species at concentrations of 0.32 to 1.00 mg/l. A water quality criterion for iron of 0.3 mg/l has been suggested for domestic uses. For aquatic life, maximum iron content of 1.0 mg/l is the criterion. Iron is a very common element in rocks and soils of the Al Dhaid area. However, because the upper aquifer is free to semi-confined, where enough amounts of oxygen persist, low iron concentrations were measured in groundwater samples collected from most of the study area. Iron content >0.31 exist in the southwestern corner of the study area (Figure 4.28). This area, as indicated from previous discussions, has highest salinity and least quality water.

Water hardness results from the presence of abundant concentrations of Ca^{2+} and Mg^{2+} . The groundwater in the Al Dhaid area varies from soft (total hardness as CaCO_3 is <100 mg/l) to very hard (total hardness as CaCO_3 is >1500 mg/l). Groundwater in the eastern part of the study area is soft, whereas groundwater in the northern, western and southwestern parts is hard to very hard (Figure 4.29).

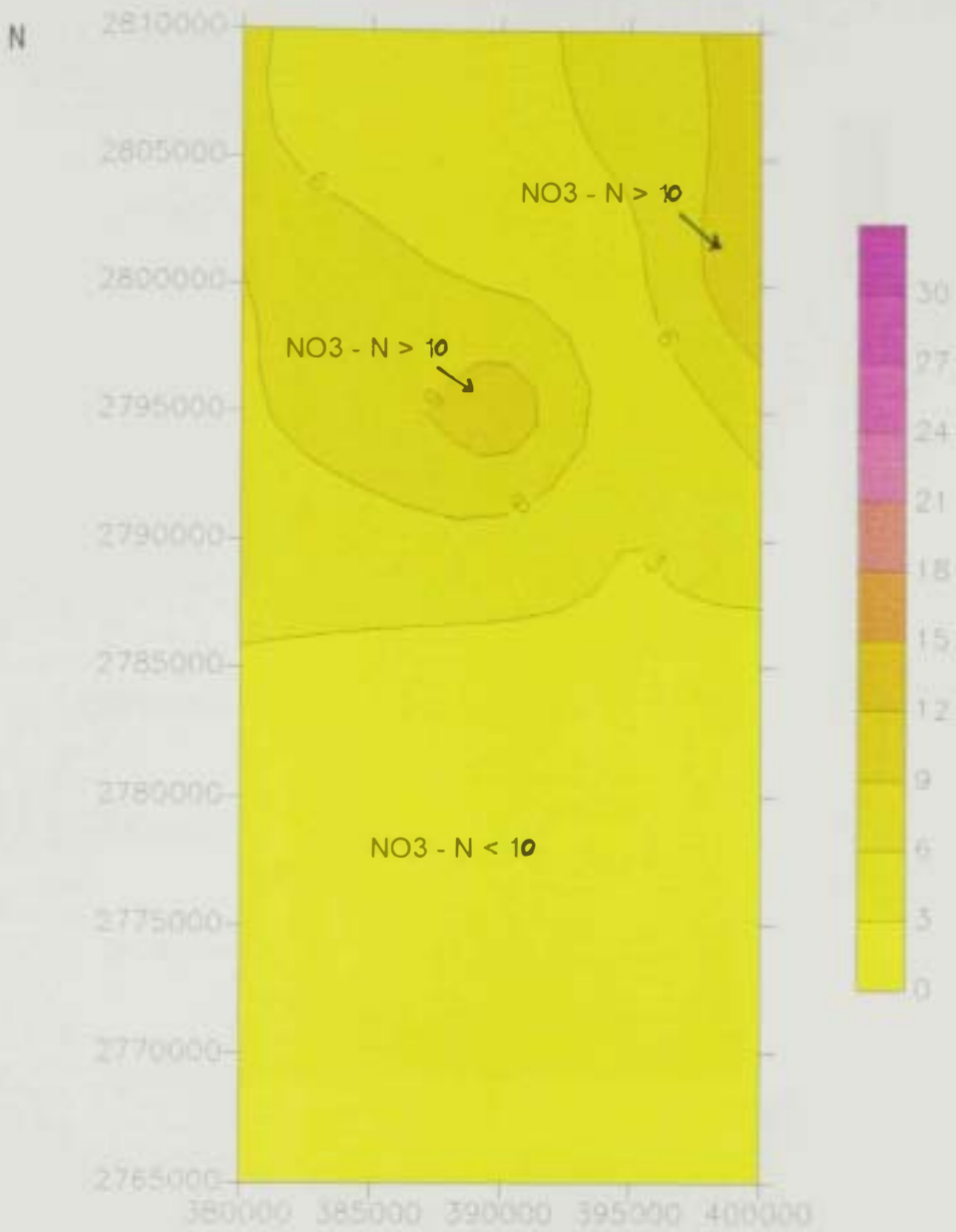


Figure 4.27. Iso-concentration map (mg/l) of the NO₃ in the groundwater of the study area in 1996.

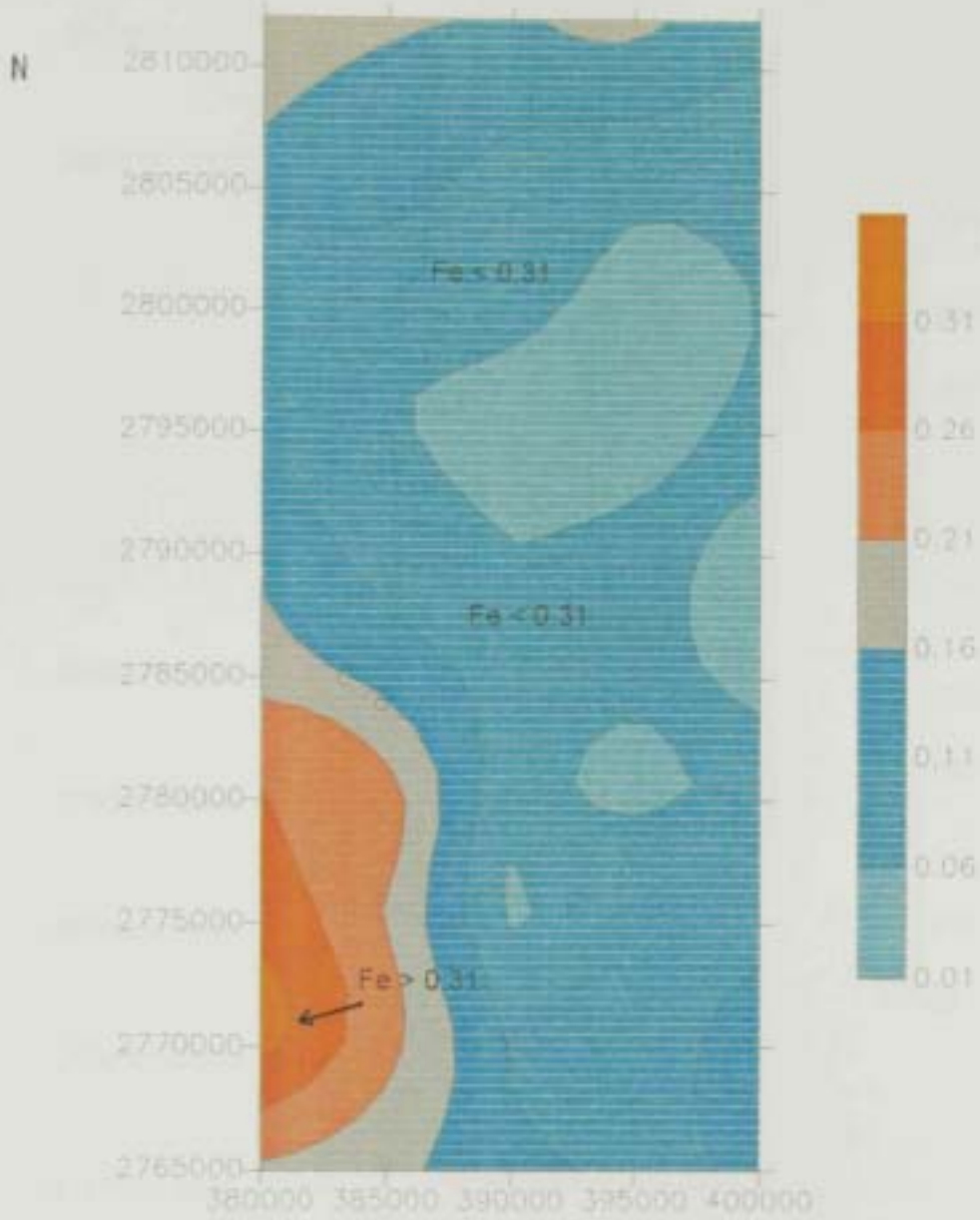


Figure 4.28. Iso-concentration contour map (mg/l) of total iron (Fe) in groundwater of study area in 1996.

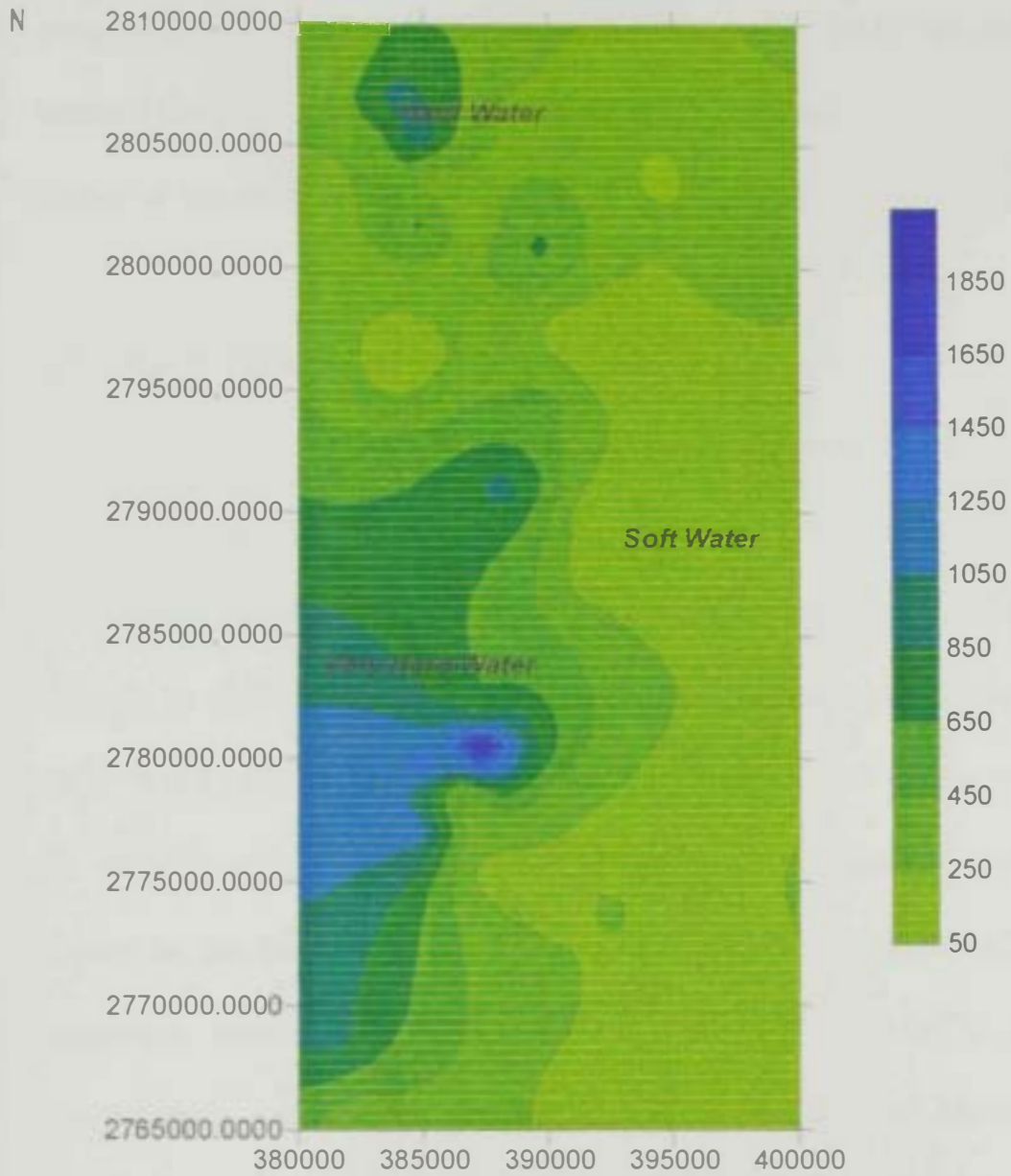


Figure 4.29. Iso-total hardness contour map (mg/l) of groundwater in study area in 1996.

The sodium adsorption ratio (SAR) of groundwater in the Al Dhaid area is predominantly <10 , which is good for irrigation water. But, groundwater in the Fayah limestone Mountains has $\text{SAR} >16$, which is harmful for plants if this water were used for irrigation. The northeastern corner of the study area has SAR values in excess of 13 (Fig. 4.30).

4.3.6 Water Types

The main purpose of the trilinear diagram proposed by Piper (1944) is to show different water types in a particular area. The diamond-shaped field of this diagram consists of two equal triangular fields. Water which appears in the upper triangle has secondary salinity properties, where $(\text{SO}_4^{2-} + \text{Cl}^-)$ exceed $(\text{Na}^+ \text{ and } \text{K}^+)$ and the characteristic water types are Ca and Mg chlorides and sulphates. On the other hand, those which appear in the lower triangle are considered to have primary alkalinity properties where $(\text{CO}_3^{2-} + \text{HCO}_3^-)$ exceed $(\text{Ca}^{2+} + \text{Mg}^{2+})$, and the characteristic water types are Na and K carbonates and bicarbonates (Walton, 1970).

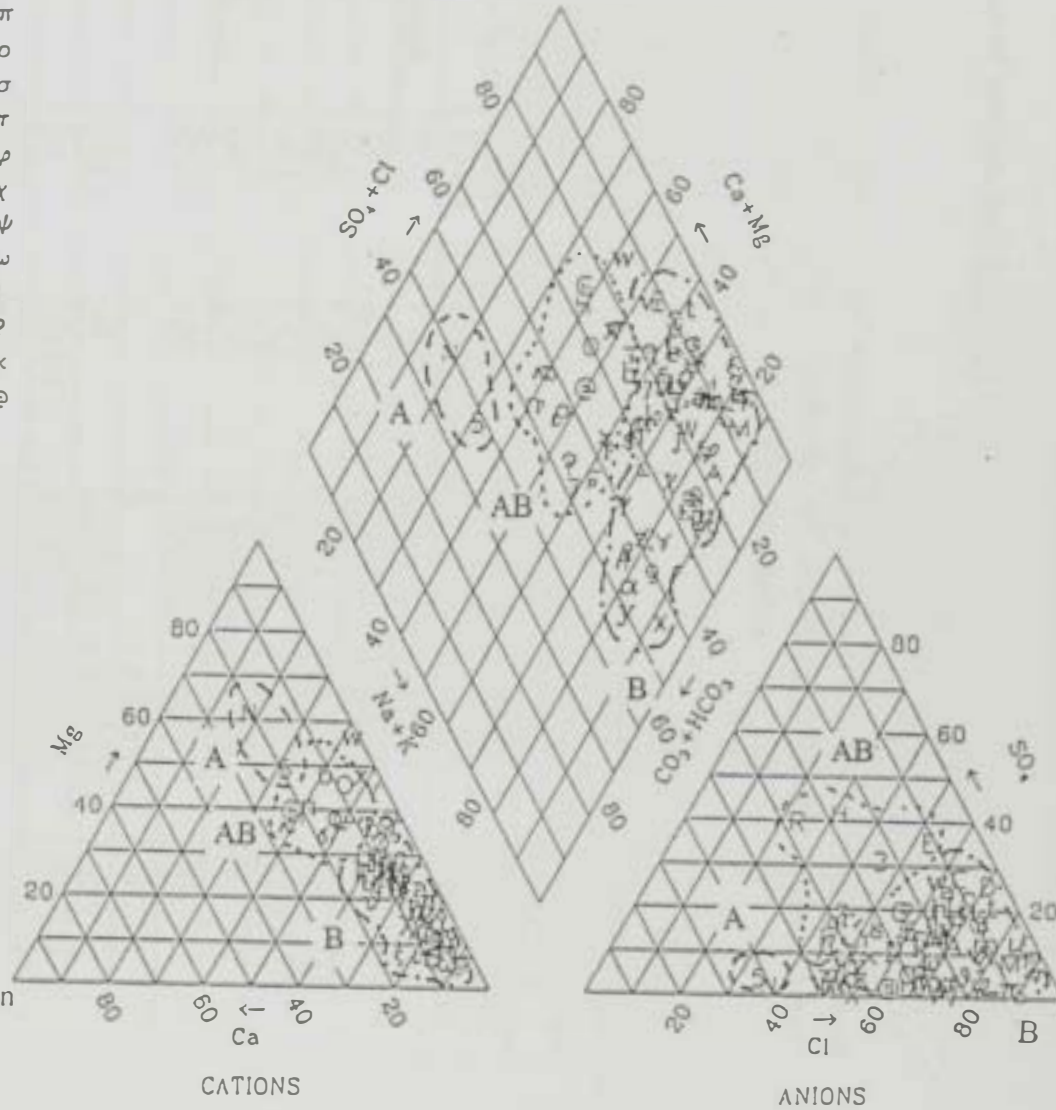
Figure 4.31 shows a trilinear plot groundwater samples from the Al Dhaid area, on which three water types can be distinguished: Type-A water is characterized by High Ca^{2+} and Mg^{2+} ions. This type represents groundwater samples collected from the Northern Oman Mountains in



Figure 4.30. Iso-SAR contour map of groundwater in the study area in 1996.

Figure 4.51. A ternary plot of all groundwater samples collected from the study area in 1996.

1	1	Q	30	p	π
2	3	R	31	q	ρ
3	4	S	32	r	σ
4	5	T	33	s	τ
5	6	U	34	L	ϕ
6	7	V	35	u	χ
7	8	W	36	v	ψ
8	9	X	37	w	ε
9	11	Y	38	x	ι
A	12	Z	39	y	?
B		a	40	z	x
C	14	b	41	α	@
D	16	c	42	β	
E	17	d	43	γ	
F	18	e	44	δ	
G	19	f	45	ε	
H	20	g	49	ζ	
I	21	h	51	η	
J	22	i	53	θ	
K	23	j	54	ι	
L	24	k	55	κ	
M	26	l	56	λ	
N	27	m	58	μ	
O	28	n	59	ν	
P	29	o	60	ξ	



Type A : Water of Northern Oman Mountain
 Type B : Water of gravel plain
 Type AB: Water of mixed origin

UAE, which is located in the eastern part of the study area. Type-B water is dominated by Na^+ and Cl^- ions and represents water samples collected from the gravel plain. Type-AB waters are groundwater samples of mixed origin of both A and B types.

Table 4.3 Comparison of water-quality parameters in the study area and the drinking water standards of the World Health Organization (WHO, 1984) and GCC (1993) standards.

Parameter	Study area			WHO	GCC
	Maximum	Minimum	Mean	Guideline	Max. level
PH	11.20	6.95	7.81	6.5 – 8.5	605 – 8.5
Temp. °C	43.10	28.20	34.32		
TDS	1420	440	894	1000	100 - 1000
EC	9170	366	2759	1400	160 - 1400
Hardness	?	?	?	500	500
Ca^{2+}	271	6	39	75 - 200	200
Mg^{2+}	379	6	75	30 - 150	30 – 150
Na^+	1615	15	422	200	200
HCO_3^-	488	37	243.99		
Cl^-	2379	55	632.82	250	250
NO_3^-				10	10
SO_4^-	1861	4	228.99	200 – 400	400
<i>F</i>	14	0.10	4.84	1.50	0.6 – 1.7
<i>Fe</i>	0.35	0	0.01	0.3 – 1	0.30
<i>Zn</i>	0.20	0.10	0.15	5	5
<i>Cu</i>	0.10	0.10	0.10	1 – 1.5	1
<i>Pb</i>	0.20	0.01	0.06	0.05	0.05

CHAPTER 5

GEOGRAPHICAL INFORMATION SYSTEM (GIS) MODELING OF GROUNDWATER POTENTIALITY

CHAPTER 5

GEOGRAPHICAL INFORMATION SYSTEM (GIS) MODELING OF GROUNDWATER POTENTIALITY

5.1 Introduction

The geographic information system (GIS) is an efficient tool for studying, assessment and management of natural resources (Lang, 1998). Rofail, et al. (1998) defined GIS as “an organized collection of computer hardware, software, geographic data and personal design to efficiently capture, store, update, manipulate, analyze and display all forms of geographically referenced information“.

In the present study, GIS technique were used to cross correlate soil suitability map, groundwater quality and hydraulic head maps, in addition to the prevailing geologic structures. The results of this correlation could guide future groundwater development plans and agriculture activities in the study area and other areas in the country as well.

5.2 Model Construction

The analyses were carried out using ArcView GIS 3.2 package (ESRI products) with ArcView Spatial Analyst. Figure 5.1 is the flow chart of the analytical model developed to achieve the objectives of this part of the study. Two sets of data were included in the database constructed by

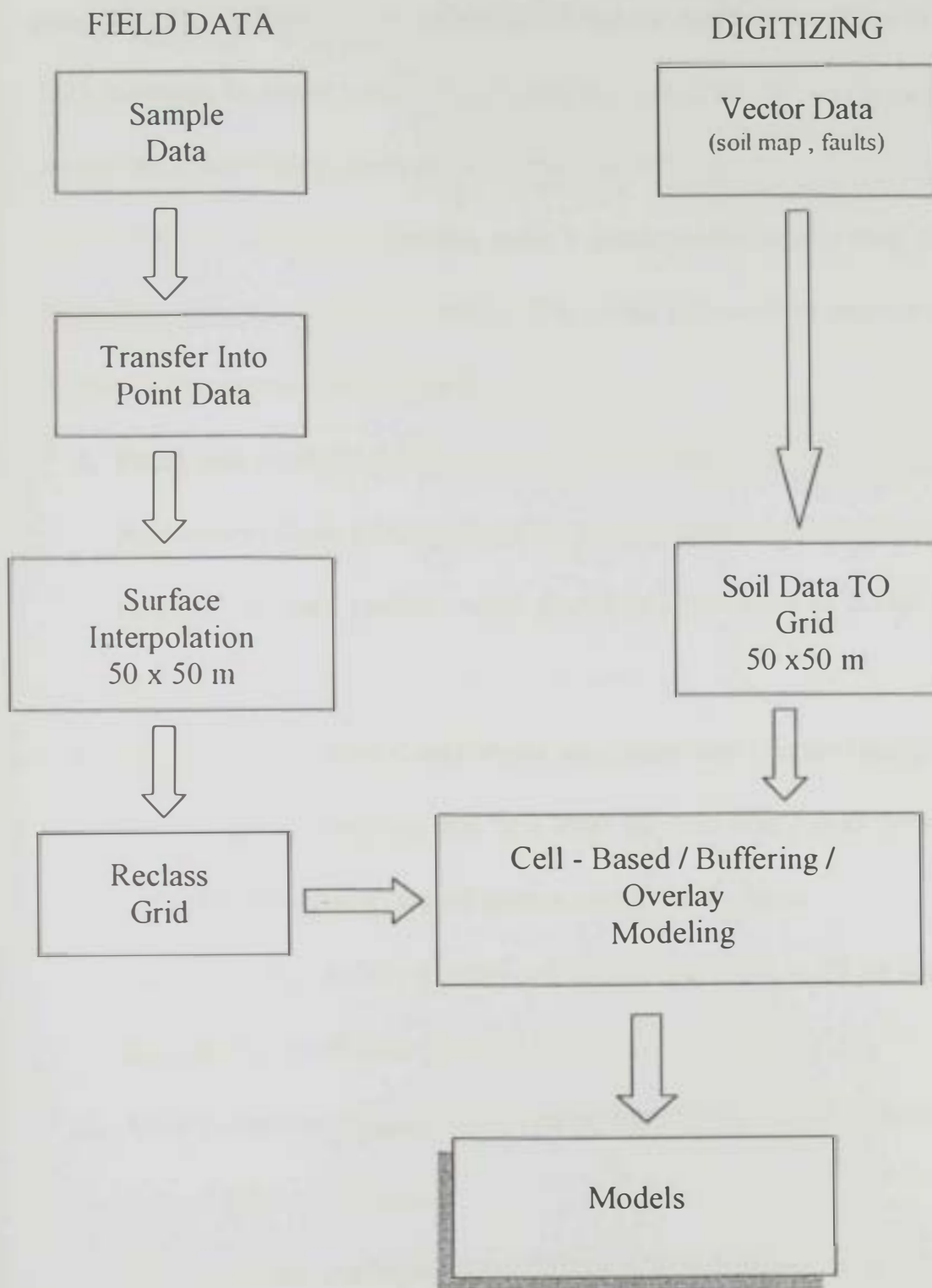


Figure 5.1. A flow chart of the GIS analytical model of the study area

the researcher for the purpose of this study; field surveyed data and digitized data. The field data describe specific parameters such as geographic coordinates (x,y) of different values such as water level and TDS contents in water wells. These data are based on the result of field survey and laboratory analyses of groundwater samples. The digitized data included a soil classification map, a geologic structures map and a map showing major drainage basins. The steps followed in construction of the present model are as follows:

- a. Field data including point data of TDS, total hardness, Sodium Adsorption Ratio (SAR), depth to groundwater and coordinates (x,y) of all data points were stored in data base of a dbf 4 format.
- b. Field data were then transformed into point data (vector) using a unified grid, based on the soil map for the study area as an extend (coordinates) for all output maps and models.
- c. Surface interpolation (raster) of an accuracy 50 x 50 m was assigned for each data point.
- d. Data points were regroup according to selected criteria into re-classed grid-zone maps.
- e. The soil map, geologic structures map and drainage lines map were digitized into 50 x 50 m grid data (raster).

- f. Selected layers of grid data were superimposed according to certain criteria using the cell-based modeling technique.
- g. Other models were constructed, based on buffering and overlaying techniques of drainage lines, major geologic structures and TDS zoned maps.

The input data of the GIS model of the Al Dhaid area can be generally described as follows:

a. Groundwater Observation Wells

Two groups of groundwater observation wells were used. The first group was the observation wells of Ministry of Agriculture and Fisheries (MAF). These wells were used to measure the groundwater depth from the land surface (depth to water). The second group of wells was the pumping wells in private farms. These wells were used for collection of water sample for chemical analysis.

b. Total Dissolved Solids (TDS)

The groundwater salinity values in milligrams per liter (mg/l) were deduced from the electrical conductivity values. Iso-salinity contour maps were constructed as illustrated in Figures 5.2 and 5.3.

c. Total Hardness (TH)

The iso-total hardness zoned map of groundwater in the study area is illustrated in Figure 5.4. The dark blue zones represent areas of



Figure 5.2.
Distribution of Total Dissolved Solids (TDS) in mg/L
of groundwater samples from the study area.



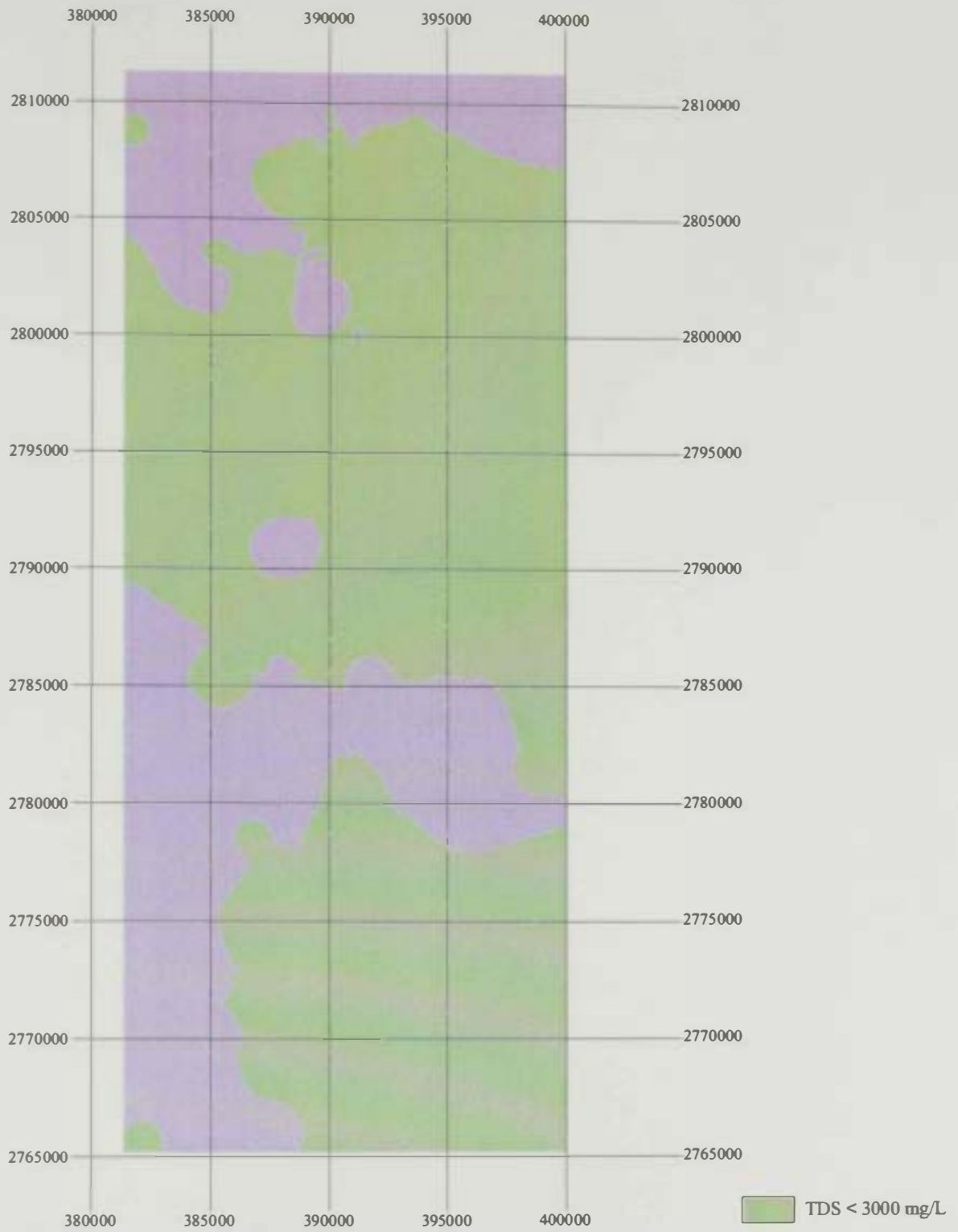
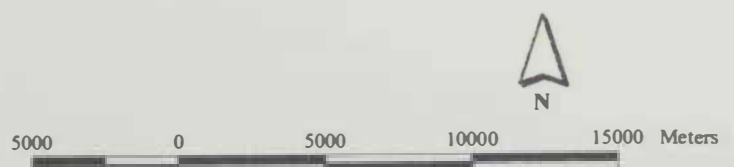


Figure 5.3
Distribution of Total Dissolved Solids (TDS) in mg/L
of groundwater from the study area.



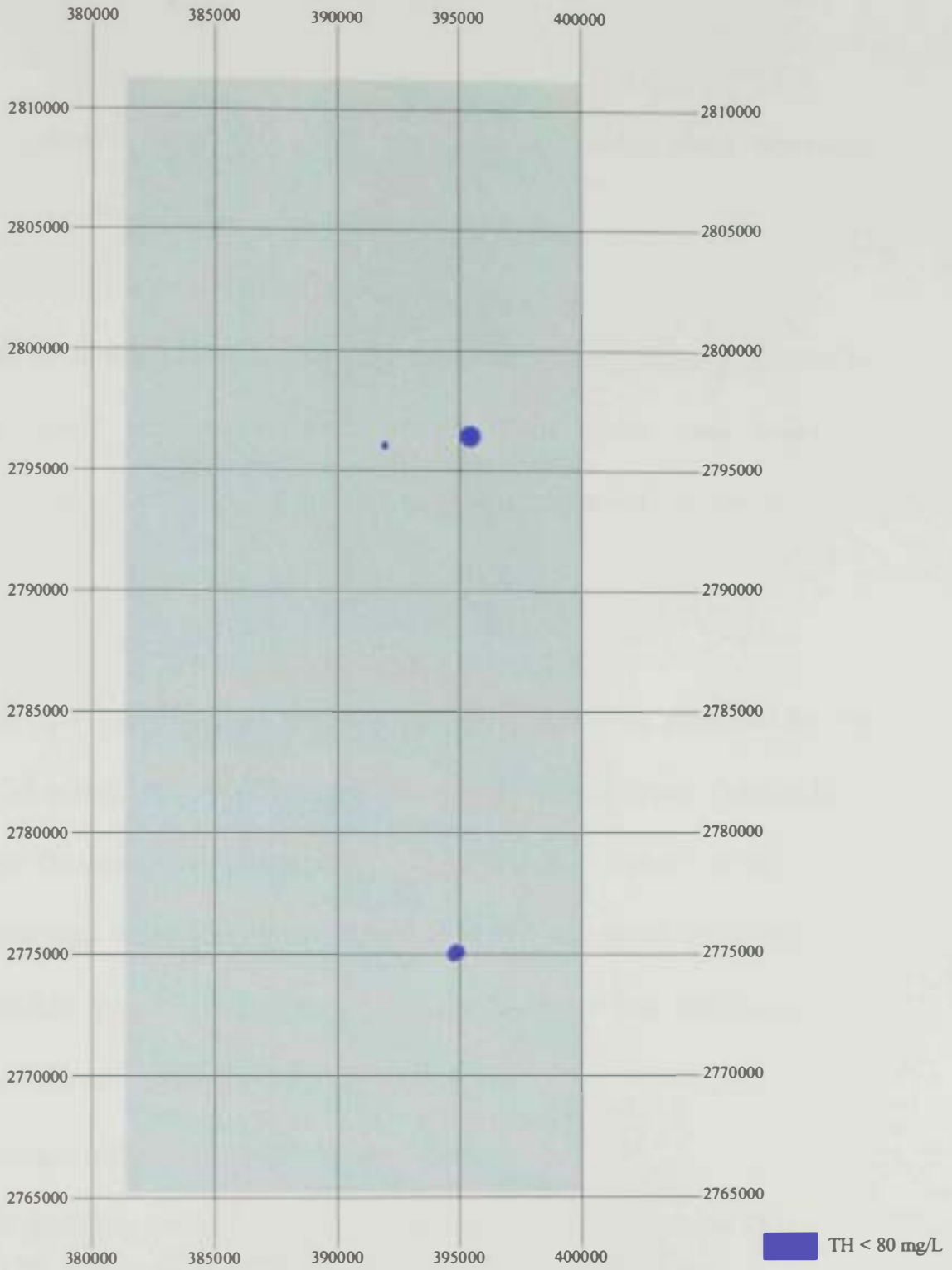
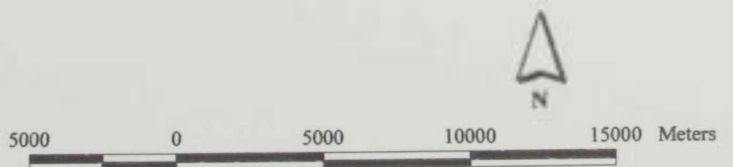


Figure 5 4
Distribution of Total Hardness (TH) in mg/L
of groundwater samples from the study area.



groundwater with $TH \leq 80$ mg/l. the light blue zone represent groundwater with $TH > 80$ mg/l.

d. Sodium Adsorption Ratio (SAR)

The SAR was calculated for all groundwater samples and presented in the zoned map on Figure 5.5. The light violet zone refers to groundwater with $SAR \leq 10$. The dark violet zone refer to groundwater with $SAR > 10$

e. Soil Classification

The soil classification map for the study area was prepared by the JICA project in 1996. The map contains seven soil types: Calciorthids, Torrifluvents, Torripsaments-2, Gypsiorthids, Torriorthents, Wadi Beds and Rock Outcrops. The first three soil types are considered suitable types for agriculture, whereas the other four soil types were considered unsuitable types for agriculture.

f. Geologic Structures and Drainage Lines.

The geologic structures were deduced from the geophysical data presented in Chapter 3. The drainage lines were traced and digitized from soil classification map of the study area.

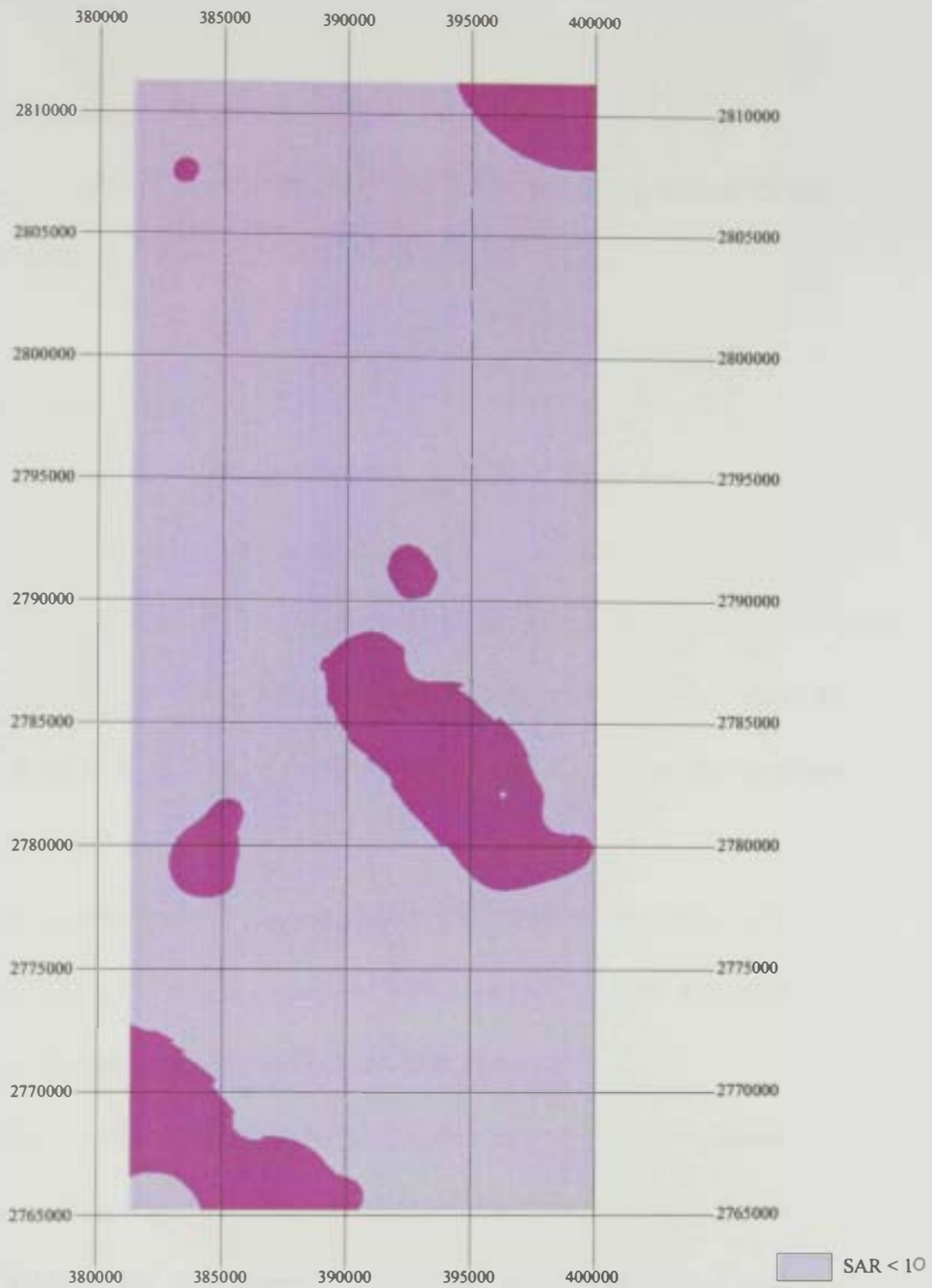
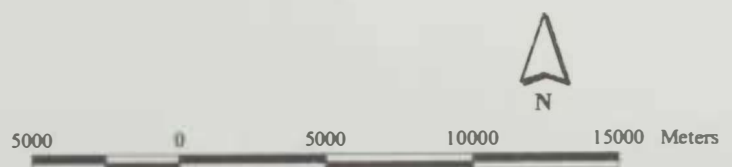


Figure 5.5.
Distribution of Sodium Adsorption Ratio (SAR)
in groundwater from the study area.



5.3 Discussion of Results

The following discussion includes the zoned maps, output models and interrelation between different parameters.

5.3.1 Zoned Maps

The groundwater salinity distribution maps show two distinct zones. Figure 5.2 shows that the groundwater with $\text{TDS} \leq 1500 \text{ mg/l}$ occurs parallel to the eastern and southeastern boundary of the study area; close to the Northern Oman Mountains and along the course of main wadis. The $\leq 3000 \text{ mg/l}$ TDS exist into two zones occupying the western and southwestern parts of the study area.

The groundwater in the study area is mainly hard to very hard. Soft water ($\text{TH} \leq 80 \text{ mg/l}$) occurs as two isolated rounded circles along the eastern boundary of the study area (Fig. 5.4).

The calculated SAR values of groundwater in the Al Dhaid area are illustrated in Figure 5.5. Most of the groundwater within the study area has $\text{SAR} \leq 10$. Localized zones in the northeastern and southeastern corners of the study area have SAR values > 10 . Groundwater in these areas is hazardous to soil and plants when it is used for irrigation. The course of wadi kadra is also characterized by high SAR values. The high

SAR values usually characterize the groundwater moving through limestone aquifers.

The depth to groundwater around Al Dhaid is mostly ≤ 45 m except for the area east of Al Dhaid, where the depth to water is greater than 45 m (Fig. 5.6).

JICA (1996) constructed a soil map for the study area. This map shows seven soil types: Calciorthids, Torrifluvents, Torripsaments-2, Gypsiorthids, Torriorthents, Wadi Beds and Rock Outcrops (Fig. 5.7). The Calciorthids, Torrifluvents and Torripsaments-2 soil types are considered as one group which is suitable for agriculture according to the available soil types in UAE (Abrol, 1988). On the other hand, Gypsiorthids, Torriorthents, Wadi Beds and Rock Outcrops represent the second group which was considered unsuitable for agricultural purposes (Fig. 5.8).

The drainage lines dissecting the study area originate in the Northern Oman Mountain in UAE. Almost all wadis move from east to west and northernwest converging in a single wadi channel (Wadi Lamaha). This wadi reaches the Arabian Gulf in the northernwestern corner of the study area (Fig. 5.9). The drainage lines in the mountainous areas are controlled as indicated by the rectangular and parallel patterns, whereas the drainage pattern of wadis crossing the gravel plain in western part of the study area is mainly dendritic. The major fault lines affecting the study area are the

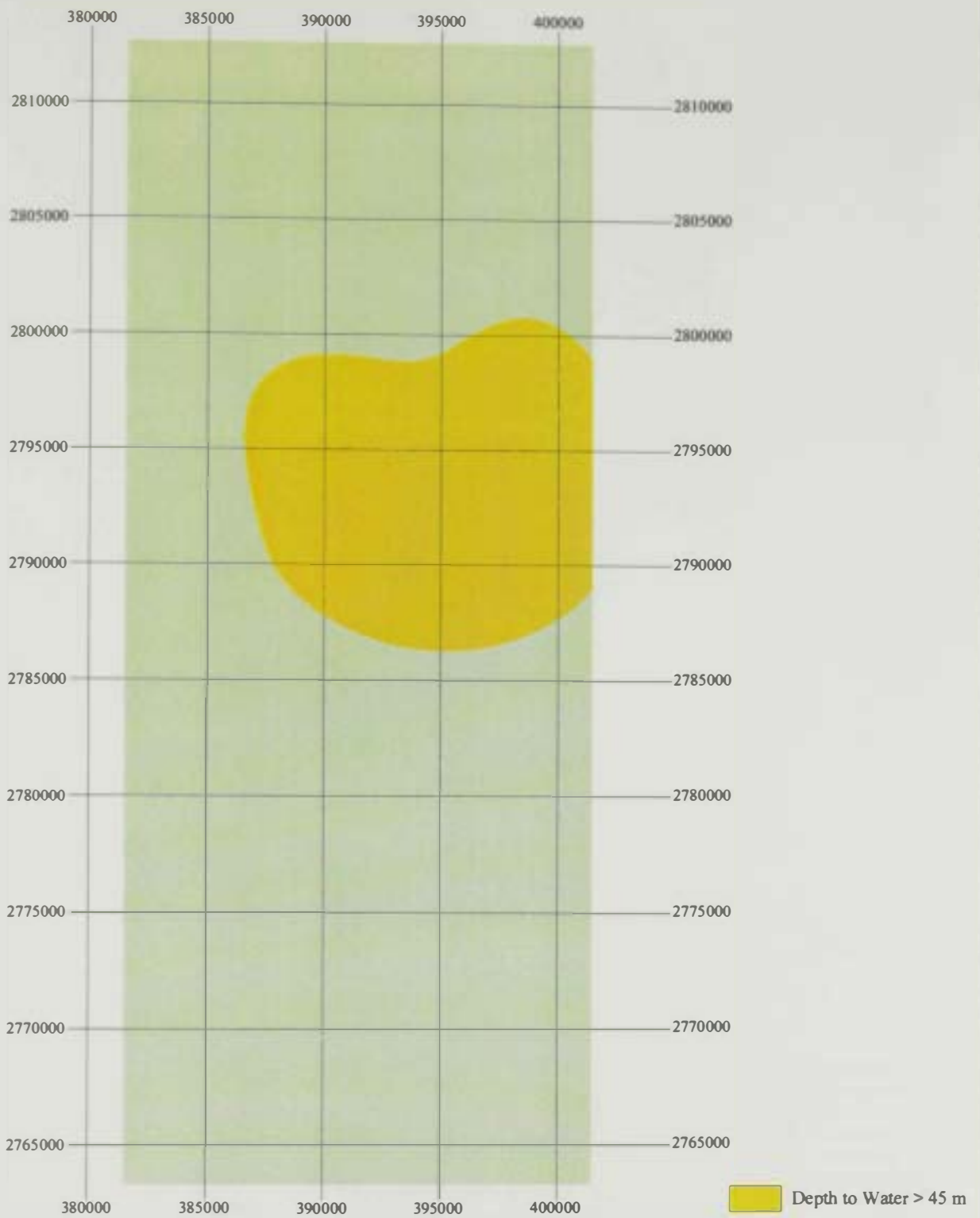
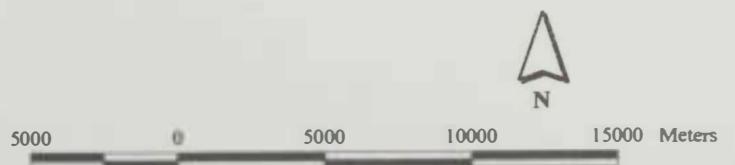


Figure 5.6.
Dipth to groundwater in the study area.



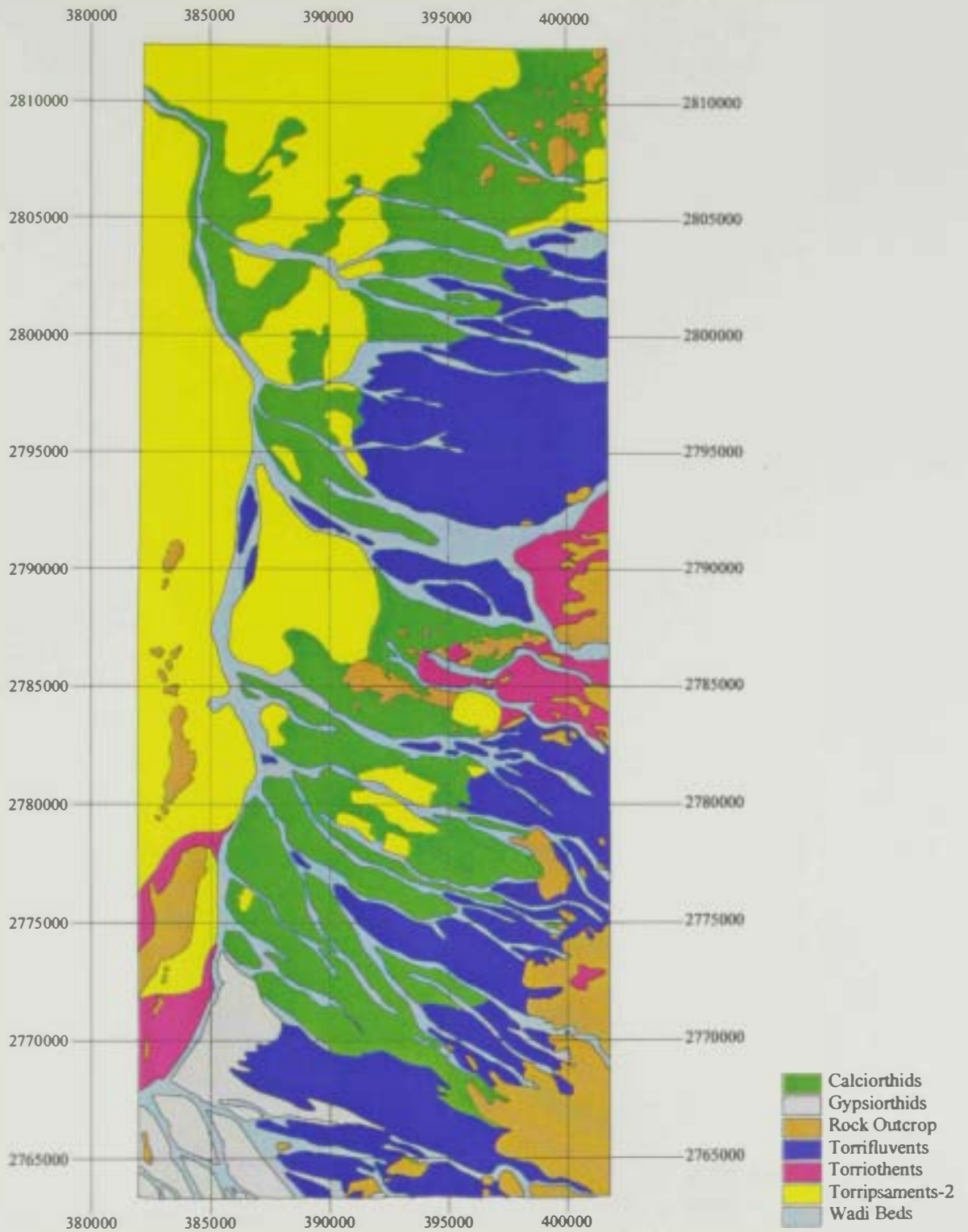
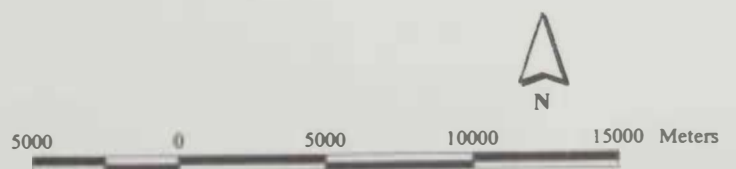


Figure 5.7
Soil Classification for the study area.
Source: JICA 1996.



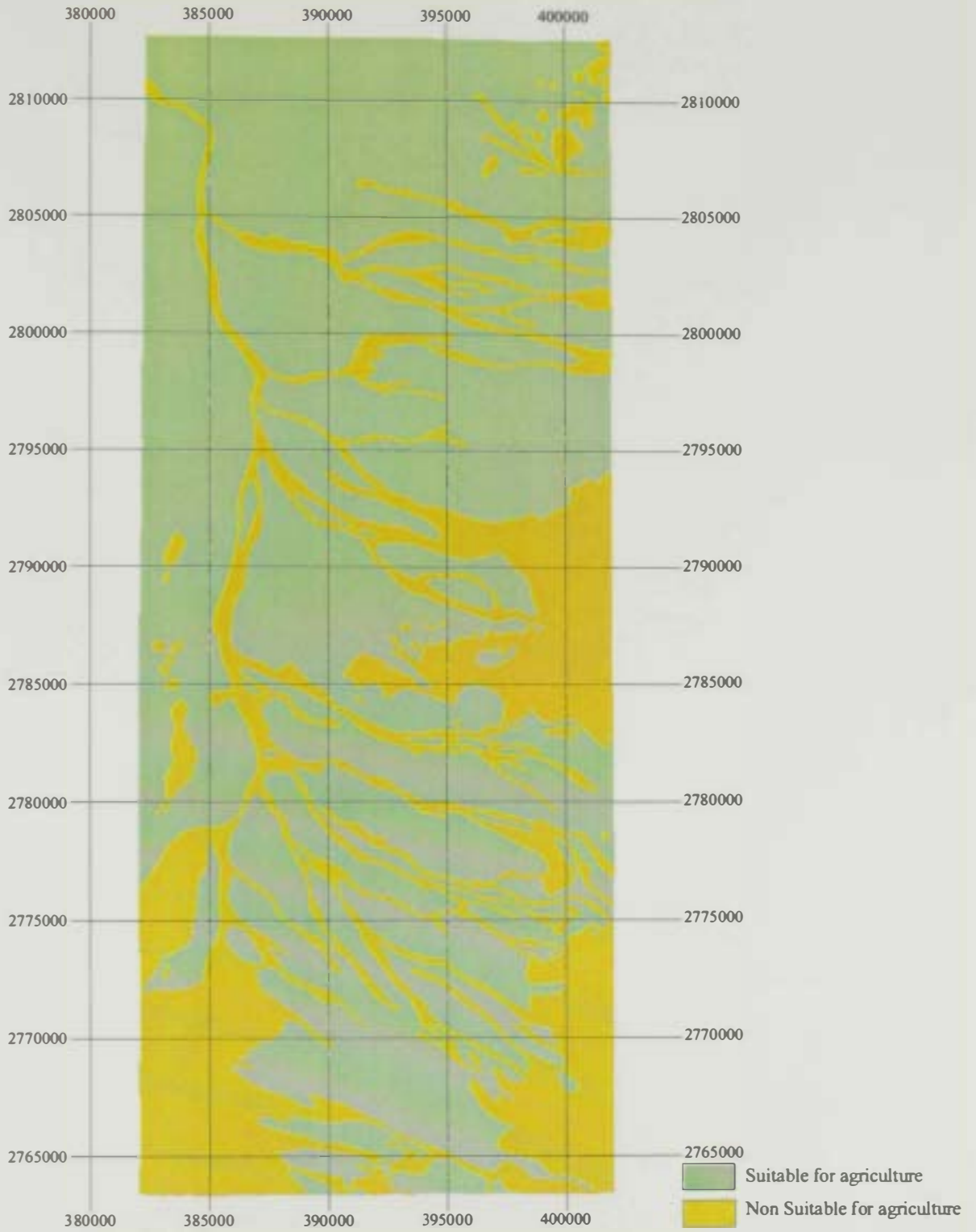
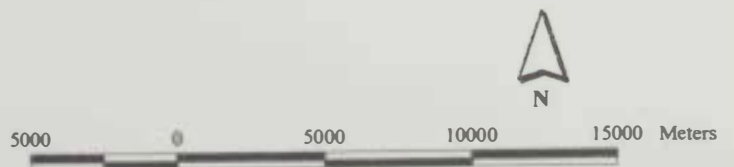


Figure 5.8
Different soil categories within the study area.



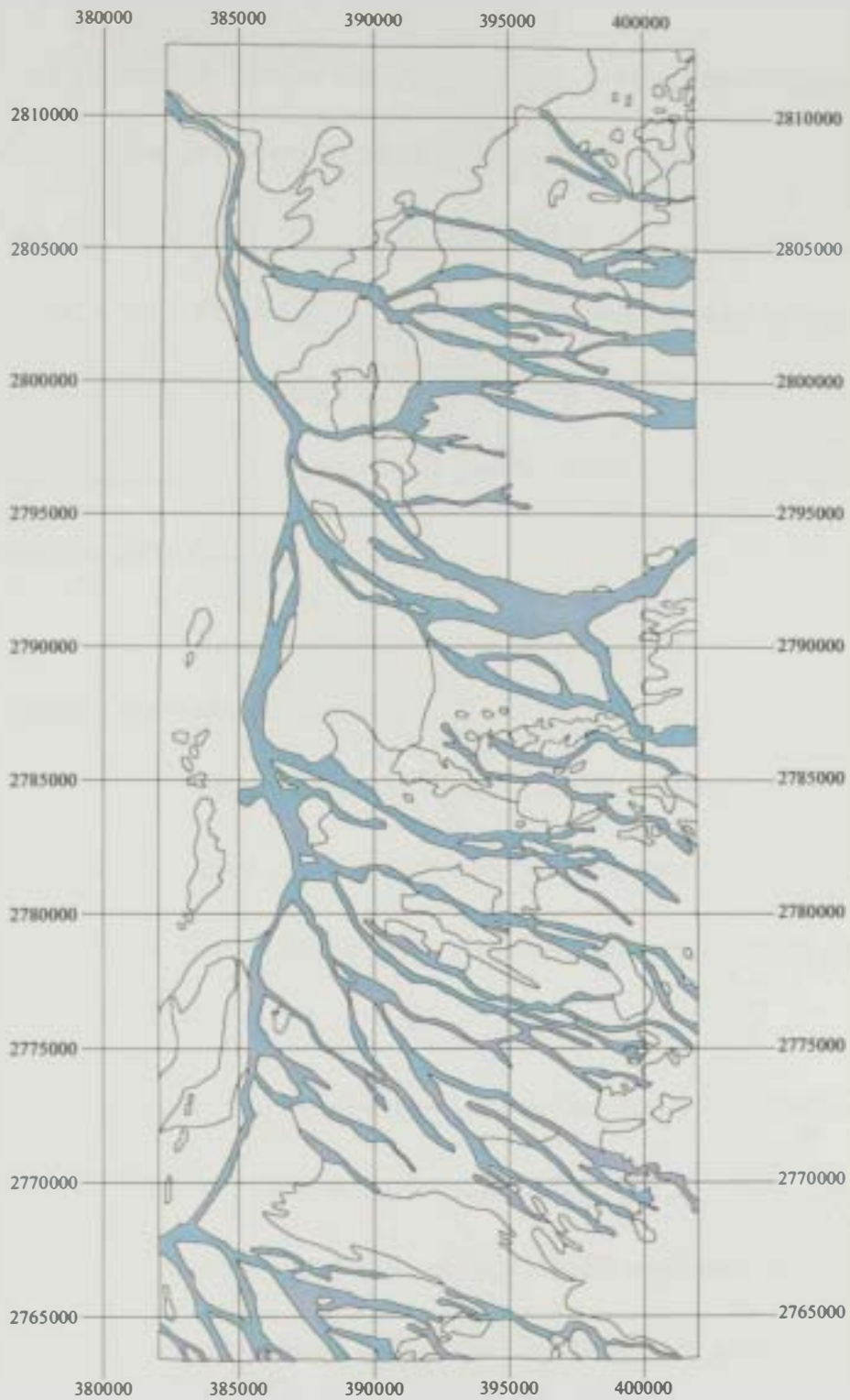
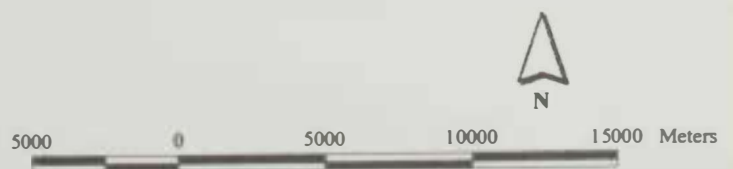


Figure 5.9
The main drainage lines within the study area.



northeast-southwest Dibba zone trend, the northwest-southeast Wadi Ham line and the east-west trend of Hatta zone (Fig. 5.10)

Both the Dibba zone trend and Wadi Ham line have major influence on the study area. Figure 5.11 illustrates a combined map of major fault trends and the main drainage lines. This map shows that several stream segments coincide with certain fault trends, especially in the eastern and southeastern parts of the study area.

5.3.2 Cross Correlation Models

The following discussion is based on combination of selected parameters represented on the previously discussed maps in order to assess the groundwater potentiality and land use planning in the study area.

The combination of groundwater salinity (expressed in TDS contents) and total hardness (TH) zoned maps (Fig. 5.12) show that most groundwater in the study area has salinity >1500 mg/l and TH > 80 mg/l. Only two small rounded areas east of Al Dhaid contain groundwater with TDS ≤ 1500 mg/l and TH ≤ 80 mg/l.

A combination of groundwater of TDS ≤ 3000 mg/l and SAR ≤ 10 is illustrated in Figure 5.13. The figure shows that the groundwater in most of the study area is suitable for irrigation. Areas in the north and

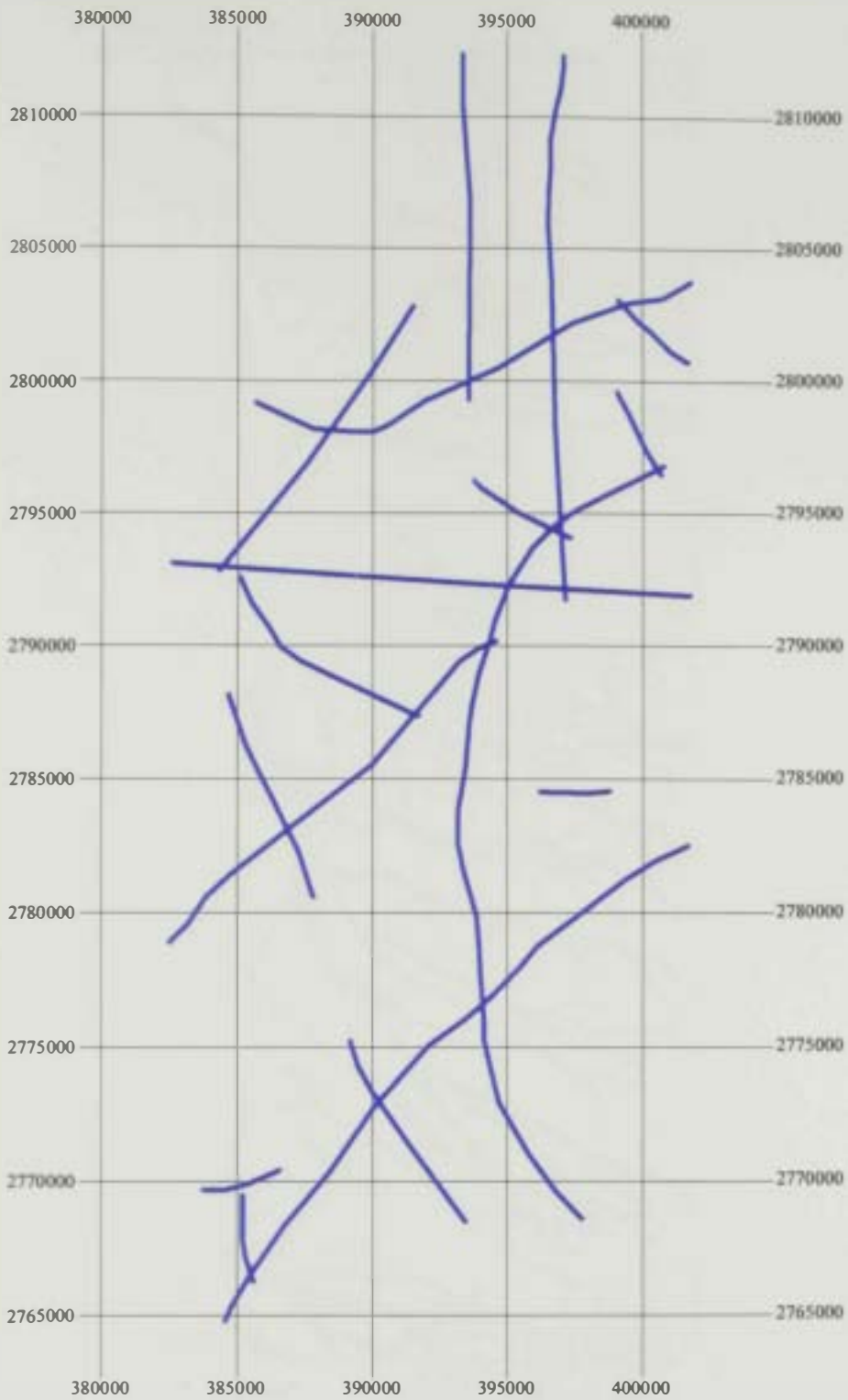
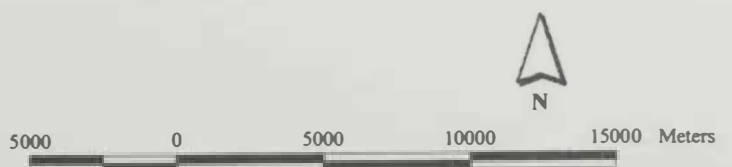


Figure 5.10
Major fault trends affecting the study area, Digitized from gravity data.



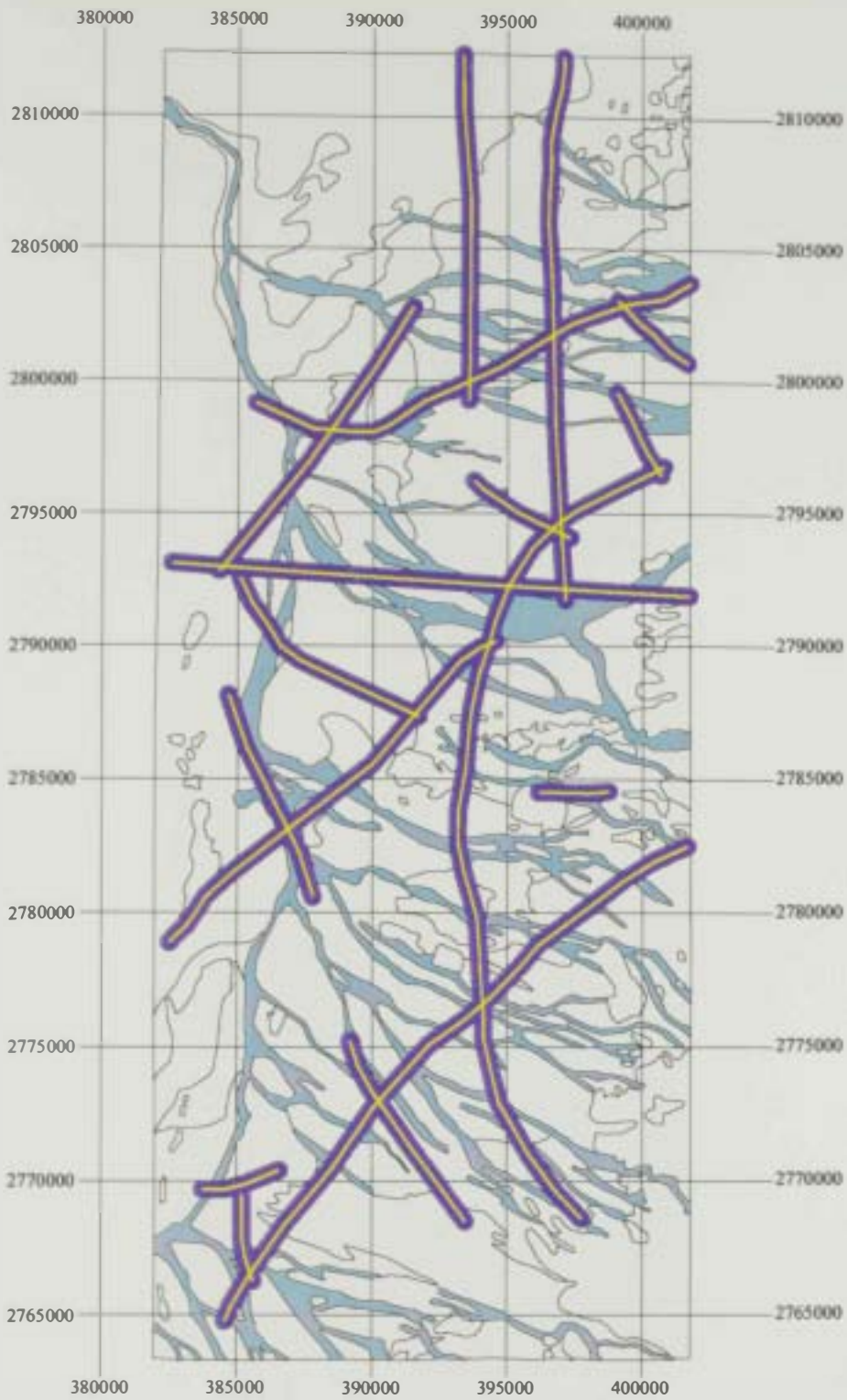
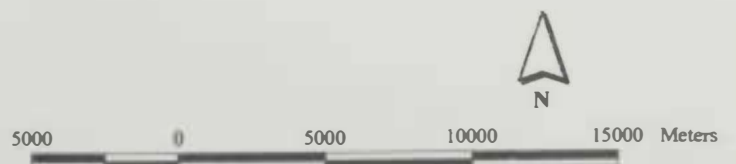


Figure 5.11.
Influence of structural trends on the drainage network of the study area.



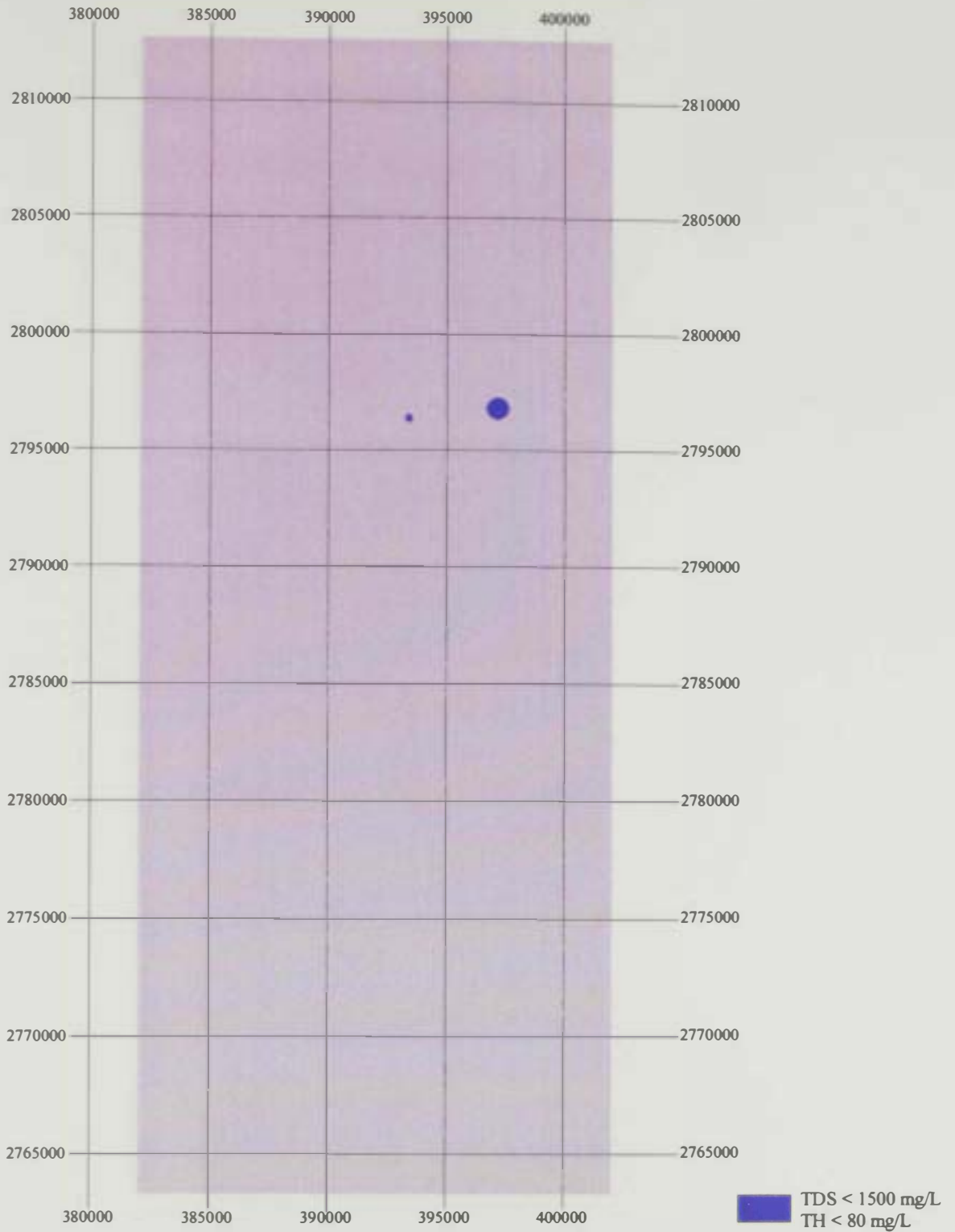


Figure 5.12
Total Dissolved Solids (TDS) in mg/L & Total Hardness in mg/L
of groundwater samples from the study area.



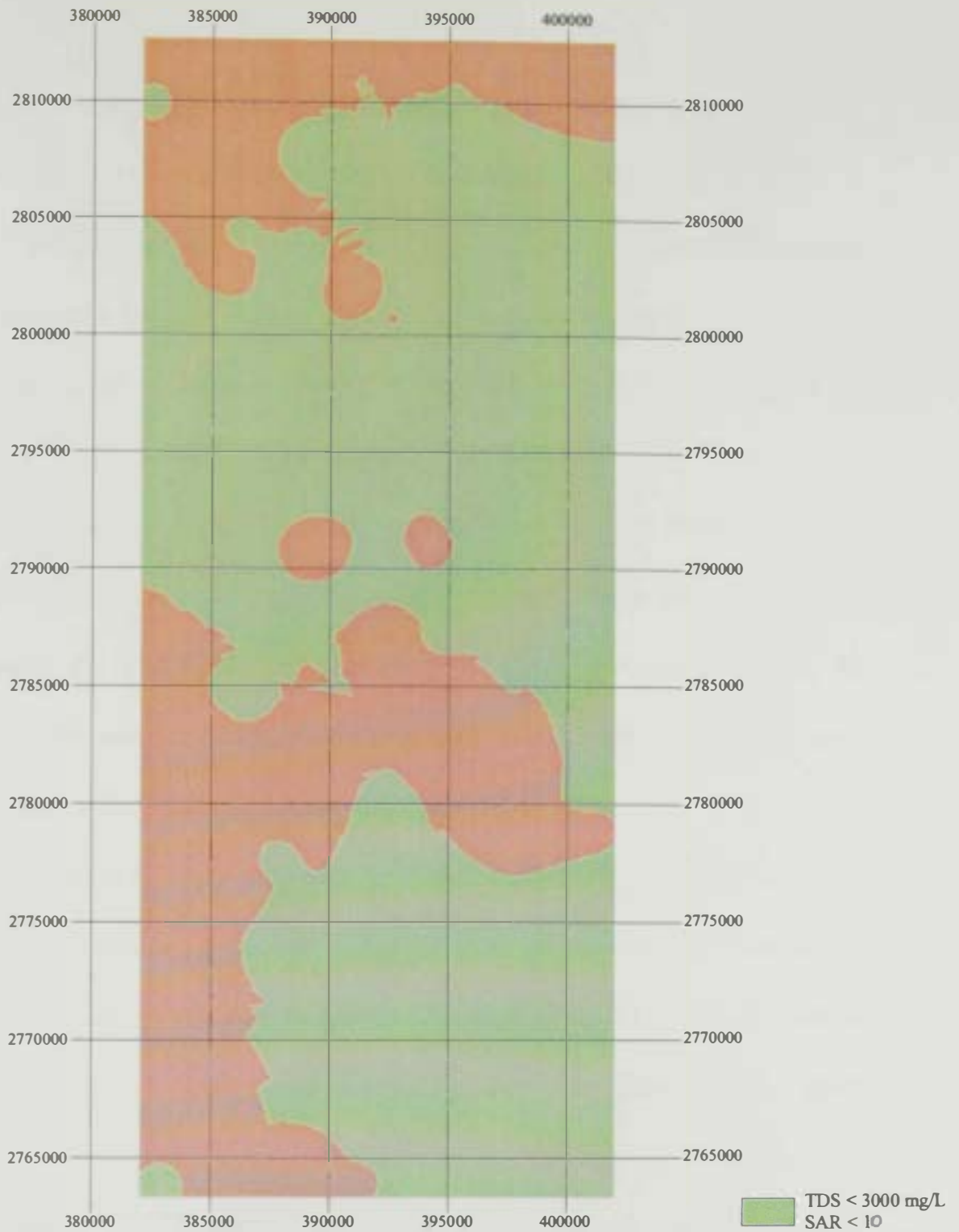


Figure 5.13.
Total Dissolved Solids (TDS) in mg/L
and Sodium Adsorption Ratio (SAR) for the study area.



southwestern parts have high values of salinity and SAR and their groundwater is not suitable for irrigation of traditional crops.

The shallow (depth to water ≤ 45 m) fresh groundwater (TDS ≤ 1500 mg/l) occurs in the southern part of the study area (Figure 5.14). There were no areas of depth to water ≤ 45 m, TDS ≤ 1500 mg/l and TH ≤ 80 mg/l.

The zones of moderate salinity groundwater (TDS ≤ 3000 mg/l), low SAR values (≤ 10) and soil type suitable for agriculture are illustrated in Figure 5.15. The north central part of the study area, including the Al Dhaid city, and the south central part meet these criteria. Both areas are, therefore, suitable for agriculture.

The shallow (depth to water ≤ 45 m), moderate quality groundwater (TDS ≤ 3000 mg/l) with low SAR (≤ 10) occurs to north and west of the Al Dhaid city in addition to the south central area (Figure 5.16). These areas coincide with the zones suitable for agriculture illustrated in Figure 5.15.

Figure 5.17 show the zones within the study area in which groundwater is shallow (depth to water ≤ 45 m), of a moderate salinity (TDS ≤ 3000 mg/l), low SAR (SAR ≤ 10) and soil types suitable for agriculture. This model again supports the results illustrated in Figures 5.15 and 5.16.

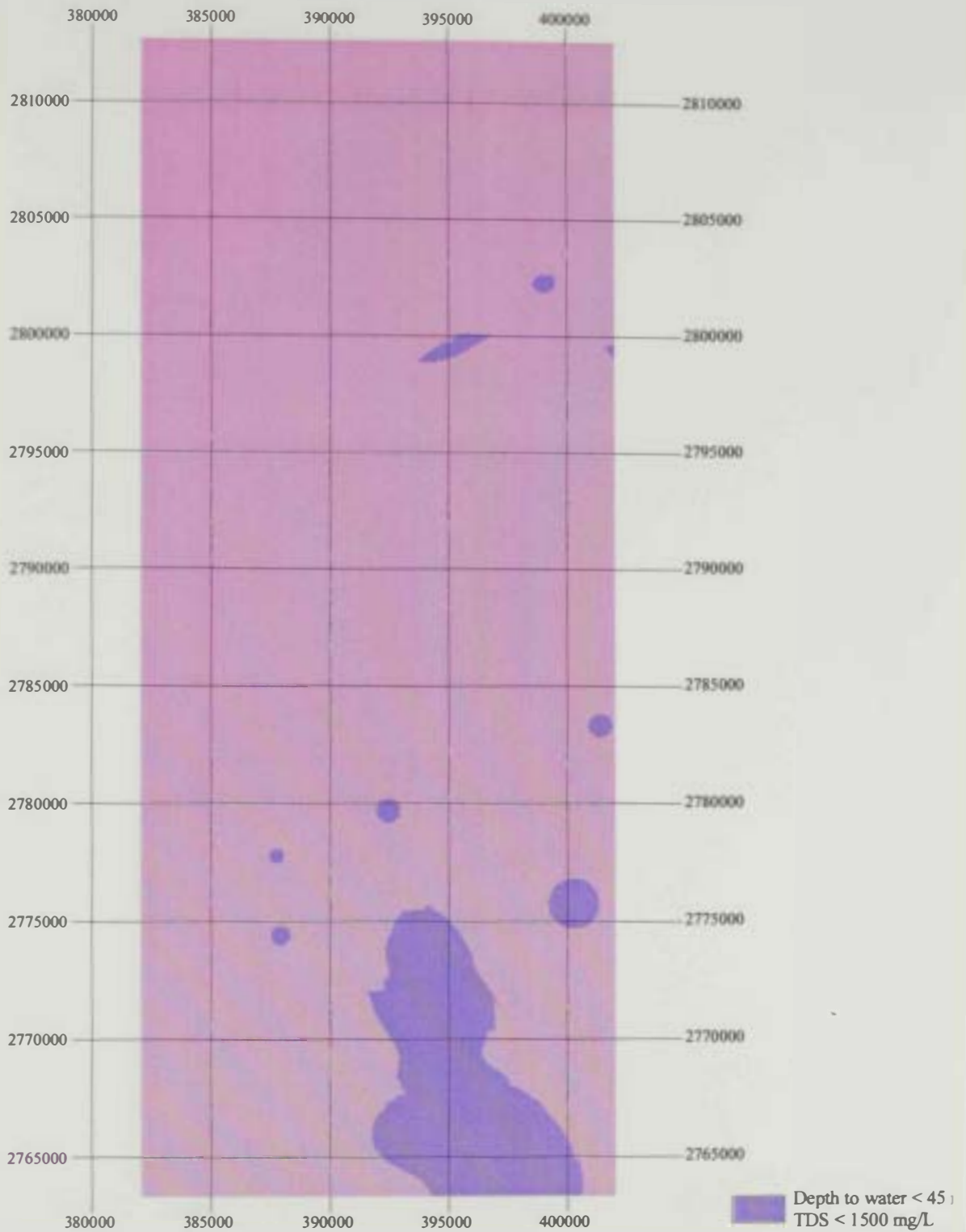
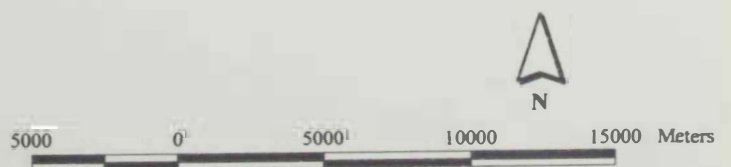


Figure 5 14.
 Depth to groundwater and Total Dissolved Solids (TDS) in mg/L



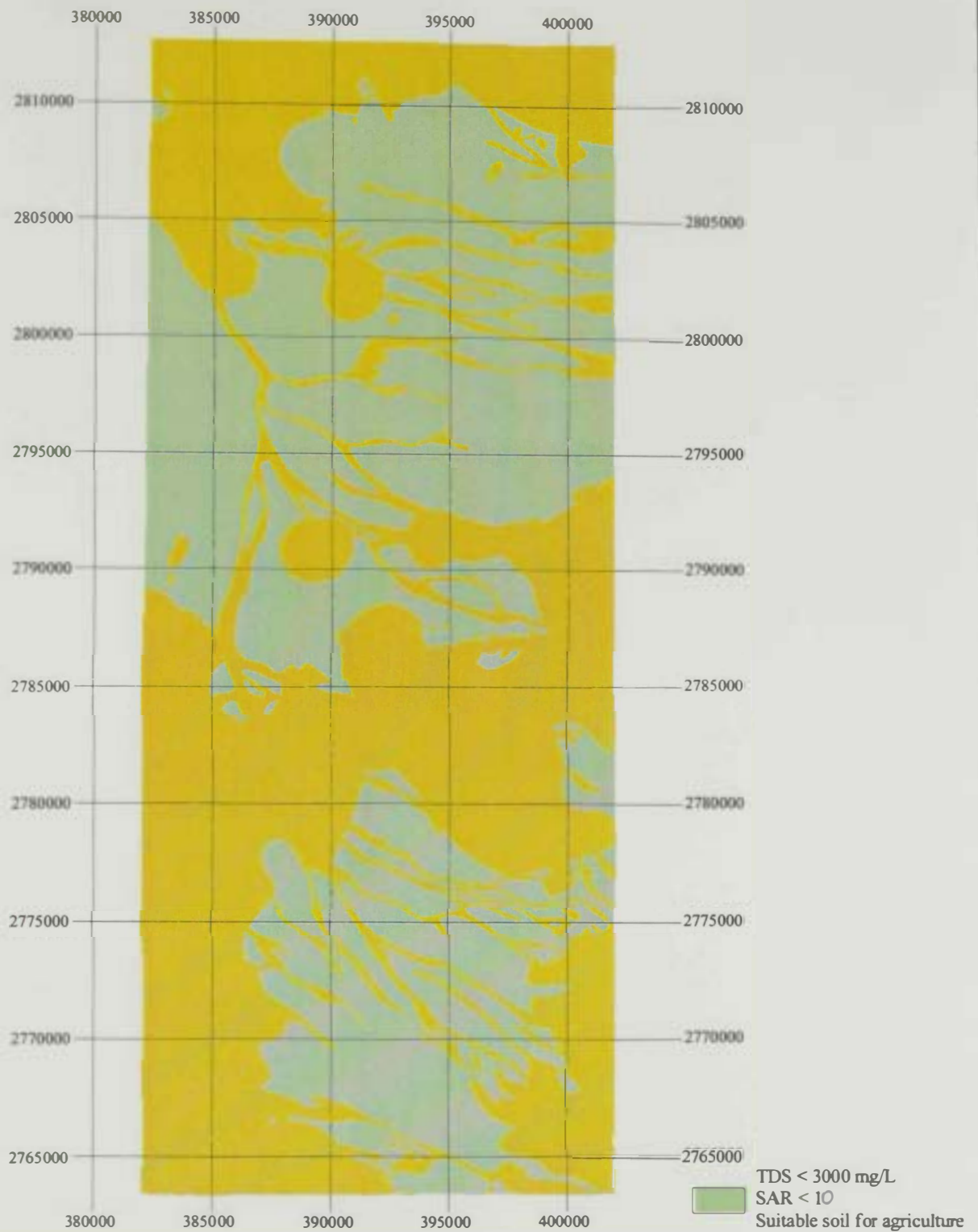
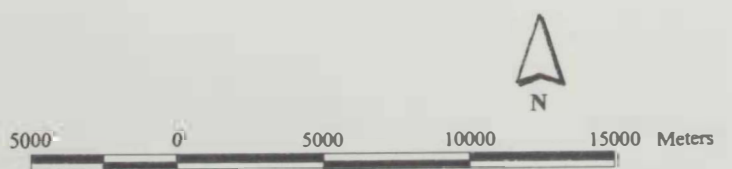


Figure 5. 5.15.
Total Dissolved Solids (TDS) in mg/L, Sodium Adsoption Ratio (SAR)
and suitable soil for agriculture.



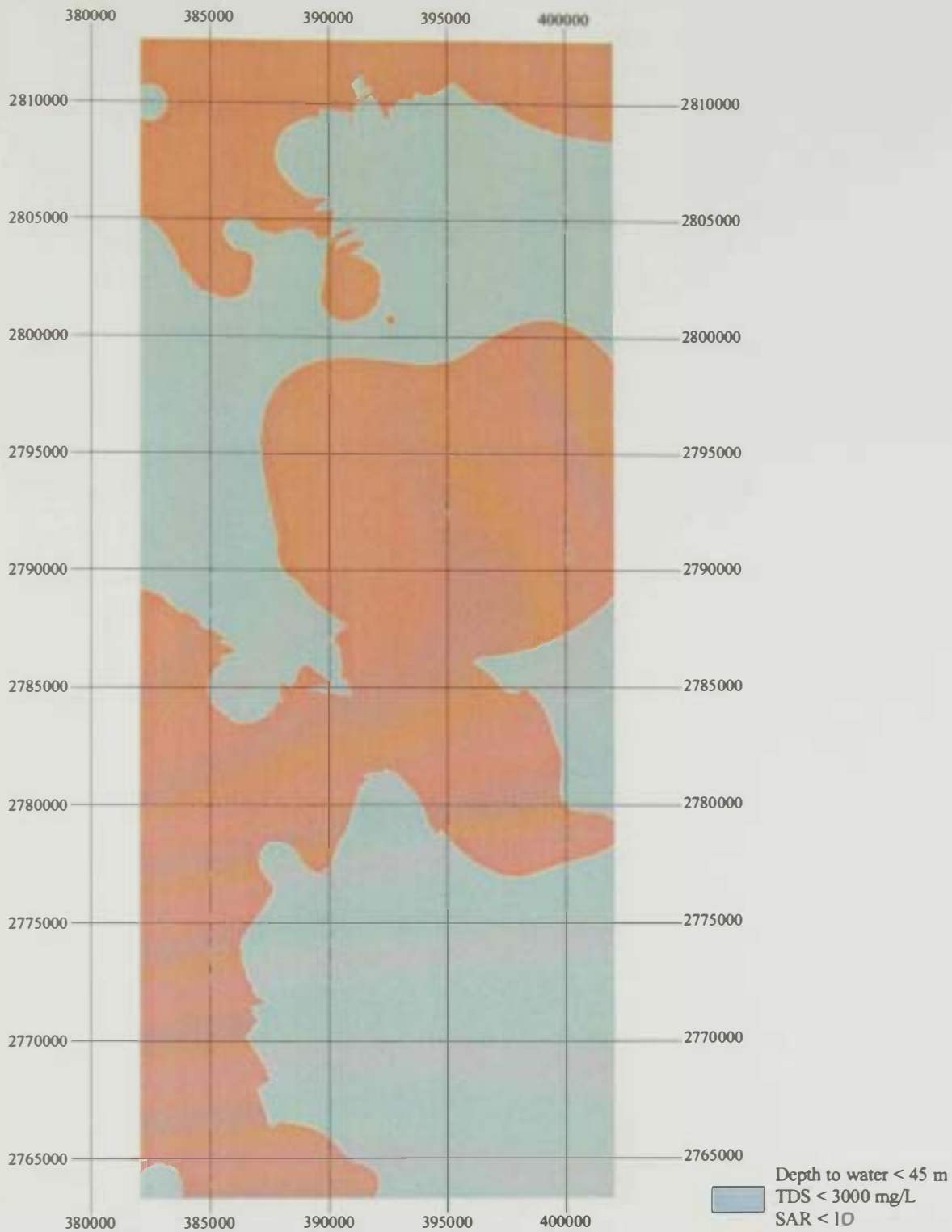
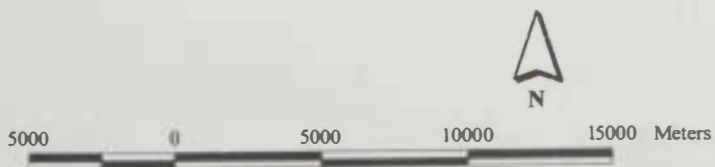


Figure 5.16
Depth to groundwater, Total Dissolved Solids (TDS) in mg/L
and Sodium Adsorption Ratio (SAR).



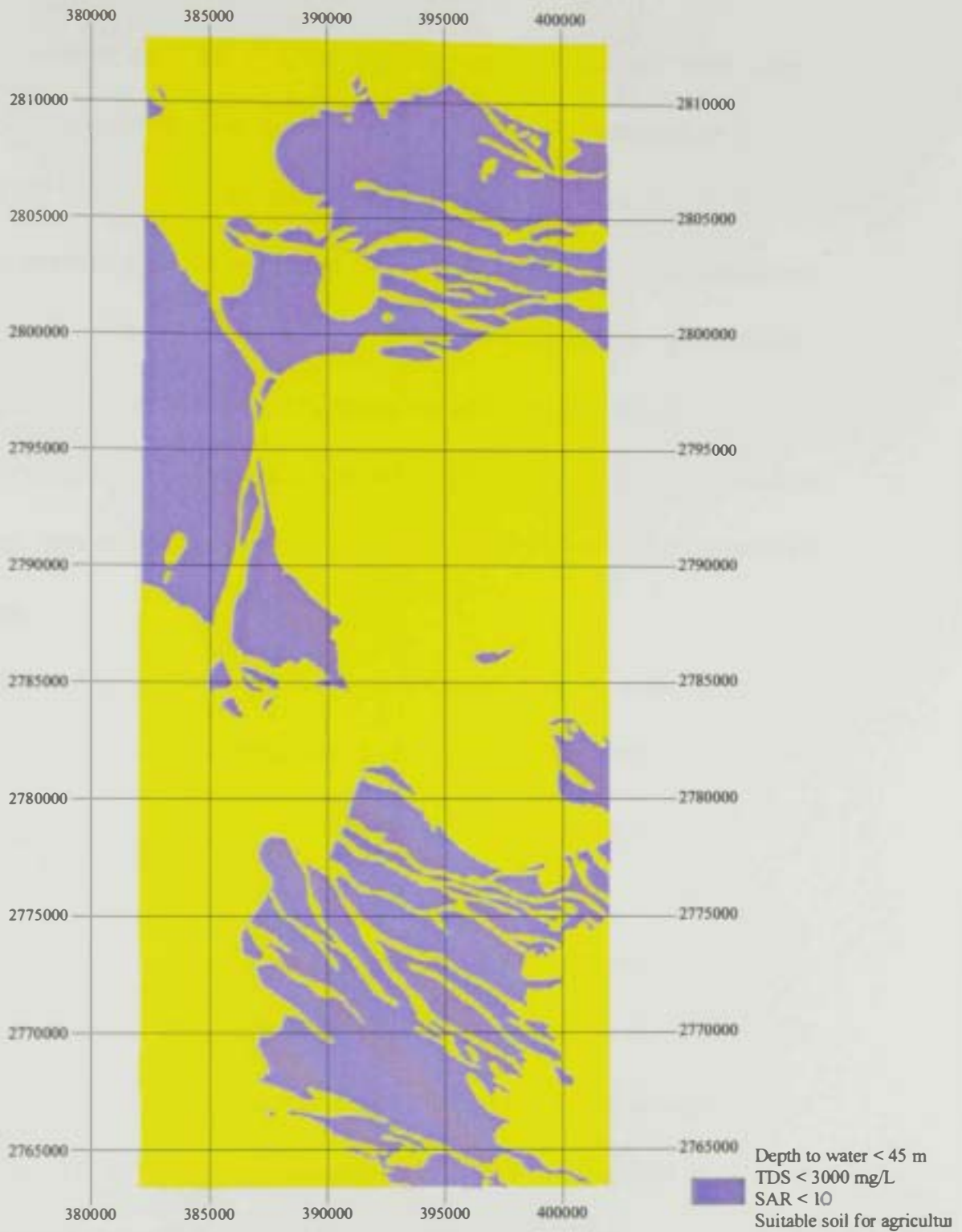
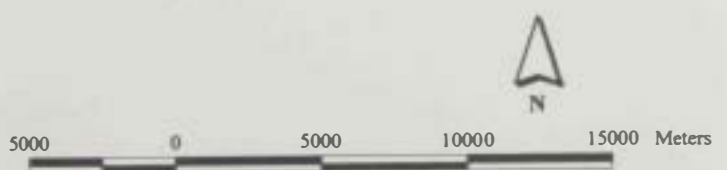


Figure 5.17.
Depth to groundwater, Total Dissolved Solids (TDS) in mg/L,
Sodium Adsoption Ratio (SAR) and suitable soil for agriculture.



An overlay of TDS ≤ 1500 mg/l, drainage lines and fault zones (given a suggested buffer zone of 300 m wide) is illustrated in Figure 5.18. This overlay reveals the areas of high groundwater potentiality which represent preferable sites of future new farms and high production water wells. These areas are characterized by high groundwater potentialities and presence of soil types suitable for agriculture.

The correlations described above can provide guidance for land use planning, groundwater availability and suitability of soil for agriculture purposes.

Because most wadi sides encompass farms, a 50 m wide protection zones are proposed. In these zones no dumping of wastes should be allowed and human related activities must be kept at the minimum level (Fig. 5.19)

Figure 5.20 shows the location of groundwater observation wells. It is also suggested that protection zones must be applied for them and other water supply well fields. An arbitrary distance of 300 m is suggested in this model. However, more accurate calculation of required protection distance can be obtained from pumping test results.

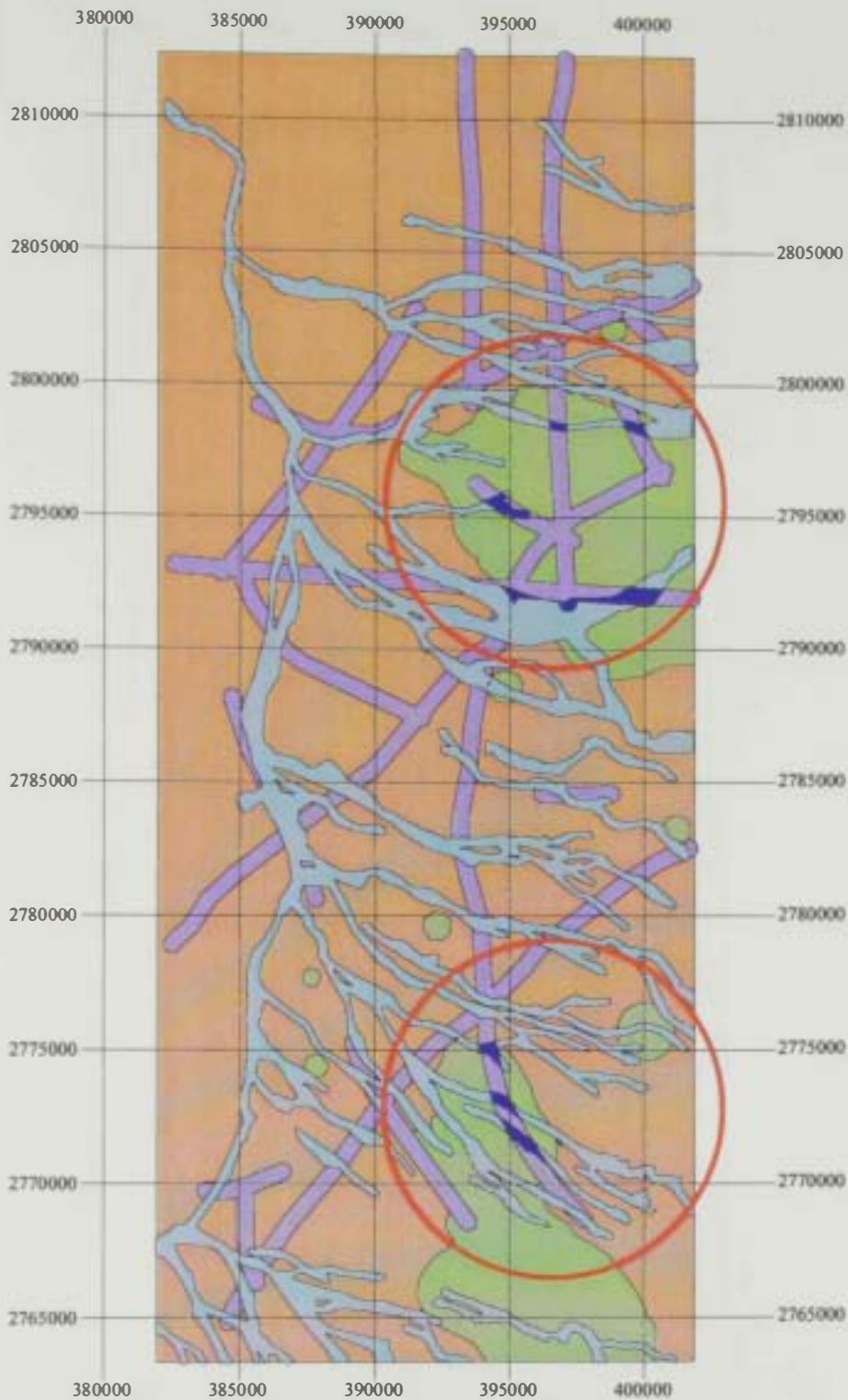
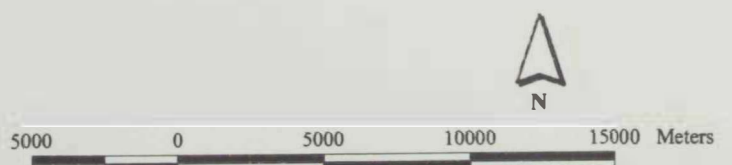


Figure 5.18. Combination of groundwater salinity, drainage lines and major structural zones affecting the study area.



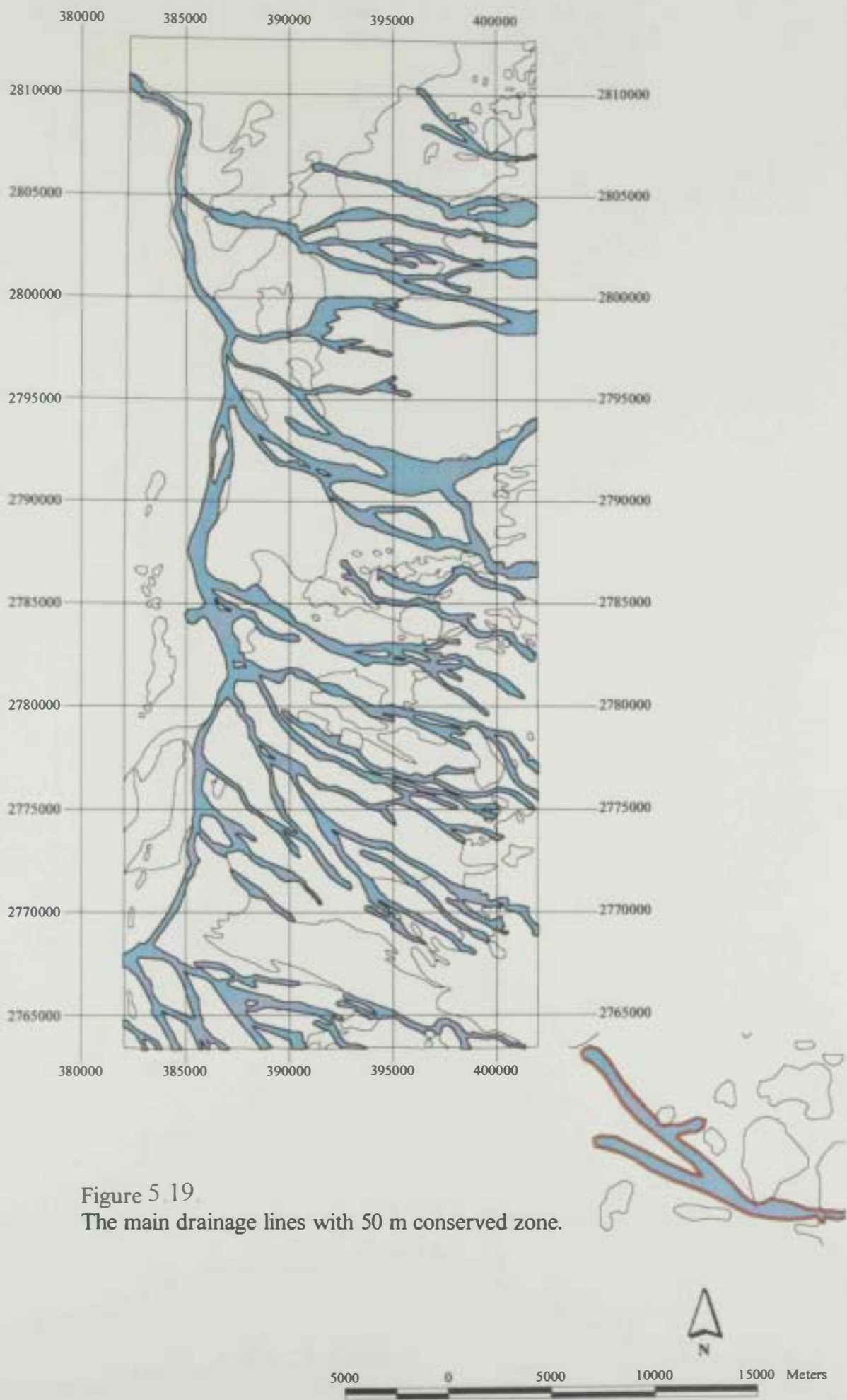


Figure 5 19
The main drainage lines with 50 m conserved zone.

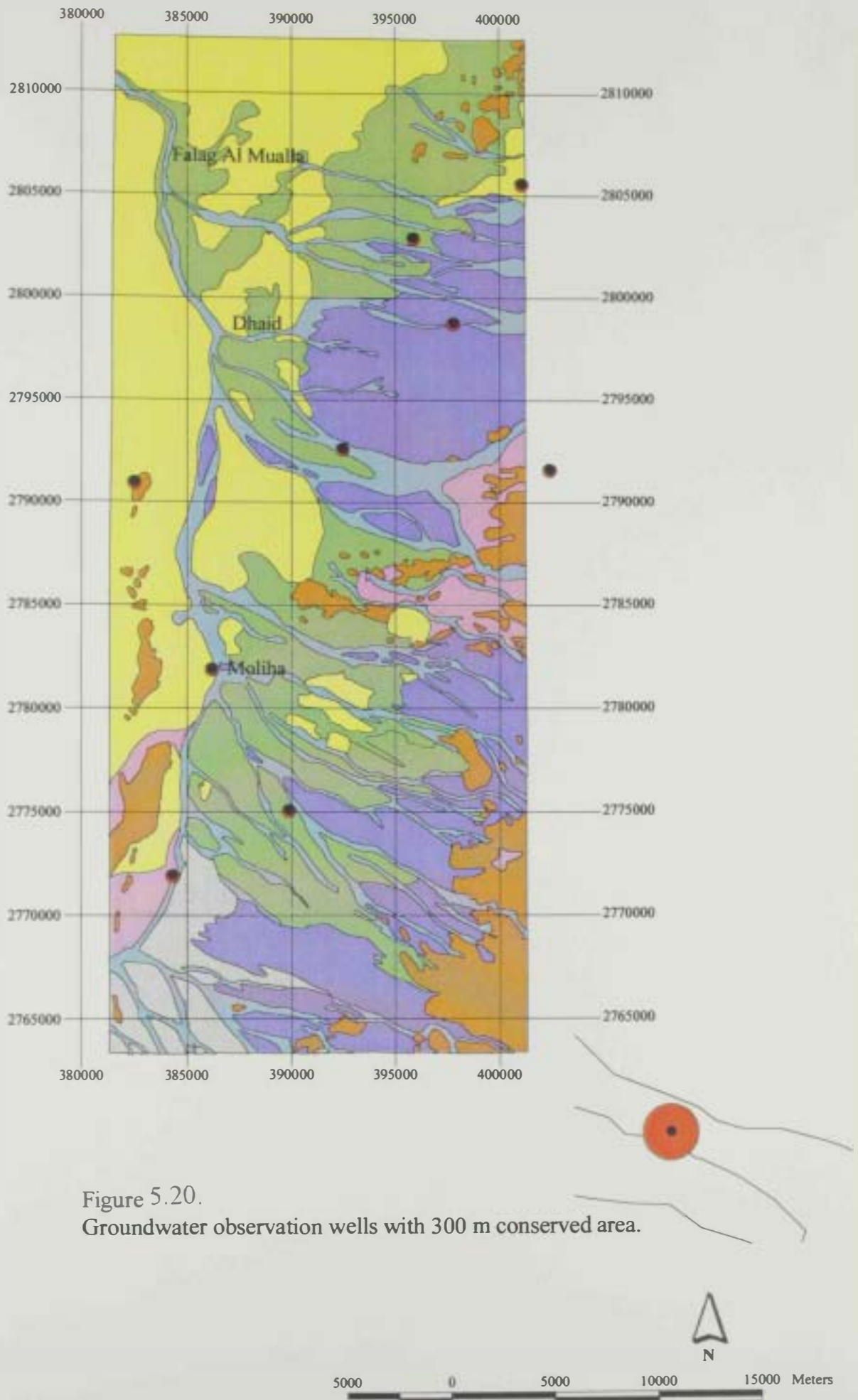


Figure 5.20.
Groundwater observation wells with 300 m conserved area.

CHAPTRE 6

CONCLUSIONS

CHAPTRE 6

CONCLUSIONS

6.1. Introduction

The findings of previous studies, in addition to the results of the present geophysical investigations, hydrogeologic and hydrogeochemical studies, water quality analysis and GIS modeling techniques were used in this study.

The following is description of the main conclusions reached based on the results of this study:

6.2. Conclusions based on geophysical investigations

1. Results of gravity analysis outlined the structural picture of the Al Dhaid area. The gravity anomalies yielded three fault trends; the ENE-WSW, NNW-SSE and E-W. The fault displacements range from 70 m to 320 m. The calculated thickness of the sedimentary section above the ophiolite series varies between 700 m at the southeastern end of the profile and more than 3500 m at its northwestern end. The majority of faults have their downthrown sides towards the northwest.
2. The geoelectrical resistivity survey included DC-electrical resistivity and time domain electromagnetic. The TDEM measurements were interpreted in the present work and the results are given in terms of

thicknesses, resistivities and total dissolved salts in different geoelectric layers:

- a. The thickness of the first layer ranges from 1.5 m in the northwest to 5 m in the west. The resistivity ranges from 500 to 2000 Ohm.m and the total dissolved salts (TDS) are very small, ranging from 10 to 50 ppm.
- b. The thickness of the second layer varies between 5 m in the southern part and >5 m in the central and northern parts. In the southern part, the resistivity is low (205 Ohm.m), while the highest resistivity value of this layer (605 Ohm.m) was calculated in the northern part of the study area. The TDS in this layer ranges from 200 to 2000 ppm.
- c. The thickness of the third layer varies between 28 m in the southeastern corner and 150 m in the northern part of the area. The calculated true resistivity is about 10 Ohm.m in the northwestern corner, while values of >1000 Ohm.m were calculated in the middle part of the study area. The TDS ranges from 100 ppm at the eastern corner of the study area and 300 ppm at the western part.
- d. The fourth geoelectric layer has a thickness of 80 m in the western corner and 450 m in the northern part of the study area. The true resistivity is 2 Ohm.m in the northwestern corner and 100 Ohm.m

in the northeastern part of the study area. The TDS distribution shows a great fluctuation, ranging from 100 ppm to 7500 ppm.

3. The analysis geophysical well logs yielded information about petrophysical parameters of the different layers and the characteristics of saturating fluids. Analyses of caliper, gamma rays, resistivity, neutron, density, sonic, temperature, conductivity and hydrochemistry logs gave information about the rock type, porosity, fracturing, permeability, bed attitude, structure, clay content, total dissolved salts and groundwater flow directions in the study area.
 - a. Porosities of <5% Lst were calculated in some carbonate rocks, while values >40% Lst were found in some dolomitic rocks. The presence of fractures facilitates greatly the movement of groundwater through rock cracks and voids.
 - b. The calculated TDS pattern gave an idea about salt-water intrusion in some localities, which can be fully understood if fracture analyses are considered in the future.

A comparative study of salinity distribution in salt-water intruded areas, fractures pattern in different layers and temperature anomalies, shows the direction of groundwater flow, which can be either a recharge or salt-water intrusion into the aquifer.

6.3. Conclusions based on hydrogeological studies

1. Three hydrogeologic units were identified in the Al Dhaid area; an upper free to semi-confined aquifer, an aquiclude and a lower confined aquifer.
2. The regional groundwater flow direction occurs from the Northern Oman Mountain in east towards the Arabian Gulf in the west and northwest.
3. Between 1984 and 1999, a 20 km diameter cone-of-depression, centered around the observation well GP-15, resulted from excessive groundwater pumping for different purposes. In 1999, a maximum drawdown of 50 m was observed is well GP-15.
4. The Northern Oman Mountains are the main recharge area for groundwater in the Al Dhaid area, while the Arabian Gulf is the main natural discharge area.
5. The average hydraulic gradient is steep (0.025) along the foothills of the Northern Oman Mountains in the east and gentle (0.005) in the western region.

6.4. Conclusions based on hydrogeochemical studies

1. The total dissolved solids (TDS) in groundwater of the Al Dhaid area changes from <750 mg/l in the northeast to 3000 mg/l in the central area and >7500 mg/l in the southwest.
2. The sequence of cation dominance in groundwater of the Al Dhaid area is $\text{Na}^+ > \text{Mg}^{2+} > \text{Ca}^{2+}$, whereas the sequence of anion dominance is $\text{Cl}^- > \text{SO}_4^{2-} > \text{HCO}_3^-$.
3. Based on the TDS contents, concentrations of major ions and total hardness, groundwater in some parts in and around the Al Dhaid city is not suitable for drinking or domestic purposes.
4. The calculated total hardness of groundwater in Al Dhaid area shows that this water is hard around the Al Dhaid city and very hard everywhere else. Soft water exists in the eastern part of the study area and along the courses of main wadis.
5. The electrical conductivity (EC) and concentrations of calcium, sodium, potassium, chloride and sulphate ions are all increasing from the east towards the west and northwest, in the direction of groundwater flow.
6. The concentrations of nitrate in the study area are above the WHO (1984) recommended limits for drinking water in the north central part

of the study area due to intensive application of chemical fertilizers in agriculture in this area.

6.5 Conclusions based on GIS modeling

1. The results of GIS modeling indicate that the eastern strip of the study area is the most favorable region of high groundwater potentiality because:
 - a. Both areas witness the intersection of more than one structural trend, which seems to control groundwater movement and recharge.
 - b. Both areas have soft groundwater ($TH \leq 80$ mg/l) with of low salinity ($TDS \leq 1500$ mg/l).
 - c. Both areas are near the upstream of Wadi Al Dhaid in the north and Wadis of Kadra and Shoka in the south.
2. The area around the Al Dhaid city and the south central area are favorable for agriculture due to the followings:
 - a. Both areas have $TDS \leq 3000$ mg/l.
 - b. SAR values ≤ 10 in both areas.
 - c. Soil types are suitable for agriculture.
 - d. Depth to groundwater shallow (≤ 45 m).
3. Because wadi channels within the study area contain several water production wells, which are used mainly for domestic purposes, it is proposed to minimize or even prohibit urban and agricultural activities

in the upstream side of these wells and assign them as groundwater protection zones to maintain good quality groundwater supply.

4. Because of the presence of farms within the courses of several wadi channels, it is also suggested to control urban activities that can impose negative effects on groundwater feeding these farms.
4. For further investigations and continuous monitoring of the impact of urban and agricultural development on groundwater resources of the Al Dhaid and similar areas in UAE utilizing the GIS capabilities, the following is needed:
 - a. Aerial photograph with accepted accuracy to be used as base maps of these studies.
 - b. A GIS laboratory and a comprehensive environmental database at the Ministry of Agriculture and Fisheries.

Generally the results obtained represent a contribution to understanding the factors affecting groundwater flow, recharge, quality, groundwater potentiality and land use for agricultural purposes. It is recommended that the results of present field investigations and GIS modeling to be considered by the MAF in the future to improve the groundwater augmentation and land use planning in the study area and other areas as well.

REFERENCES

REFERENCES

- Abrol, I.P, Yadav, J.S.P and Massoud, F.I, 1988, Salt-affected soils and their management: FAO Soils Bulletin 39. UN. Rome, 131 p.
- Al-Farraj,A.M. and Harvey,A.M.,2000, Use of Desert pavement characteristics to correlate wadi terrace and alluvial fan surface : Wadi Al Bih , UAE and Oman.Georphology,35p,279-297.
- Al-Farraj,A.M., in prap, Quaternary geomorphic evolution of wadi drainage basin in the northern UAE.
- Al- Farraj A.M., 1996, Late Pleistocene geomorphology in Wadi Al-Bih northern UAE and Oman: with special emphasis on wadi terrace and alluvial fans (Ph.D. thesis): Liverpool. The University of Liverpool.
- Alleman, F., and Peters, T., 1972, The ophiolite-radiolarite belt of the north Oman Mountain. *Ecologiae Geologicae Helventiae*, 65, 657-697.
- Al Shamesi, M.H., 1993, Drainage basins and flash flood hazards in the Al Ain area, United Arab Emirates: M. Sc. Thesis, Fac. Sci., UAE University,151 p.
- Alsharhan,A.S., and Kendall,C. St. C.,1986,Precambrian to Jurassic rocks of Arabian Gulf and adjacent areas: their facies, depositional setting, and hydrocarbon habitat. *The American Association of Petroleum Geologists Bulletin.*, 70,8, 977-1002.
- Alsharhan, A.S., and Naim, A. E. M., 1988, A review of the Cretaceous formation in the Arabian peninsula and the Gulf: part II, Mid-Cretaceous (Wasia Group) stratigraphy and palaeogeography. *Journal of Petroleum Geology.* 13,247-277.
- Bassiouni, Z.,1994, Theory, measurement and interpretation of well logs.SPE Textbook series vol.4, Richardson, TX, 372 p.
- Davis, S.N., and De Weist, R.J., 1966, Hydrogeology: John Wiley and Sons, New York, 463 p.

- Domenico, P.A., and Schwartz, F.W., 1990, Physical and chemical hydrogeology: John Wiley and Sons, New York, 824 p.
- Environmental System Research Institute (ESRI), 1996, Using the ArcView spatial analyst, USA, 148 p.
- Freeze, R.A., and Cherry, J.A., 1979, Groundwater: Prentice-Hall, Englewood Cliffs, N.J., 604 p.
- Garamoon, H.K., 1996, Hydrogeological and geomorphological studies on the Abu Dhabi-Al Ain-Dubai rectangle, United Arab Emirates: Ph. D. Thesis, Ain Shams University, Cairo, Egypt, 277 p.
- Glennie, K.W., Pugh, J.M., and Goodal, T.M., 1994, Late Quaternary Arabian desert models of Permian Rotliegend reservoirs. Exploration Bulletin, 274, 1-19
- Grant, F.S. and West, G.F., 1965, Interpretation Theory in Applied Geophysics, McGraw-Hill, New York, 583 p.
- Hem, J.D., 1985, Study and interpretation of chemical characteristics of natural water: U. S. Geological Survey Water Supply Paper no. 1473, 363 p.
- Hounslow, A.W., 1995, Water quality data - Analysis and interpretation: Lewis Publishers, New York, 397 p.
- IWACO, 1986, Drilling deep wells at various locations in the UAE: IWACO Consultants for Water and Environment, The Netherlands, v. 6, Groundwater development in the central agricultural region, 117 p.
- JICA, 1996, The master plan study on the groundwater resources development for agriculture in the vicinity of Al Dhaid in the UAE: Japan International Cooperation Agency – Final Report.

- Keller, G. V. and Frischknecht, F. C., 1979, *Electrical methods in geophysical prospecting*. Pergamon, London.
- Lang, L., 1998, *Managing natural resources with GIS*, Environmental System Research Institute, Inc (ESRI), California. 117 p.
- Ministry of Agriculture and Fisheries, 1993, *Climatological data, v. 3, 1979-80 to 1991-1992: Department of Soil and Water, MAF, UAE*, 443 p.
- Ministry of Communication, 1996, *UAE Climate*. 237p.
- Piper, A.M., 1944, A graphic procedure in the geochemical interpretation of water analysis: *Trans. Amer. Geophysical Union*, v. 25, pp. 914-928.
- Rofail, N., Zahraa, S. and Ibrahim, Y., 1998, *Application of geographic information systems in natural resources management in arid zones: Water Resources Division (ACSAD/WS/R 122)*. The Arab Center for the Studies of Arid zones and Dry lands, Syria, 103 p.
- Walton, W.C., 1970, *Groundwater resources evaluation*: McGraw-Hill Book Company, New York, 664 p.
- WHO (World Health Organization), 1971, *International standards for drinking water, 3rd edition*: Geneva, Switzerland.
- World Health Organization, 1984a, *WHO guidelines for drinking water quality: Volume 1, Recommendations*, Geneva, Switzerland, 130 p.

ARABIC SUMMARY

أ. كلا المنطقتان بميزان مياه حوفية متوسطة الملوحة (الأملاح الكلية الذائبة أقل من ٣٠٠٠ ملليجرام في اللتر).

ب. نسبة إدمصاص الصوديوم في المياه الجوفية منخفضة في كلا المنطقتين ، أقل من ١٠ ، حيث لا يحتمل أن يكون لتلك المياه تأثير ضار على النباتات عند استخدامها في الري.

ت. أنواع التربة في كلا المنطقتين صالحة للزراعة كما أن المياه الجوفية بهما ضحلة ولا يتعدى عمقها ٤٥ متر من سطح الأرض مما يعني الاقتصاد في نفقات حفر آبار الري.

٣. لأن مجاري الأودية الرئيسية في منطقة الدراسة تحوي العديد من آبار المياه التي تستخدم مياهها في الشرب وفي الأغراض المنزلية فإنه من المقترح منع أو الإقلال قدر الإمكان من الأنشطة الحضرية أو المشروعات الزراعية إلى الشرق من تلك الآبار وإعتارها مناطق محمية حتى لا تؤثر تلك الأنشطة سلباً على جودة المياه الجوفية لتلك الآبار.

٤. يلزم للدراسات المستقبلية والمراقبة المستمرة لتأثير المشروعات الحضرية والزراعية على موارد المياه الجوفية وغيرها من مناطق الدولة والاستفادة الكاملة من قدرات تقنيات الاستتعار عن بعد و نظم المعلومات الجغرافية مايلي:

أ. الحصول على صور حوية ذات دقة مقبولة لإستخدامها كخرائط أساس للدراسات المستقبلية.

ب. بناء قاعدة معلومات بيئية وتجهيز معمل كامل لنظم المعلومات الجغرافية بوزارة الزراعة والثروة الحكيمة بدمشق.

تعنبر النتائج التي تم التوصل إليها في هذه الأطروحة إضافة إلى فهمنا للعوامل التي تؤثر على إعادة شحن الخزانات الطبيعية للمياه الجوفية وكمياتها ونوعيتها بالإضافة إلى إستخدامات الأراضي في الأغراض الزراعية. لذا فإنه يوصى بأن تأخذ نتائج الدراسات الحقلية الحالية ونتائج نموذج نظم المعلومات الجغرافية الذي تم إعداده من خلالها في الإعتبار بواسطة وزارة الزراعة والثروة الحكيمة في المستقبل لترشيد وتحسين وتخطيط إستخدام موارد المياه الجوفية والأراضي في منطقة الدراسة وفي غيرها من مناطق الدولة.

٤. أوضع حساب العسر الكلي للمياه الجوفية في منطقة الدراسة لفا حصة في منطقة الليد ورحوط وعسرة حاداً في المناطق الأخرى ماعدا الشريط الشرقي الموازي لجبال عمان الشمالية في الإمارات العربية المتحدة وفي بحاري الوردان الرئيسية.

٥. درجة التوصل الكهول للمياه الجوفية بالاضافة الى تركيز الأيونات الرئيسية -ماعدا اليكربونات- تزداد جميعا من الشرق نحو الغرب والشمال العربي ، في اتجاه حركة المياه الجوفية من مناطق التغذية نحو مناطق التصريف.

٦. يزيد تركيز أيون النترات عن الحد المسموح به في مياه الشرب من قبل منظمة الصحة العالمية وذلك في الجزء الشمالي الأوسط من منطقة الدراسة. تلك المنطقة تعرف بكثافة السطاط الزراعي واستحمام المحاصيل الكيماوية من بينها الأسمدة النتروجينية.

رابعاً: نتائج نموذج نظام المعلومات الجغرافية

١. أوضحت نتائج نموذج نظام المعلومات الجغرافية الذي تم إعداده أن الأجزاء الشمالية الشرقية والجنوبية الشرقية من منطقة الدراسة هي أكثر المناطق إجمالاً من حيث إمكانات المياه الجوفية ها وذلك للأسباب التالية:

أ. كلا المنطقتان تنبعها تتابع أكثر من اتجاه تركيزي من تتفق وكهيف الطبقات الجاملة للمياه الجوفية وبالتالي سهولة حركتها وإعادة تغذيتها عن طريق تسرب مياه الأمطار والسيول إليها.

ب. كلا المنطقتان هما مياه عسرة والعسر الكلي أقل من ٨٠٠ ملليجرام في اللس وتركيز محض من الأملح الكلية الذائبة أقل من ١٥٠٠ ملليجرام في اللس مما يعنى إمكانية استخدامها في الشرب والأغراض المنزلية الأخرى.

ج. كلا المنطقتان تقعان عند الأطراف الشمالية لأحواض صرف رئيسية هي وادي اللبيد في الشمال الشرقي ووادي كدرة وشوكة في الجنوب الشرقي وبالتالي فهما يقعان بالقرب من مناطق تغذية المياه الجوفية وهي جبال عمان الشمالية في الإمارات العربية المتحدة.

٣. الأجزاء التي تشمل مدينة الليد والمناطق المحيطة بها والمنطقة الوسطى الجنوبية هما أكثر المناطق ملائمة للزراعة في منطقة الدراسة وذلك للأسباب التالية:

ثانياً: نتائج الدراسات الهيدروجيولوجية

١. تم التعرف على ثلاثة وحدات هيدروجيولوجية في منطقتي الدراسة هي: الحزان المائي الطبيعي الحزالي شبه الحز العلوي والطبقة الحامسة الوسطى والحزان المائي الطبيعي السفلي.
٢. الإتجاه العام حركة المياه الجوفية في منطقة الدراسة يتم من جبال عمان الشمالية في الإمارات العربية المتحدة والتي تقع في شرق منطقة الدراسة نحو الخليج العربي في الغرب والشمال الغربي.
٣. بين عامي ١٩٨٤م و ١٩٩٩م تكون منخفض ضخ يتمركز حول بئر الملاحظة رقم ١٥ نتيجة الضخ الزائد للمياه الجوفية للأغراض المختلفة في منطقة الدراسة. حيث بلغ أقصى إنخفاض الماء الجوفي حوالي ٥٠ متر.
٤. تعتم جبال عمان الشمالية في الإمارات العربية المتحدة والتي تقع في شرق منطقة الدراسة هي منطقة التغذية الرئيسية للمياه الجوفية أما منطقة التصريف الطبيعي الرئيسية فتتمثل في الخليج العربي والذي يقع على الجانب الغربي والشمال الغربي من منطقة الدراسة.
٥. يختلف التدرج الهيدروليكي من شديد (٠,٢٥) بطول الجهة الشرقية لمنطقة الدراسة إلى خفيف (٠,٠٥) في المنطقة الغربية.

ثالثاً: نتائج الدراسات الهيدروجيوكيميائية

١. يتراوح تركيز الأملاح الكلية الذائبة في المياه الجوفية بمنطقة الدراسة بين أقل من ٧٥٠ ملليجرام في اللتر في الجزء الشمالي الشرقي و ٣٠٠٠ ملليجرام في اللتر في المنطقة الوسطى و ٧٥٠٠ ملليجرام في اللتر في الجزء الجنوبي الغربي.
٢. تتابع شيوخ الأيونات الموجبة الرئيسية في المياه الجوفية بمنطقة الذيد هي: الصوديوم يليه الماغنسيوم ثم الكالسيوم. بينما تتابع الأيونات السالبة الرئيسية فهو: الكلوريد يليه الكبريتات فالبكربونات.
٣. بناءً على تركيز الأملاح الكلية الذائبة الكلية في المياه الجوفية عسرها الكلي فإن تلك المياه في العديد من أجزاء منطقة الدراسة - خاصة في المنطقة الوسطى - لا يصلح للشرب والأغراض المنزلية الأخرى.

٢. **الطبقة الثانية:** يتراوح سمك الطبقة الثانية بين ٥ أمتار في الجنوب وأكثر من ١٥ متر المناطق الوسطى والشمالية من منطقة الدراسة. أما المقاومة النوعية للطبقة الثانية فتتراوح بين ٢٠٥ أوم-متر في الجنوب و ٦٠٥ أوم-متر في شمال منطقة الدراسة. أما الأملاح الكلية الذائبة فإنها تتراوح بين ٢٠٠ و ٢٠٠٠ جزء في المليون.

٣. **الطبقة الثالثة:** يتراوح سمك الطبقة الثالثة بين ٢٨ متر في الجنوب الشرقي و ١٥٠ متر المناطق الشمالية من منطقة الدراسة. أما المقاومة النوعية للطبقة الثالثة فتتراوح بين ١٠ أوم-متر في الجزء الشمالي الغربي و ١٠٠٠ أوم-متر في وسط منطقة الدراسة. أما الأملاح الكلية الذائبة فإنها تتراوح بين ١٠٠ جزء في المليون في شرق منطقة الدراسة و ٣٠٠ جزء في المليون في غربها.

٤. **الطبقة الرابعة:** يتراوح سمك الطبقة الرابعة بين ٨٠ متر في الغرب و ٤٥٠ متر المناطق الشمالية من منطقة الدراسة. أما المقاومة النوعية للطبقة الثالثة فتتراوح بين ٢ أوم-متر في الجزء الشمالي الغربي من منطقة الدراسة و ١٠٠ أوم-متر في الشمال الشرقي. أما الأملاح الكلية الذائبة فإنها تتراوح بين ١٠٠ و ٧٥٠٠ جزء في المليون.

٣- أوضحت نتائج سجلات الآبار المعاملات الصخرية الطبيعية ودرجة تشبعها بالسوائل. ويعطي تحليل سجلات الحفر وأشعة جاما وسجل النيوترون والسجل الصوتي وسجل الكثافة وسجل الحرارة وسجل التوصيل الكهربائي والسجلات الهيدروكيميائية معلومات عن نوع الصخر ومساميته ودرجة تكهفه ونفاذيته ووضع الطبقات والتراكيب الجيولوجية ومحتواها من معادن الطين والأملاح الذائبة الكلية وإتجاهات حركة المياه الجوفية وتداخل المياه المالحة.

١. تراوحت المسامية التي تم حسابها بين أقل من ٥% في بعض الصخور الجيرية وأكثر من ٤٠% في بعض صخور الدولوميت حيث يؤدي وجود التكهفات داخل الصخور إلى سهولة حركة المياه الجوفية عبرها.

ب. أوضحت قيم الأملاح الذائبة الكلية التي تم حسابها عن تداخل المياه المالحة في بعض مناطق الدراسة. ويمكن تحديد تلك المناطق بدقة إذا تم عمل تحليل للشروخ الصخرية في المستقبل.

ج. أوضحت المقارنة الميدانية بين توزيع الأملاح الذائبة الكلية وتوزيع الشروخ الصخرية مع مناطق الشدوذ الحراري إتجاه حركة المياه الجوفية ونوعية المياه ، هل هي مياه أمطار تغذي الخزان الجوفي أم أنها مياه مالحة من طبقات صخرية مجاورة.

بِسْمِ اللَّهِ الرَّحْمَنِ الرَّحِيمِ

الملخص العربي

عن

تطبيق التقنيات الجيوفيزيائية والبيدرولوجية ونظام المعلومات الجغرافية للكشف عن موارد المياه الجوفية في منطقة الخيد حولة الإمارات العربية المتحدة

إستهدمت في إعداد هذه الأطروحة نتائج الدراسات المسابقة بالإضافة إلى الدراسات الحالية بإستخدام الطرق الجيوفيزيائية والبيدرولوجية والبيدرولوجيو كيميائية ودراسة لنموذج بنظام المعلومات الجغرافية.

فيما يلي وصف متسلل وتختصر للاستنتاجات الرئيسية التي تم التوصل إليها بناءً على نتائج الدراسات الحالية:

أولاً: نتائج الدراسات الجيوفيزيائية

١- أوضحت نتائج تحليل بيانات الجاذبية صورة التوزيع الجسوليوجي لمنطقة الذيد حيث أظهرت تلك النتائج وجود ثلاثة إتجاهات للفرق الرئيسية هي: شرق شمال شرق - جنوب جنوب غرب وشمال شمال غرب - جنوب جنوب شرق وشرق - غرب. أما الإزاحة عبر مستويات تلك الفرق فتتراوح بين ٥٠ متر إلى ٣٢٠ متر وأن إتجاه الرمية السفلية لتلك الفرق هو الشمال الغربي. أما سمك الطبقات الرسوبية التي تعقلو تتابع منحور الأفيوليت فيتراوح بين ٧٠٠ متر في الجنوب الشرقي لمنطقة الدراسة وأكثر من ٣٥٠٠ متر في شمالها الغربي.

٢- أما المسوحات الجيوكهربية فقد إبتسملت على المقاومة النوعية والطرق الكهرومغناطية والتي ترجمت نتائجها في شكل معلومات محددة من المقاومة النوعية والسمك والأملاح الكلية الذائبة في كل طبقة جيوكهربية.

- ١- الطبقة الأولى: يتراوح سمك الطبقة الأركلي (الطوية) بين ٥ ، امتري في الشمال الغربي و ٥٠٠ أمتار في الجزء الغربي من منطقة الدراسة. أما المقاومة النوعية للطبقة الأركلي فتتراوح بين ٥٠٠ و ٢٠٠٠ أوم-متر. أما الأملاح الكلية الذائبة فأما تتراوح بين ١٠ و ٥٠ جزء في المليون.

تطبيق التقنيات الجيوفيزيائية والهيدروجيولوجية ونظام المعلومات الجغرافية
للكشف عن موارد المياه الجوفية في منطقة الذيد
دولة الإمارات العربية المتحدة

إعداد

محمد مصطفى محمد الملا

بكالوريوس علوم زراعية

١٩٩٤م

رسالة مقدمة إلى

كلية العلوم - جامعة الإمارات العربية المتحدة

لاستكمال متطلبات الحصول على

درجة الماجستير في

علوم البيئة

كلية العلوم

جامعة الإمارات العربية المتحدة

يناير ٢٠٠١م

